Characterization of the insect specific putative kinase *banshee* in *Drosophila melanogaster*

by

Lindsay Christine Canham

A thesis submitted in partial fulfillment of the requirements for the degree of

Master of Science

in
Molecular Biology and Genetics

Department of Biological Sciences
University of Alberta

Abstract

In differentiating cells, genes are silenced or transcribed through changes in chromatin organization. Active chromatin is known as euchromatin and repressive chromatin is known as heterochromatin. These active or repressive states are initiated and maintained by modifying residues of the core histone tails. Previous work has identified *Su(var)* and *E(var)* genes as modifiers of histone, with some roles in initiating heterochromatin or maintaining euchromatin, respectively. The gene *bshe* (*CG8878*) was identified in a forward genetic screen looking for recessive lethal *Drosophila E(var)* mutants. The amino acid sequence of this previously unstudied gene is predicted to be a protein kinase, based on its similarity to a known histone kinase.

My research has begun to explore the function of *bshe*, and how it contributes to the heterochromatin/euchromatin balance. The predicted BSHE polypeptide has a kinase domain within the sequence. However, it also has a large interruption in the middle of the catalytic regions of the kinase domain, calling in to question whether it truly has kinase activity. Through phylogenetic analysis I characterize *bshe* to be an insect specific kinase of either an ancient or rapidly evolving clade. Predictions of the protein structure suggest that despite the large interruption, the main catalytic regions of the kinase domain are still in correct confirmation, suggesting that it still functions as a kinase. My observations of *bshe* mutant phenotypes show the majority of mutant hemizygotes to die by second instar larvae, with a maternal effect leading to earlier lethality. I completed an initial optimization of three antibodies, made against three polypeptides from BSHE, for Western blots and immunofluorescence. Initial observations show in syncytial embryos BSHE is localized to the cytoplasm.

Preface

This thesis is an original work by Lindsay Canham. An undergraduate researcher, Brian McNish, assisted in data collection for all experiments in Chapter 5 under Lindsay Canham's supervision. No part of this thesis has been previously published.

Acknowledgements

I would like to thank Dr. John Locke for his mentorship, wisdom and guidance during my graduate studies.

I thank NSERC for Dr. Locke's Discovery Grant that supported this research, and the University of Alberta Department of Biological Sciences for TA Support.

I thank Dr. Warren Gallen for his essential help in creating the phylogenetic trees; Dr. Shelagh Campbell and Dr. Ellen Homola for helping set up our lab for protein antibody work, and teaching me the techniques; Dr. Ted Allison for the use of his fluorescent dissecting microscope for all the mutant GFP experiments.

Importantly, I want to send the most heartfelt thanks to my partner Adam Maunder, who daily teaches me computer skills that have been invaluable for my degree, and provided support throughout the emotional rollercoaster that is graduate school.

Table of Contents

List of Figures

List of Tables

List of Symbols and Abbreviations

+: wild type allele

(2R): chromosome 2 right arm

A: Adenine or Alanine depending on context

aa: amino acids

A488: Anti-Rabbit IgG Conjugated-Fluorophore absorbance 488nm

act: actin gene

ash1: *absent, small or homeotic discs 1* gene

AK: Atypical kinases

APE: Conserved Alanine-Proline-Glutamate motif

BAF: Barrier-to-Autointegration Factor

ball: *ballchen* gene, also known as *nhk-1*

BEAUTi: Bayesian Evolutionary Analysis Utility

BEAST: Bayesian Evolutionary Analysis by Sampling Trees

BLAST: Basic Local Alignment Search Tool

bp: base pairs

BSA: bovine serum albumin

bshe: *bshe* gene

C- carboxy, Cytosine or Cysteine depending on context

ºC: degrees Celcius

C-score: confidence score

ci: cubitus interruptus gene

cg: *combgap* gene

CG8878: Computer Generated gene 8878

CK1: Casein Kinase

ck1α: casein kinase 1 α

CSF-1: colony-stimulating factor 1

Cy: *Curly* gene 1

CyO: Curly of Oster chromosome

D: Aspartic acid

Df(2): chromosome 2 deficiency

dH_2O: distilled water

disc: *discs overgrown* gene

dp$^{:}$ *dumpy* gene

D1: D1 chromosomal protein gene

DNA: deoxyribonucleic acid

E: Glutamic acid

e: ebony gene

E1: P{lacW}ci^{E1}

E2: P{lacW}ci^{E2}

ECL: Enhanced Chemoluminescence

eIF2: eukaryotic initiation factor 2

elav: *embryonic lethal abnormal vision* gene

EMS: ethylmethane sulfonate

en: *engrailed* gene

Erk: Extracellular signal-regulated kinase

ey: *eyeless* gene

E(var): Enhancers of variegation

F: Phenylalanine

G: Guanine or Glycine depending on context

g: grams

GFP: Green fluorescent protein

GAL4: yeast transcription activator protein

gish: gilgamesh gene

H: Histidine

H1: histone 1

H3: histone 3

H3.3: Histone 3, variant 3

H3K4: Histone 3, lysine 4 residue

H3K9: Histone 3, lysine 9 residue

HDAC: histone deacetylases

Hh: *Hedgehog* gene

HMM: hidden Markov models

HP1: heterochromatin protein 1

hPEV: heterochromatic Position Effect Variegation

HRP: horse radish peroxidase

Hu: *humeral* allele of *Antennapedia* gene

hsp83: *heat shock protein 83*

H3S10: Histone 3, serine 10 residue

I: Isoleucine

IAL: *Ipll-auora-like* kinase gene

I-TASSER: Iterative Threading Assembly Refinement

K: Lysine

Kb: Kilobase pair

kDa: kiloDaltons

L: liter or Leucine

M: molar or Methionine

MAPK: mitogen-activated protein kinase

MCMC: Baysian Markov chain Monte Carlo

MEK: MAPK/Erk kinase

mg: milligram

ml: millilitres

mM: millimolar

mod (mdg4): modifier of midgut 4 gene

mRNA: messenger RNA

MUSCLE: MUltiple Sequence Comparison by Log-Expectation

µg: micrograms

µl: microliters

N-: amino or Asparagine

neur: neuralized gene

p: phosphate

P: Proline

PBS: phosphate buffered saline

PcG: Polycomb Group

Pci: *P{lacW}ciD*^{plac}

PCR: polymerase chain reaction

PDB: Protein Data Bank

PDGF: Platelet-derived growth factor

PDS: *P* element dependent silencing

PEV: position effect variegation

PH3: Phospho-histone 3 serine 10

PKR: interferon-induced protein kinase

Q: Glutamine

R: Arginine

RAS/MAPK pathway:

RNA: ribonucleic acid

RNAi: ribonucleic acid interference

RpS3A: *Ribosomal protein S3A* gene

S: Sulphur, Synthesis or Serine depending on context

SDS-PAGE: sodium dodecyl sulphate - polyacrylamide gel electrophoresis

SIN: conserved Serine-Isoleucine-Asparagine motif

SMP: skim milk powder

Su(var): Suppressors of variegation

Su(var)205: suppressor of variegation 205 gene

Su(var)3-7: suppressor of variegation 3-7 gene

Su(var)3-9: suppressor of variegation 3-9 gene

SuUR: Supressor of underreplication gene

T: Thymine or Threonine depending on context

TBST: Tris buffered saline with 0.1% Tween 20

TAF4: *TBP-associated factor 4* gene

TM6B: third multiply inverted chromosome 6B

TTBK1: *Tau-tubulin kinase* 1 gene

TTBK2*: tau-tubulin kinase* 2 gene

TK: typical kinases

Trx: *trithorax* gene

TTBK: Tau-Tubulin Kinase

UAS: Upstream Activation Sequence

V: Valine

vasa-IVS3-beta-*geo*: a germline specific reporter construct

vrk-1: vaccinia-related kinase 1 gene

VRK: Vaccinia-Related Kinase

VDRC: Vienna Drosophila Resource Center

WNT pathway: Wingless-related integration site pathway

w^{m4-}:*Inversion (1) white-mottled 4*

w: *white* gene

$w^{--:}$ *white mutant allele*

w^{+}: uniform red eye color phenotype

Y: Tyrosine

y-: yellow mutant allele

1. Chapter 1 - Introduction

An important feature in multicellular organisms is the ability of a cell to develop from a population of stem cells into a differentiated cell, specialized for their tissue type. Each cell, no matter the tissue has the same DNA, and so the individual cells need ways to turn on or off genes to allow only the appropriate compliment of genes to be expressed according to the tissue or specific cell. Genes appropriate for the specific cell also need to be regulated so they are only induced in the necessary conditions, in times of stress for example. There are a variety of ways cells decide to regulate gene expression and silencing, including but not limited to: chromatin structure, transcriptional initiation through activator or repressor proteins, RNA processing and modification, transcript stability, translational initiation, small non-coding RNAs, post-translational modification, and protein transport and stability. The method that I am most interested in is through chromatin structure.

Chromatin is defined as a complex of proteins and DNA that allows the DNA to coil into a tighter secondary structure for packaging and prevention of DNA damage (1). A higher degree of the secondary structure can also allow for control of gene expression. Chromatin is generally categorized into two opposing states: the loosely packaged and transcriptionally active euchromatin, and the tightly packaged and transcriptionally repressed heterochromatin. Further classification of chromatin will be described later. Modification to the histone tails can create areas of euchromatin or heterochromatin, depending on the modification, where genes are transcriptionally active or inactive. Chromatin silencing is most commonly used in tissues that are differentiated to silence genes associated with stem cells, or genes that are not associated with the specific tissue type.

Background

Histone modifications

A DNA polymer is negatively charged, which if left on its own is unable to fold in a way to fit into a cell due to its size and electrostatic repulsion (2). The DNA wrapping around a positively charged protein complex, known as a nucleosome, solves this. Four histone proteins in an octamer form the nucleosome: Histone 2A, 2B, 3 and 4. 147 base pairs (bp) of DNA wrap around each nucleosome 1.67 times, with 20-80 bp of linker

DNA between each nucleosome. Together, the nucleosome and the linker, or region of DNA between two nucleosomes, makes up what is called the 10nm fibre. Histone H1 is a linker protein that works to pull the DNA in a closer conformation, making a 30nm fibre. Further higher order chromatin structures can be formed from there, with 200nm fibres seen in mitotic chromosomes. Chromatin is dynamic and is often not found consistently in any one distinct fibre width (3).

Each histone protein has a globular core, with an exterior N-terminus known as the 'histone tail'. The presence or absence of modifying marks such as acetyl, methyl, ubiquityl or phosphate groups on the histone tails provide heritable marks. These marks will still be in place, maintaining the chromatin in that region following cell division in subsequent daughter cells.

Other proteins will recognize the specific tags on the histone tails and recruit protein complexes to move the nucleosomes into a tighter or looser conformation, to prepare the chromatin for mitosis, or to allow for DNA repair. A well-known example is with heterochromatin protein 1 (HP1). Simply put, euchromatic chromatin is often marked through modifications to histone 3 (H3), specifically an acetyl group on H3K9 and a methyl group on H3K4. When H3K4 methyl group is removed it induces deacetylation at H3K9 and encourages methylation at H3K9. HP1 recognizes methylated H3K9 and when interacting recruits DNA methyltransferases that add methyl groups to the DNA itself, inducing a transcriptionally silent heterochromatic state (4).

Changes to H3K4 and H3K9 are just a few of many histone modifications that can lead to either transcriptionally active or repressive chromatin regions. Table 1.1 summarizes a few of the other modifications known to be involved in chromatin states, and the list is ever growing. Changes that affect cellular traits without directly affecting the DNA sequence are known as epigenetic changes. Studying these secondary modifiers of histones to induce chromatin changes is one aspect of studying epigenetics.

Chromatin types

It is important to first understand the nature of chromatin and the modifications that occur on histones to induce a heterochromatin or euchromatin state.

I previously stated that chromatin is found in two typical states: euchromatin and heterochromatin. Historically, heterochromatin was also broken up into two groups: constitutive and facultative heterochromatin (5). Constitutive heterochromatin was classified as the more structural heterochromatin, such as is found in centromeres to survive the pulling forces of mitosis. It is never seen in a euchromatin form. Facultative heterochromatin are in regions where there are genes, but have been selectively chosen to be silenced using heterochromatin. Facultative is used for gene silencing, and can be more or less permanent depending on the signals received.

The three forms of chromatin described above are helpful for a general understanding of chromatin, they are an older model of chromatin dynamics. Recent studies have shown that there are more separations of different types of chromatin. Within Drosophila there are five different types of chromatin that could possibly be broken down into further sub-categories(6). The five basic types described are named by colours to prevent semantic confusion.

Green and Blue chromatin are types of heterochromatin that have already previously been described. Green looks like classic heterochromatin, with classic markers such as HP1, HP1 interacting proteins, and *Su(var)3-9*. This chromatin looks most similar to the constitutive heterochromatin described previously, found predominantly around the centromere and on the highly heterochromatinized Drosophila 4^{th} chromosome. This type of chromatin is particularly marked by H3K9me2, which is caused by Su(var)3-9 and bound by HP1. Blue chromatin is distinct by being caused by Polycomb Group (PcG) proteins. H3K27me3 is the mark that is caused by PcG proteins are found in regions of Blue heterochromatin. Some proteins are found associated with both Blue and Green heterochromatin, but because they have specific interactions with the distinct proteins in both groups.

Black chromatin is a repressive form of chromatin that covers 48% of the genome with little to no transcriptional activity coming from this region. Black chromatin is universally marked by H1, D1, IAL and SUUR proteins. Black chromatin actively silences genes, instead of just appearing secondarily in regions of low transcriptional activity. It also appears to have the ability to change to other chromatin types to allow expression

of the genes in its region in a tissue specific manner, showing that it likely has a developmental role.

Red and Yellow chromatin are types of euchromatin. These regions have high amounts of transcriptional activity and bound RNA polymerase, along with H3K4me2 and H3K27me3 transcription marks. Yellow chromatin markers are mostly found in regions of typically constitutive genes like ribosomes and DNA repair genes, along with genes that are found in a wide range of developmental tissues. Red chromatin is found in regions of distinctively timed active genes, like transcription factors or signal transduction.

Chromatin types are regional

Heterochromatin gene silencing, when set up in distinct regions, has the ability to spread. The mechanism for the spreading is still not completely known, and there are likely multiple ways that spreading occurs (7). The HP1 example described previously shows one mechanism by which heterochromatin spreading can occur. Once HP1 is bound to the methylated H3K9, it recruits more methyltransferases and deacetylases to nearby nucleosomes and encourages similar marks, causing more HP1 proteins to bind and so on spreading heterochromatin to nearby regions (8,9). What terminates the spreading is also not well understood.

One hypothesis is the factors involved in the spreading of heterochromatin are limited and spreading occurs until the factors are used up (10,11). Another proposed model is that discrete histone marks set up the boundaries of heterochromatin and euchromatin. An example is the protein JIL-1, in which studies suggest that both methods could work in different contexts (12-15). JIL-1 phosphorylates H3S10 in regions of euchromatin. This mark made by JIL-1 is able to suppress the spread of heterchromatinization, particularly blocking Su(var)3-9 from methylating H3K9 (12,15). If the JIL-1 function is lost, heterochromatin can spread, which then depletes available heterochromatinizing factors from the pericentric regions (14).

An example of support of the barrier method is with histone variant H3.3. H3.3 is incorporated into regions that are actively transcribed (16,17). The incorporation of H3.3

acts as a boundary, preventing heterochromatin spreading and maintaining the regions of actively transcribed euchromatin (18).

Maintaining the balance of heterochromatin and euchromatin within each gene, and preventing unnecessary spreading of heterochromatin is essential for proper cellular functions. Mutations in any of these chromatin-modifying genes can upset this balance, and cause improper activation or silencing of genes. Silencing of obvious phenotypes has been used in *Drosophila* for almost a century to learn more about these chromatin modifiers using a phenomenon called position effect variegation.

Position effect variegation

The first studies into the spreading heterochromatin gene silencing started with position effect variegation (PEV) (19). This was done in Drosophila, using the *white* gene. *white* is responsible for the migration of pigment into the ommatidia, causing the red eye normally seen in *Drosophila melanogaster* . When mutated, or silenced, we see a lack of pigment in the eye or a white eye colour. *white* is typically found on the X-chromosome, in a transcriptionally active euchromatic region. Chromosomal rearrangements were discovered where an inversion places the *white* gene near the centromere, and its constitutive heterochromatin. These flies have a variegated eye colour, or in other words, there was some pigment seen in individual ommatidia, but other had a lack of pigment and so were white. This chromosomal rearrangment leading to the variegation is called *white mottled,* and an example is w^{m4} (20). The differences seen in *white* gene expression has to do with the location close to the constitutive heterochromatin and that heterochromatin in causing silencing of the gene in a stochastic manner.

The discovery of w^{m4} provided researchers with a tool for assaying a gene's involvement in the initiation or maintenance of different chromatin states. When a mutation is in a gene involved in these processes, then the stochastic amount of silencing seen changes, to having more or less ommatidia with red pigment. Genes that dominantly cause less red pigment are known as *Enhancers of variegation* (*E(var)*) and genes that dominantly cause more red pigment are known as *Suppressors of variegation* (*Su(var)*). We can also use w^{m4} to track the inheritance of the epigenetic changes that cause the gene silencing.

Two models are provided for the mechanism of PEV, known as the mass action model and nuclear compartmentalization model. The mass action is seen by the *cis*-spreading of heterochromatin across the inversion breakpoint, causing heterochromatin in a typically euchromatin region, in an 'oozing' fashion. This is dosage dependent, and the levels of any specific chromatin modifier can affect the spreading of heterochromatin, through the law of mass action in a stochastic fashion (10).

The second model is the nuclear compartmentalization model. In this the chromosomal rearrangement, or *trans* pairing, could cause a normally euchromatic gene to be found in a portion of the nucleus that doesn't have the transcriptional environment to induce its expression, therefore causing a silencing phenotype. This could result from that location having a lack of appropriate transcription factors, or could be a nuclear compartment that contains only heterochromatin, and so activates heterochromatin of chromatin in the area (21,22).

Su(var) genes include such genes as the histone methyltransferase *Su(var)3-9*, the chromo domain protein HP1 and histone deacetylases like HDAC1 (13). They are generally involved in initiating and maintaining DNA in a heterochromatin state. When these genes are mutant in a variegating system, heterochromatin does not form, or does not spread as normal, so less gene silencing is observed.

E(var) genes include genes like *trithorax*, *trithorax-like*, *ash1*, *additional sex combs*, *mod (mdg4)*. They are all constituents of euchromatin, factors that resist epigenetic silencing, or negative regulators of enzymes involved in heterochromatin formation. When mutant, because these genes can no longer prevent heterochromatin from forming, you see an expansion of heterochromatin and as a result see a more-white eyed phenotype.

<u>*P* elements in *Drosophila*</u>

P elements are a transposon found in *Drosophila melanogaster* (and some other *Drosophila* species). They can be up to 2907 base pairs (bp) long, depending whether it is complete or if internal regions are deleted. Each end has terminal 31-bp inverted repeats (23). *P* elements have only recently invaded the *Drosophila melanogaster* genome through horizontal gene transfer from *Drosophila willistoni* in the last 100 years

(reviewed in (24)). Some laboratory strains of *D. melanogaster* have been collected prior to the *P* element spread, and so do not have them yet (25). These are called M-cytotypes. Wild or more recently developed strains have *P* elements stabilized in their genome are called P-cytotypes.

P elements encode one gene that can be alternatively spliced into either a functional transposase or a repressor protein (26,27). When the 2-3 intron of the mRNA is spliced, a transposase is made. The transposase binds to the *P* element ends and excises the DNA from its location in the chromosome and inserts into another location in the same or different chromosome. When the 2-3 intron is prevented from splicing, the 66kDa repressor protein is made (28).

Splicing of the 2-3 intron, thus making a transposase, only occurs in the germline. In somatic tissues the protein P-element somatic inhibitor (PSI) is made which prevents splicing and allows the repressor protein to be translated (29). In P cytotype flies, PSI is also expressed in low levels in the germ line, allowing sufficient repressor protein to be produced to repress *P* element transposition, and so the *P* elements remain relatively stable (30).

When a P cytotype female is crossed with an M cytotype male, offspring maintain repression and stable P elements. This shows that this repression can also be maternally inherited (30). M cytotypes have no suppression system, because the lack of *P* elements means no repressor protein is produced. When an M cytotype female is crossed with a P cytotype male, there is no maternally deposited repressor protein and so PSI, the splice blocking protein, is overwhelmed (30). This causes excessive production of transposase, and excessive P element transposition. This leads to a syndrome called hybrid dysgenesis, which causes sterility, elevated rates of mutation and chromosome rearrangement (31).

<u>*P* element Dependent Silencing (PDS)</u>

The *P* element enhancer trap of *cubitus interruptus* (*ci*) with a mini-white transgene has a similar silencing phenotype as those seen in PEV (32). This *P* element is *P{lacW}ciD*^{plac} (here on known as *Pci*) and is found on chromosome 4 between *Ribosomal protein S3A* (*RpS3A*) and *ci* (32). Variegation in the eye is seen, similar to

PEV when in a w^- background and a P-cytotype (33). This silencing is location specific due to nearby heterochromatinization centre, and only silences the w^+ mini transgene (33,34).

In M cytotype flies with *Pci* there is no variegation and the red pigment is expressed uniformly. In P cytotype flies or flies with KP elements variegation occurs in the eye. KP elements are P-elements missing approximately 60% of its sequence (35). This form of silencing became known as P element Dependent Silencing (PDS). The silencing is caused in a presumably similar mechanism as PEV, through heterochromatin spreading. Support for this is seen in the P cytotype transcriptional repression of germ line hsp83 or *vasa*-IVS3-beta-*geo* reporter transgenes (36). Neither of these contain *P* element repressor binding sites, suggesting that this transcriptional repression could occurs through chromatin silencing (36). *Pci* and another w^+ insert *P{hsp26-pt-T}ci*$^{2M1021.R}$, which is inserted nearby, are so far the only visually noticeable examples of PDS to date. Insertions of the same *P* element construct in different parts of the genome, and chromosomal translocations of *Pci* in chromosome 4 show no such variegation (34). *Pci* also responds to *Su(var) 205* and *Su(var 3-7)* in the same manner as w^{m4}, but not *Su(var)3-9* .(34). *Su(var) 205*$^+$, *Su(var)3-7*$^+$ and *Su(var)3-9*$^+$ are all involved in constitutive heterochromatin in telomeres and centromeres, or Green chromatin as described earlier. PDS is based upon spreading of heterochromatin on the fourth chromosome, where *Pci* is located. The fourth chromosome is extensively heterochromatinized. *Su(var)3-9*$^+$ has roles specifically in centromeric heterochromatin, but is not often found at other regions of heterochromatin, like those found on the fourth chromosome (37). *Su(var)205* and *Su(var)3-7* on the other hand have broader roles in heterochromatin gene silencing, and so mutations in those will affect the *Pci* locus.

Because of *Pci*'s proximity to *ci, Pci* should also be sensitive to the proteins that regulate *ci*. The CI protein is a zinc finger transcription factor required for anterior-posterior boundary formation in embryos and imaginal discs, as a part of the *Hedgehog* (*Hh*) pathway. *Ci* is found in the anterior and *engrailed* (*en*) in the posterior compartment(38).

Pci is useful in studying factors of heterochromatin maintenance, studying the interactions with the P-cytotype, and learning the interactions and regulation of the *ci* locus. Chromosome 4 is has extensive heterochromatin, and so provides a great system to study more suppressors and enhancers.

E1 and E2

While studying PDS at *Pci*, two spontaneous mutants, *P{lacW}*^{ciE1} (referred to as *E1*) and *P{lacW}*^{ciE2} (referred to as *E2*) were found that showed the variegated eye phenotype, rather than the typical uniform reddish eye colour found in M cytotype flies. *E1* and *E2* each have a gypsy element insertion 1 kb upstream from *Pci*, in opposite orientations 547 base pairs apart. Analysis of known suppressors and enhancers show that the variegation seen in *E1* and *E2* is not a result of gypsy insulator activity (34).

When heterozygous with the *Pci* allele, both *E1* and *E2* trans-silenced w^+ expression of *Pci*. However, when these two chromosomes are prevented from pairing, such as with a translocation (with the exception of one, where the effect was weaker) this trans-silencing is inhibited. Therefore either nuclear position or pairing with the *Pci* contributes to the *trans*-silencing (34).

E1 and *E2*'s variegation has a similar mechanism of PDS as *Pci* in a P-cytotype background. The same modifiers as PEV and PDS modify *E1* and *E2*. The variegation without the P-cytotype allows for easier screening of enhancers or suppressors than just *Pci* alone.

E(var) Genetic Screen

*E(var)*s loci are underrepresented in the collection of modifiers of PEV, so by using the *E1* variegation system in a forward genetic screen it would help identify overlooked *E(var)* genes.

A former member of the lab, Allen McCracken, was looking for *E(var)* mutants in PDS. He did this through EMS mutagenization of *E1* homozygous males, looking for an enhancer eye phenotype of increased white silenced cells. Many *E(var)* mutations were recovered that were also recessive lethal. These mutations were put into recessive lethal complementation groups (assuming the *E(var)* and recessive lethal phenotypes were due to the same lesion) and mapped to their specific loci. Where possible,

complementation tests were done against extant alleles of candidate genes to confirm/refute the allelism. The mutant alleles were sequenced to confirm the mutant lesion, and the extant mutant alleles had pigment analysis to confirm a similar PDS phenotype. Around 44 000 flies were screened, and 58 of those were recessive lethal *E(var)*. Those mutants fell into 8 complementation groups, which included *absent, small or homeotic discs 1* (*ash1*), *trithorax* (*trx*), *TBP-associated factor 4* (*Taf4*), *combgap* (*cg*), *CG8878* and 3 unmapped groups. *ash1* and *trx* are histone lysine methyltransferases, and *Taf4* and *cg* are transcription factors.

At that time *CG8878* had not been studied previously, but according to predicted amino acid sequence domains it is a serine-threonine kinase. The investigation of the *CG8878* gene is the subject of this thesis.

Trx, *ash1*, and *cg* have all previously been shown to act at the *ci* locus, though all also showed PEV with w^{m4} as well (39).

Rational for the research

After finding *CG8878* in his screen, Allen McCracken briefly explored it during his PhD in the lab. *CG8878* at the time had not been studied before, and all that was known about it was that it showed an *E(var)* phenotype in this screen with E1. Thus, it likely has either a direct or indirect role in chromatin. Since the dominant mutant caused an enhancer phenotype (a spread of heterochromatin silencing), then the molecular role of CG8878 may involve maintaining a euchromatin state and/or maintaining the heterochromatin/euchromatin boundaries. Further studies have shown *CG8878* to be a suitable candidate for continuing research to broaden the understanding of chromatin modification.

<u>*CG8878* variegation</u>

Quantification of eye pigment variegation in *CG8878* mutant heterozygotes identified it as an *E(var).* Using *E1* both male and female *CG8878* mutant heterozygotes went from a variegated eye to near white, in every mutant allele (40). As confirmation that this was a PDS modifier, enhancement of variegation was also seen in flies with *Pci*, in a P-cytotype background (40). Enhancement of variegation was also seen in w^{m4} flies, identifying *CG8878* also as a modifier of PEV (40).

CG8878 gene and protein features

The first interesting feature of the *CG8878* gene is that its entire transcript is found within the intron of another gene: *hen1*. (Figure 1.1) It was determined that the *E(var)* mutant phenotype is caused by *CG8878* and not *hen1*. This is based on *hen1* not being a recessive lethal gene, and all *CG8878* alleles (as defined by failure to complement) isolated in the screen had lesions within the annotated *CG8878* transcript, and are all found within the intron of *hen1*. *Hen1*'s role is in processing *Piwi* interacting RNAs, which silence invading transposable elements (41,42). If *hen1* was responsible for the silencing of the w^+ transgene through PIWI, then enhanced silencing should also occur in the same *P* element construct inserted in another location, and no enhanced silencing would be seen in the w^{m4}. This observation does not occur, as no silencing is seen with *P* elements in different locations, and there is enhancement of silencing with w^{m4}. This all suggests that the mutations within *CG8878* is the source of *E(var)* phenotype.

Initial observations of the CG8878 amino acid sequence predict it to have a kinase domain. But upon a more detailed inspection, the kinase domain is not continuous, but has a large interruption in the middle (Figure 1.2)(40). Since *CG8878* has not been studied previously, there is no evidence whether this kinase domain is still functional, or if the interruption removes that function. Additional domains found within the CG8878 protein are three regions that have a high frequency of acidic amino acids. One is within the interrupted region of the kinase domain; while the other two are in the C-terminus of the protein. Acidic domains are occasionally associated with transcriptional activation (43).

CG8878 has a homolog in *Drosophila* known both as *ballchen* and *nhk-1*. Here after, I will be referring to it as *ballchen* (*ball*). *ballchen* is an essential gene, known to histone H2A (44). Mutants in *ballchen* show both developmental mitotic defects and meiotic fertility problems (45-49). The human homolog of *ball* is *vrk-1*, which has a variety of roles ranging from cell cycle regulation, chromatin condensation, golgi fragmentation and DNA damage response (50-53). *ballchen*'s role in histone phosphorylation provides support for *CG8878* acting in a similar manner and thus might be involved in chromatin modification. Initial queries into other species with *CG8878* homologs show that it is found in other species in the order Diptera, including all other

Drosophila and mosquitos, as well as in the Lepidopteran species *Bombyx mori*, the silkworm moth (40). Further detail was not sought at that time, but will constitute Chapter 3 of this thesis.

Characterization of *banshee* (*CG8878*)

This thesis describes the characterization of *CG8878*, which I have named *banshee* (*bshe*), as I will refer to here after. Scottish/Irish banshees are known for washing the blood from clothing before a person dies. Because the screen identifying *banshee* was looking for lethal *E(var)* mutants, or mutants that causes the eye to be less red and more white, I thought this name would be appropriate.

At the beginning of my research, no information of possible roles of *bshe* had been published. Since then, a couple articles have described screens in which *bshe* (referenced in all as *CG8878*) has been found. BSHE has been shown to be involved in the MAPK/ERK pathway, as well as the WNT pathway (54,55). *bshe* is was found in the MAPK/ERK pathway through a genome-wide RNAi screen in *Drosophila* S2 cells, looking for modulation of phosphorylated MAPK. In the RAS/MAPK pathway it is a positive regulator of RAS signaling, and epistasis has shown it to act downstream of RAF and upstream of MEK in the pathway (54). In the WNT pathway, it is identified as a positive WNT pathway regulator that functions downstream of the ligand-receptor interaction in cells receiving the signal, but is doesn't involve Notch (55).

Since *bshe* mutations are recessive lethal, it must have an essential function within Drosophila. A role as a chromatin modifier would be a good candidate. I more fully characterized the relatedness of *bshe* to other proteins, finding that it is an insect specific gene that is, along with *ball*, either an older class of gene or is under high evolutionary pressure. I went on to attempt to quantify which stage in development is lethal and characterize any mutant phenotypes. I lastly began optimization of antibodies against the *bshe* protein, which would in the future be used for protein analysis.

Summary of Research

Phylogenetics and Bioinformatics of the BSHE protein

A phylogenetic tree was built based on the most conserved sequences of similar proteins found in the Phylum Arthropoda. *bshe* and five other main groups of the known

Casein Kinase 1 (CK1) family were found as the most similar proteins: *ballchen*, *asator*, *casein kinase 1α*, *gilgamesh*, and *discs overgrown*. Based upon *bshe* being present in all the insect species observed, but not found in other Arthropoda subphylum, *bshe* is predicted to be an insect specific protein. The most similar kinase domain to *bshe* is *ball.* Both *bshe* and *ball* form the most ancient clade in the phylogenetic tree based upon the branch lengths. This could be due to the origin of the clade occurring earlier than the other CK1 family members, or that it is under greater selective pressures. All other BSHE proteins have an insert within the kinase domain, but the size and sequence is not consistent or conserved.

The predicted protein structure of BSHE shows the potential for a functioning kinase domain. The inserted region, described previously, loops away from the catalytic domains, allowing them to rest in what appears to be a functional conformation. This would predict that, despite the large interruption within the kinase domain, it still would be able to have functioning kinase activity. Future research should next experimentally determine kinase function.

Analysis of *bshe* mutants

Understanding the timing and appearance of the lethal mutants can aid in understanding more about *bshe*'s function. Through observing hemizygous mutants I observed conflicting results on the stage of lethality, either embryonic or mid-larval stage. This conflict occurred depending on whether the parents were deletion or mutant. Therefore it appears to be a maternal affect that is a cause of early lethality.

RNAi knockdowns were done using a GAL4-UAS system. Some neural drivers show mild bristle defects. Eye drivers show mild to severe eye degeneration. Ubiquitous GAL4 drivers have pupal lethality. The penetrance is variable based upon which UAS inverted repeat transgene construct is used. Results indicate that *bshe* does have roles that are essential for survival in those cells. Certain RNAi knockdowns may be useful in future experiments to further explore BSHE's function.

Optimization of BSHE specific antibodies

Three antibodies were designed for three different peptides of BSHE. These antibodies were chosen for optimization of Western blots and immunofluorescence with

the goal of understanding more of BSHE's function based upon its intracellular localization. Also, antibodies would be useful for future purification of BSHE and other experimental assays.

In the Western blots each antibody produces bands in the approximate expected size of BSHE, which is approximately 114kDa. Many smaller background bands are also present in the Western blots. At this time, controls have not been completed to confirm whether the bands at 114kDa are the BSHE protein or not.

Immunofluorescence results for one antibody show that BSHE has cytoplasmic localization in the early embryo. No specific localization changes are noticed based upon the stages of the cell cycle. Negative controls appear to confirm that the antibody is specific to BSHE. Additional test are required in order to confirm that the negative controls are true protein nulls.

Figures and Tables

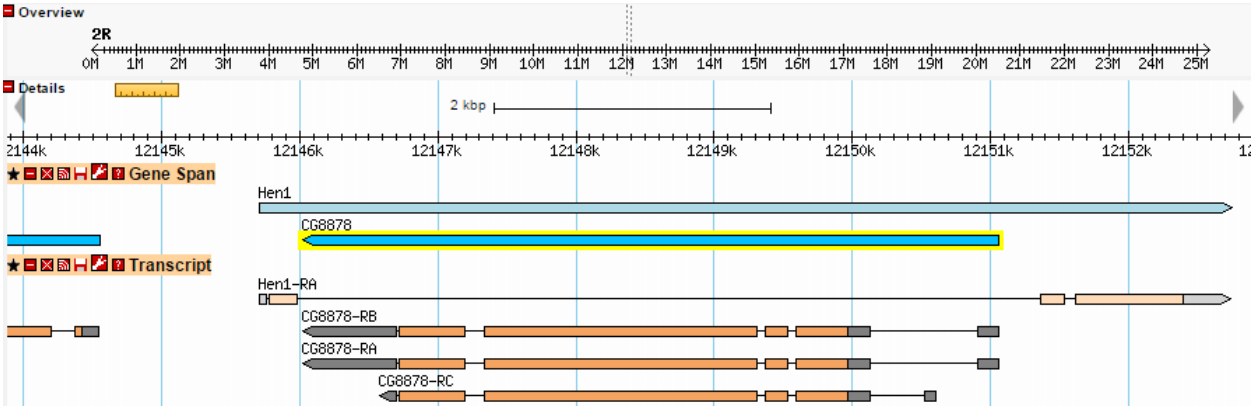

Figure 1.1. Location and transcript of *bshe* (*CG8878*) and *hen1*. The entire *bshe* transcript is found entirely within the second intron of *hen1*. Transcription of *bshe* is in the opposite orientation of *hen1*. Image is taken from GBrowse on flybase.org, 2015.

Figure 1.2. Location of *bshe* mutations. Seven independent mutations were recovered from a genetic screen for Enhancers of *Pci* previously done in our lab. Two recovered mutants had the same mutagenic lesions as two other mutations, making five unique mutations. The five mutations separate into four with premature stop codons (3a22a and 3a97a had the same change) and one pair (3a90a and 4a7a) with a four base pair deletion in the enhancer box (E-box) of the promoter region. The purple sections show where the interrupted kinase domain is.

Table 1.1. Select summary of transcriptionally active and transcriptionally repressive histone marks. These are listed by mark, the amino acid letter code, and the amino acid sequence position. This table is not meant to be inclusive of every mark known to cause chromatin-based activation or silencing, and is not meant to be encompassing of all or any one species. Table compiled from information in the following reviews (6,56-58).

Histone	**Transcriptionally Active Marks**	**Transcriptionally Repressive Marks**
Histone 2A		Phospho-S10
Histone 2B		
Histone 3	Methyl-K4, Acetyl-K9, Phospho-S10, Acetyl-K14, Methyl-K36, Methyl-K79	Methyl-K9, Methyl-K27
Histone 4	Methyl-R3, Acetyl-K5	Acetyl-K12

References

1. Takata H, Hanafusa T, Mori T, Shimura M, Iida Y, Ishikawa K, et al. Chromatin compaction protects genomic DNA from radiation damage. PLoS ONE. 2013;8(10):e75622.

2. Bloomfield VA. DNA condensation. Curr Opin Struct Biol. 1996 Jun;6(3):334–41.

3. Maeshima K, Imai R, Tamura S, Nozaki T. Chromatin as dynamic 10-nm fibers. Chromosoma. 2014 Jun;123(3):225–37.

4. Bártová E, Krejcí J, Harnicarová A, Galiová G, Kozubek S. Histone modifications and nuclear architecture: a review. J Histochem Cytochem. 2008 Aug;56(8):711–21.

5. Trojer P, Reinberg D. Facultative heterochromatin: is there a distinctive molecular signature? Mol Cell. 2007 Oct 12;28(1):1–13.

6. Filion GJ, van Bemmel JG, Braunschweig U, Talhout W, Kind J, Ward LD, et al. Systematic protein location mapping reveals five principal chromatin types in Drosophila cells. Cell. 2010 Oct 15;143(2):212–24.

7. Talbert PB, Henikoff S. Spreading of silent chromatin: inaction at a distance. Nat Rev Genet. 2006 Oct;7(10):793–803.

8. Schotta G, Ebert A, Reuter G. SU(VAR)3-9 is a conserved key function in heterochromatic gene silencing. Genetica. 2003 Mar;117(2-3):149–58.

9. Grewal SIS, Elgin SCR. Heterochromatin: new possibilities for the inheritance of structure. Curr Opin Genet Dev. 2002 Apr;12(2):178–87.

10. Locke J, Kotarski MA, Tartof KD. Dosage-dependent modifiers of position effect variegation in Drosophila and a mass action model that explains their effect. Genetics. 1988 Sep;120(1):181–98.

11. Zuckerkandl E. A possible role of "inert" heterochromatin in cell differentiation. Action of and competition for “locking” molecules. Biochimie. 1974;56(6-7):937–54.

12. Bao X, Deng H, Johansen J, Girton J, Johansen KM. Loss-of-function alleles of the JIL-1 histone H3S10 kinase enhance position-effect variegation at pericentric sites in Drosophila heterochromatin. Genetics. 2007 Jun;176(2):1355–8.

13. Ebert A, Schotta G, Lein S, Kubicek S, Krauss V, Jenuwein T, et al. Su(var) genes regulate the balance between euchromatin and heterochromatin in Drosophila. Genes Dev. 2004 Dec 1;18(23):2973–83.

14. Lerach S, Zhang W, Bao X, Deng H, Girton J, Johansen J, et al. Loss-of-function alleles of the JIL-1 kinase are strong suppressors of position effect variegation of the wm4 allele in Drosophila. Genetics. 2006 Aug;173(4):2403–6.

15. Zhang W, Deng H, Bao X, Lerach S, Girton J, Johansen J, et al. The JIL-1 histone H3S10 kinase regulates dimethyl H3K9 modifications and heterochromatic spreading in Drosophila. Development. 2006 Jan;133(2):229–35.

16. Ahmad K, Henikoff S. The histone variant H3.3 marks active chromatin by replication-independent nucleosome assembly. Mol Cell. 2002 Jun;9(6):1191–200.

17. Schwartz BE, Ahmad K. Transcriptional activation triggers deposition and removal of the histone variant H3.3. Genes Dev. 2005 Apr 1;19(7):804–14.

18. Nakayama T, Nishioka K, Dong Y-X, Shimojima T, Hirose S. Drosophila GAGA factor directs histone H3.3 replacement that prevents the heterochromatin spreading. Genes Dev. 2007 Mar 1;21(5):552–61.

19. Girton JR, Johansen KM. Chromatin structure and the regulation of gene expression: the lessons of PEV in Drosophila. Adv Genet. 2008;61:1–43.

20. Muller HJ. Types of visible variations induced by X-rays inDrosophila. Journ of Gen. 1930 Jul;22(3):299–334.

21. Csink AK, Bounoutas A, Griffith ML, Sabl JF, Sage BT. Differential gene silencing by trans-heterochromatin in Drosophila melanogaster. Genetics. 2002 Jan;160(1):257–69.

22. Dernburg AF, Broman KW, Fung JC, Marshall WF, Philips J, Agard DA, et al. Perturbation of nuclear architecture by long-distance chromosome interactions. Cell. 1996 May 31;85(5):745–59.

23. O'Hare K, Rubin GM. Structures of P transposable elements and their sites of insertion and excision in the Drosophila melanogaster genome. Cell. 1983.

24. Engels WR. The origin of P elements inDrosophila melanogaster. Bioessays. 1992 Oct;14(10):681–6.

25. Kidwell MG, Frydryk T, Novy JB. The hybrid dysgenesis potential of Drosophila melanogaster strains of diverse temporal and geographical natural origins. Drosoph. Inf. Serv; 1983. 7 p.

26. Rio DC. Molecular mechanisms regulating Drosophila P element transposition. Annual review of genetics. 1990.

27. Misra S, Rio DC. Cytotype control of Drosophila P element transposition: The 66 kd protein is a repressor of transposase activity. Cell. 1990.

28. Gloor GB, Preston CR, Johnson-Schlitz DM, Nassif NA, Phillis RW, Benz WK, et al. Type I repressors of P element mobility. Genetics. 1993 Sep;135(1):81–95.

29. Siebel CW, Rio DC. Regulated splicing of the Drosophila P transposable element

third intron in vitro: somatic repression. Science. 1990 Jun 8;248(4960):1200–8.

30. Lemaitre B, Ronsseray S, Coen D. Maternal repression of the P element promoter in the germline of Drosophila melanogaster: a model for the P cytotype. Genetics. 1993 Sep;135(1):149–60.

31. Kidwell MG, Kidwell JF, Sved JA. Hybrid Dysgenesis In Drosophila Melanogaster: A Syndrome Of Aberrant Traits Including Mutation, Sterility And Male Recombination. Genetics. 1977.

32. Eaton S, Kornberg TB. Repression of ci-D in posterior compartments of Drosophila by engrailed. Genes Dev. 1990.

33. Sameny A, Locke J. The P-element-induced silencing effect of KP transposons is dose dependent in Drosophila melanogaster. Genome. 2011 Sep;54(9):752–62.

34. Bushey D, Locke J. Mutations in Su (var) 205 and Su (var) 3-7 suppress P-element-dependent silencing in Drosophila melanogaster. Genetics. Genetics Soc America; 2004;168(3):1395–411.

35. Black DM, Jackson MS, Kidwell MG, Dover GA. KP elements repress P-induced hybrid dysgenesis in Drosophila melanogaster. EMBO J. 1987 Dec 20;6(13):4125–35.

36. Roche SE, Rio DC. Trans-silencing by P elements inserted in subtelomeric heterochromatin involves the Drosophila Polycomb group gene, Enhancer of zeste. Genetics. 1998 Aug;149(4):1839–55.

37. Schotta G. Central role of Drosophila SU(VAR)3-9 in histone H3-K9 methylation and heterochromatic gene silencing. EMBO J. Nature Publishing Group; 2002 Mar 1;21(5):1121–31.

38. Motzny CK, Holmgren R. The Drosophila cubitus interruptus protein and its role in the wingless and hedgehog signal transduction pathways. Mech Dev. 1995 Jul;52(1):137–50.

39. McCracken A. Modifiers of P-element-dependent silencing in Drosophila melanogaster. Locke J, editor. [Edmonton]: University of Alberta; 2012.

40. McCracken A, Locke J. Mutations in CG8878, a novel putative protein kinase, enhance P element dependent silencing (PDS) and position effect variegation (PEV) in Drosophila melanogaster. PLoS ONE. 2014;9(3):e71695.

41. Horwich MD, Li C, Matranga C, Vagin V, Farley G, Wang P, et al. The Drosophila RNA methyltransferase, DmHen1, modifies germline piRNAs and single-stranded siRNAs in RISC. Curr Biol. 2007 Jul 17;17(14):1265–72.

42. Saito K, Nishida KM, Mori T, Kawamura Y, Miyoshi K, Nagami T, et al. Specific

association of Piwi with rasiRNAs derived from retrotransposon and heterochromatic regions in the Drosophila genome. Genes Dev. 2006 Aug 15;20(16):2214–22.

43. Melcher K. The strength of acidic activation domains correlates with their affinity for both transcriptional and non-transcriptional proteins. J Mol Biol. 2000 Sep 1;301(5):1097–112.

44. Aihara H, Nakagawa T, Yasui K, Ohta T, Hirose S, Dhomae N, et al. Nucleosomal histone kinase-1 phosphorylates H2A Thr 119 during mitosis in the early Drosophila embryo. Genes Dev. 2004 Apr 15;18(8):877–88.

45. Cullen CF. The conserved kinase NHK-1 is essential for mitotic progression and unifying acentrosomal meiotic spindles in Drosophila melanogaster. J Cell Biol. 2005 Nov 14;171(4):593–602.

46. Lancaster OM, Cullen CF, Ohkura H. NHK-1 phosphorylates BAF to allow karyosome formation in the Drosophila oocyte nucleus. J Cell Biol. Rockefeller Univ Press; 2007;179(5):817–24.

47. Lancaster OM, Breuer M, Cullen CF, Ito T, Ohkura H. The Meiotic Recombination Checkpoint Suppresses NHK-1 Kinase to Prevent Reorganisation of the Oocyte Nucleus in Drosophila. PLoS Genet. Public Library of Science; 2010 Oct 28;6(10):e1001179.

48. Herzig B, Yakulov TA, Klinge K, Günesdogan U, Jäckle H, Herzig A. Bällchen is required for self-renewal of germline stem cells in Drosophila melanogaster. Biol Open. 2014 May 29.

49. Yakulov T, Günesdogan U, Jäckle H, Herzig A. Bällchen participates in proliferation control and prevents the differentiation of Drosophila melanogaster neuronal stem cells. Biol Open. 2014;3(10):881–6.

50. Sanz-Garcia M, Lopez-Sanchez I, Lazo PA. Proteomics Identification of Nuclear Ran GTPase as an Inhibitor of Human VRK1 and VRK2 (Vaccinia-related Kinase) Activities. Mol Cell Proteomics. 2008 Nov 6;7(11):2199–214.

51. Kang T-H, Park D-Y, Choi YH, Kim K-J, Yoon HS, Kim K-T. Mitotic Histone H3 Phosphorylation by Vaccinia-Related Kinase 1 in Mammalian Cells. Mol Cell Biol. 2007.

52. Lopez-Sanchez I, Sanz-Garcia M, Lazo PA. Plk3 Interacts with and Specifically Phosphorylates VRK1 in Ser342, a Downstream Target in a Pathway That Induces Golgi Fragmentation. Mol Cell Biol. 2009 Feb 11;29(5):1189–201.

53. Valbuena A, Castro-Obregón S, Lazo PA. Downregulation of VRK1 by p53 in Response to DNA Damage Is Mediated by the Autophagic Pathway. PLoS ONE. Public Library of Science; 2011 Feb 28;6(2):e17320.

54. Ashton-Beaucage D, Udell CM, Gendron P, Sahmi M, Lefrançois M, Baril C, et al. A Functional Screen Reveals an Extensive Layer of Transcriptional and Splicing Control Underlying RAS/MAPK Signaling in Drosophila. PLoS Biol. Public Library of Science; 2014;12(3):e1001809.

55. Swarup S, Pradhan-Sundd T, Verheyen EM. Genome-wide identification of phospho-regulators of Wnt signaling in Drosophila. Development. 2015 Apr 15;142(8):1502–15.

56. Grant PA. A tale of histone modifications. Genome Biol. 2001;2(4):REVIEWS0003.

57. Goll MG, Bestor TH. Histone modification and replacement in chromatin activation. Genes Dev. 2002 Jul 15;16(14):1739–42.

58. Jenuwein T, Allis CD. Translating the histone code. Science. 2001 Aug 10;293(5532):1074–80.

2. Chapter 2: Materials and Methods

Drosophila stocks and mutations

Drosophila melanogaster stocks were maintained at room temperature (21ºC) on standard yeast/cornmeal medium. Embryo collection cages were grown at 25ºC on grape juice agar plates, apple juice agar plates, or standard yeast/cornmeal medium as required. Stocks acquired from Bloomington Stock Center or the Vienna *Drosophila* Resource Center are listed in Table 2.1

Mutant stocks for *bshe* were isolated from a EMS mutagenic screen done by Allen McCracken (1). Mutagenesis used $w^-; dp^-; e^-; P\{lacW\}ci^{DplacE1}$ males treated with 25 mM EMS (2) mated to $y^- w^-; +/+$ virgin females and screened for a dominant enhanced eye colour phenotype in the progeny. Putative mutants were mated to $w^-; dp^-; e^-; P\{lacW\}ci^{Dplac}$ flies to confirm transmission and segregation and to determine chromosomal location. Mutant *CG8878* alleles were kept as balanced stocks with *CyO*.Certain stocks were modified by changing a *CyO* balancer to a *CyO P{act-gfp}* balancer, described in Table 2.1

Bioinformatics

All programs used for bioinformatics, and their purposes are summarized in Table 2.2.

Sequence Retrieval

Basic Local Alignment Search Tool (BLAST) version 2.2.28 online software was initially used to assemble CG8878 protein homologs within Dipterans. A HMMER profile was created from one half of the split kinase domain of those alignments (3). HMMER 3.0 software was then used to search Genbank, and to retrieve all sequences with an e-value of $9.9e^{-20}$ or lower. From this list, records were removed that weren't Insecta, and the deer tick (*Ixodes scapularis)* and the western predatory orchard mite (*Metaseiulus occidentalis)* were retained as outgroups. All sequence retrieval occurred between June 10, 2013 and July 23, 2013.

Alignment and Tree Building

Assembled amino-acid sequences were first aligned with the program MUltiple Sequence Comparison by Log-Expectation (MUSCLE) (4). All *Drosophila* species

except *D. melanogaster* and *D. virilis* were removed for simplicity. Other sequences detailed in Table 2.3 were removed because they were incomplete or incorrectly called sequences that failed to align as expected for a homolog sequence. Sequence gaps of more than 10% in the alignment were removed using GBLOCKS. This amino acid sequence alignment was reverse translated using TranslatorX comparing to the known DNA sequence for those protein sequences.

Bayesian Evolutionary Analysis Utility (BEAUTi) and Bayesian Evolutionary Analysis by Sampling Trees (BEAST) programs were used to assemble a Max Sum Clade Credibility over time tree. This was based on every 1000th tree of the last 50 million trees in a 100 million tree run. The Yang model for nucleotide sequence evolution was used (5).

FigTree was used to visualize the phylogenetic tree.

Molecular modeling

3D structure was predicted using the Iterative Threading Assembly Refinement (I-TASSER) program (6,7). Model was analyzed using Swiss PDB viewer (8).

jDotter

jDotter (9) was used to compare sequence similarity with proteins through the use of dot plots. Individual dot plots had different plot sizes defined in the figure legends. Otherwise all were set to maximum plot size of 1000 bases/pixel and sliding window size for new plots of 50. Grey map tool: 0, 20. Scoring Matrix: BLOSUM62.

Mutant phenotype

RNAi

UAS-bshe and *UAS-ball* inverted repeat transgenes were tested against a variety of GAL4 drivers (listed in Table 2.1) and scored against the balancer chromosomes to observe any aberrant phenotype. Crosses were done at room temperature (21ºC).

Homozygous mutant survival collections

Males of a mutant strain were crossed to females of the same mutant strain in vials with standard yeast cornmeal media. The strains used were *3a52a/CyO-P{act-GFP}*, *3a66a/CyO-P{act-GFP}* and *3a90a/CyO-P{act-GFP}*. After allowing to lay for 3-5 days, adult parents were removed. The media was collected and mixed in a 15% sucrose

solution. Floating larvae were collected from the top and washed with water. Larvae were scored with a fluorescent dissecting microscope for presence or absence of GFP, indicating whether it was homozygous mutant or not.

Mutant larvae lifespan

Lifespan of mutant larvae were assessed using two methods.

Method 1:

Male *3a52a/CyO-P{act-GFP}* and female *Df(2R)BSC699/CyO-P{act-GFP}* flies were crossed in an embryo collection cage on standard yeast/cornmeal medium plates at 25ºC. Plates were switched out multiple times to normalize egg laying. After a 4 hour egg lay, plates were removed and grown at 25ºC for 23 hours from start of egg lay. Any hatched larvae were removed from plates, and then waited another hour. All larvae collected after this point were considered to be the same age within an hour. Larvae were assessed for presence of GFP (control - *Df(2R) or 3a52a/ CyO-P{act-GFP})* or absence of GFP (mutant - *Df(2R)/3a52a*) using the fluorescent dissecting microscope (Dr. Ted Allison's lab), and photographs were taken for length measurement. Larvae were individually placed on their own yeast/cornmeal medium plates and grown at 25ºC. Media was wetted with drops of water if they appeared to be drying out. They were imaged every 12 hours for measurement purposes and their condition, activity (eating, crawling or sickly) and their larval stage were recorded. In order to photograph them, active larvae were gently removed from media with a wet, unfrayed, paintbrush and placed on a chilled glass slide. The cold slide briefly immobilized them in time to take the photograph, and then they were transferred back to media and watched to make sure they recovered. Larvae that were sickly were not removed from plate, but instead imaged directly on their media plate. Experiment continued till larvae pupated or died.

Method 2:

Female *3a52a/CyO-P{act-GFP}* or *3a66a/CyO-P{act-GFP}* and male *Df(2R)BSC699/CyO-P{act-GFP}* were crossed, and embryo cages were set up with yeast/cornmeal medium plates in a similar manner to Method 1. Flies were allowed to lay on the plates for between 8 and 14 hours. Then plates were removed and grown at 25ºC for a set time. Multiple plates were set up, so larvae would be represented from all

time points from hatching to 125 hours old. Then larvae were collected from plates by immersing media in 15% sucrose solution and agitating for 20 mins. Larvae were then collected from the surface of the solution, rinsed in water and scored for either presence or absence of GFP and larval stage.

Antibodies for Western and Immunofluorescence assays.

Table 2.4 summarizes antibodies used. Antibodies were designed for the N- or C-terminus of BSHE. They have been used in optimization experiments for Western blots and immunofluorescence assays.

Primary antibodies

Three primary antibodies were designed for BSHE. One antibody was created for a unique peptide sequence in the N-terminus (Antibody 1 peptide sequence: MGKRLQLERPTTDRC), and two peptide sequences were designed for the C-terminus (Peptide sequences, Antibody 2: CRGRPKGTSRKQTTS. Antibody 3: CATGEGERKLKSGRT). Peptide regions were chosen using GenScript's proprietary software OptimumAntigen Design Tool. The peptides are all in regions that have a high likelihood of being accessible and unique.

Three antibody preparations were created for BSHE and were obtained from GenScript in Piscataway, New Jersey, USA. These antibodies were affinity purified by GenScript. They were shipped at 4°C, aliquoted into 30µL samples and stored at -20°C in the 1x PBS, 0.02% Sodium Azide, pH 7.4 solution they came in. Upon use, antibodies were defrosted, diluted from 0.1-1.0µg/mL and stored in a blocking buffer solution (5% BSA/Skim Milk Powder, 0.02% Sodium Azide, 1x TBS/PBS, 0.1% Tween 20) at 4°C up to one month.

A β-Tubulin primary antibody was used for a loading control during Western Blot Analysis. This was obtained from Dr. Shelagh Campbell's Lab**.**

Antibodies were defrosted, diluted from 0.1-1µg/mL and stored in a blocking buffer solution (5% Skim Milk Powder, 1x TBS (β-Tubulin), 0.1% Tween 20, 0.02% Sodium Azide) at 4°C for up to one month.

A Phospho-histone 3 serine 10 (PH3) antibody was used for our positive control for our immunofluorescence assay that was obtained from Dr.Shelagh Campbell's Lab.

These antibodies were stored at -20°C. Upon use, antibodies were defrosted, diluted from 0.1-200µg/mL, and stored in a blocking buffer solution (5% Skim Milk Powder, 1x PBS (PH3), 0.1% Tween 20, 0.02% Sodium Azide) at 4°C for up to one month.

All primary antibodies were stored and reused after probing, up to six uses.

Secondary Antibodies

For Western blot analysis two secondary antibodies were used. The Goat Anti-Rabbit IgG HRP-linked secondary antibody was obtained from Cell Signaling Technology in Danvers, Massachusetts, USA. The Sheep Anti-Mouse IgG HRP-linked secondary antibody was obtained from GE Healthcare in Buckinghamshire, UK. These antibodies were diluted from 0.04-1.0µg/mL and stored at 4°C in a blocking buffer solution (5% Skim Milk Powder, 1x TBS, 0.1% Tween 20) for up to one month.

The Anti-Rabbit IgG Conjugated-Fluorophore (A488) secondary antibody was obtained from Dr. Shelagh Campbell's Lab and was used as a secondary both for the positive control as well as experimental immunofluorescence. The secondary antibodies were stored at -20°C. These antibodies were defrosted, diluted from 0.2-1.0µg/mL and stored at 4°C in a blocking buffer solution (5% Skim Milk Powder, 1X PBS, 0.1% Tween 20) for up to one month.

The sheep anti-mouse-HRP secondary antibody was re-used up to six times. The goat anti-rabbit-HRP was reused twice. The fluorophore secondary antibody was discarded after each use.

Western Blot Analysis

Embryo Fixation

Collected embryos were fixed immediately after collection. The agar plate covered with embryos was rinsed with dH_2O and embryos dislodged from the plate by using a paintbrush. These embryos were then transferred to a 70µm nylon strainer cup almost submerged in dH_2O. Strainer cup was rinsed with dH_2O to remove excess yeast and agar from *Drosophila* embryos. A 50% bleach solution was used for decorionation, and once dechorionated, embryos were immediately rinsed with dH_2O to remove excess bleach. Using a fine paintbrush, embryos were transferred to a tube of heptane. Embryos sat in heptane for 30-60 seconds to permeablize the embryos. A 1:1 ratio of

4% formaldehyde in PBS was added to the heptane and shook horizontally for 20 minutes on a shaker at 250-300rpm to fix the embryos. The solution was removed and a 1:1 ratio of heptane: ice cold methanol added. Samples were shaken vigorously for one minute to remove the vitelline membrane. After embryos have settled, the heptane:methanol solution was removed from the tube along with any floating embryos. Samples were washed 3x with ice cold methanol and then stored.

CG8878 deletion strain embryos were created from a cross of *Df(2R)BSC699/CyO-P{act-GFP}* to itself. Embryos were collected on apple juice agar plates, and then dislodged with dH_2O into an eppendorf tube and washed multiple times to remove yeast. Embryos were transferred to a depression slide with a drop of 40% glycerol and viewed under a fluorescent microscope. Homozygous deletion embryos were collected based on failure to fluoresce (do not contain the GFP tagged balancer). Selected embryos were transferred into a fresh Eppendorf tube containing dH_2O, and given multiple rinses with dH_2O to remove traces of glycerol. 50% bleach was directly added to the tube to remove the chorion of the embryo. Embryos were then rinsed twice with dH_2O. The dH_2O was removed and 500µl of heptane was added and procedure followed above.

Embryo Rehydration

Frozen embryos need to be rehydrated prior to sample preparation. Embryos were placed on ice and methanol removed. Embryos were rinsed 3x in 0.05% Tween-20 PBS. A 40% PBST/60% glycerol solution was added to the tube for 1 hour while on ice. Embryos were either stored in glycerol at -20°C or used immediately.

Protein Extraction

Using a compound microscope, embryos were put on a microscope slide containing minimal amounts of 80% glycerol and 1-10 embryos/10µl were added to an Eppendorf tube containing a 5x sample buffer (62.5mM Tris-HCl, 25% glycerol, 2% SDS, 0.01% bromophenol blue, pH 6.8), β-mercaptoethanol, a protease inhibitor (Complete Mini Protease Tablet Inhibitor by Roche Diagnostics, prepared per manufacturer instructions) and dH_2O. Embryos were left in sample buffer on ice for an hour. Samples were then boiled for 10 minutes to denature proteins and loaded immediately.

SDS-PAGE

Samples were subject to SDS-PAGE. BioRad Mini Trans-Blot® Cell kit was used for Both the SDS-PAGE and blotting. Various 10µl samples (containing 1-7embryos/10µl) were run on a pre-cast 10 lane 4-15% gradient polyacrylamide gel at 30-100V and 0.03-0.09A for 40-75 minutes depending on how many gels were being run simultaneously. We used a 1x SDS-Page Running Buffer (250 mM Tris, 1.92 M Glycine,1% SDS, pH 8.3) (BioRad) and loaded a Precision Plus Protein Dual Color Standards Protein Ladder (BioRad).

Membrane Transfer

After SDS-PAGE, proteins were transferred to a nitrocellulose membrane. The gel, 2 sheets of BioRad Transblot® filter paper, nitrocellulose membrane, and 2 foam pads were placed in the blotting transfer solution (25mM Tris, 192mM Glycine, 20% (w/v) methanol, pH 8.3**)** for 15-20 minutes at room temperature to equilibrate. A sandwich was made according to the BioRad User Manual and placed in an assembly rack. An ice pack and a stir bar were added to the tank to prevent overheating and maintain ion flow. The transfer occurred overnight at 30V and 0.09A for 12-20 hours or for one hour at 100V and 0.35A. Membranes could be air-dried and stored at 4°C or blocked immediately.

Membrane Blocking Probing, and Autoradiography

Dried nitrocellulose membranes were rehydrated in TBST (1x TBS, 0.1% Tween 20).

Using Tupperware containers, approximately 50mL of blocking buffer (5% BSA or fat-free skim milk powder, 1x TBS, 0.01% Tween 20, 0.02% Sodium Azide) was applied to each sample for 60 minutes at room temperature or overnight at 4°C on a shaker around 40-50rpm. After incubating with the blocking buffer, each membrane was rinsed 3x with TBST.

Primary antibodies were diluted in blocking buffer with concentrations between 0.1-1.0µg/mL. Samples were incubated with the primary antibody overnight at 4°C on a shaker at 50rpm. Primary antibody was removed from all samples and reused for further western blots. Samples were washed 4x for 5 minutes on a shaker with TBST.

Secondary antibodies were diluted in blocking buffer without sodium azide in concentrations from 0.04-1.0µg/ml and incubated with samples at room temperature for an hour. After incubation, samples were washed 4x with TBST.

For visualization, BioRad Clarity™ Western ECL Substrate Kit was used. A 1:1 ratio of substrate and peroxide was added to each membrane, with volume based on area (0.1mL/cm^2). ECL solution was applied to membranes for 5 minutes and excess dabbed over before wrapped in Saran Wrap. Membranes were subject to autoradiography and exposure times varied from 1 minute to overnight.

Membrane Stripping

Membranes could be used for more than one trial therefore membranes were stripped. Stripping solution is 200mM glycine, 1% SDS, pH 2.5. It was applied to samples for 15 minutes on a shaker at room temperature. After 15 minutes, samples were washed 3x for 3 minutes with TBST and re-blocked immediately.

Immunofluorescence

Embryo Rehydration and Blocking

Fixed embryos were rehydrated with a different protocol than in the Western Blotting. Embryos were taken out of the freezer and methanol was removed. Embryos were washed 3x with 50% methanol/ 50% PBS, then washed 4x with PBST (1x PBS, 0.1% Tween 20). Embryos were blocked immediately.

PBST was extracted and blocking buffer (5% BSA, 1x PBS, 0.01% Tween 20, 0.02% Sodium Azide) was added to each sample for 60 minutes at room temperature on a shaker around 150-200rpm. After 60 minutes, blocking buffer was removed.

Primary and secondary antibody probing

Primary antibodies were diluted in blocking buffer varying in concentrations from 0.1-1.0µg/mL. Primary antibodies were added and shaken overnight at 4°C. Next day, primary antibody was removed and samples were washed 4x for 15 minutes each with PBST on a shaker at 150-200rpm at room temperature.

Samples were wrapped in tinfoil to protect light sensitive conjugated-fluorophore secondary antibody. The conjugated-fluorophore secondary antibody was diluted 1:1000 to 1:10000 in blocking buffer solution not containing sodium azide. Secondary antibody

solution was incubated with samples for 2-2.5 hours at room temperature on a shaker at 150-200rpm. After incubation, secondary was removed and discarded.

Samples washed 4x with PBST for 15 minutes each at room temperature on a shaker. An additional two more washes were done in just PBS for 15 minutes each at room temperature to remove excess Tween 20 for the Hoechst Stain.

Hoechst Stain and Mounting

Hoechst stain was added to samples just prior to mounting. Hoechst 33342 Fluorescent Stain was supplied in a 1000x solution from Dr. Shelagh Campbell's Lab. 0.2µg/mL of Hoechst Stain was added for every 1mL of PBS to each solution. Embryos were incubated with Hoechst stain on a shaker for 5 minutes at room temperature. After application and incubation of the Hoechst Stain, all samples were washed twice with PBS for 5 minutes on a shaker at room temperature.

Embryo samples were transferred onto a frosted glass microscope slide and excess liquid was removed. Immediately after a few drops of mounting solution was applied (90% glycerol, 1x PBS, 5.5µM of p-phenylenediamine dihydrochloride (anti-quencher), pH ~8.5), a cover slip was added and sealed with nailpolish. Samples were stored in the dark at 4°C.

Figures and Tables

Table 2.1. List of *Drosophila* stocks used and made

Stock #	Genotype	Description	Origin
26551	*w^{1118}; Df(2R)BSC699 , P+P Bac{XP3.RB5}BSC699 /S M6a*	CG8878 Deletion	Bloomington
LC03	*P{act-Gal4} / CyO P{act-GFP}*	Actin Gal4 stock AND 2nd chr. GFP Balancer.	King-Jones Lab
LC06	*w ; Xa / CyO P{act-GFP}*		Canham
LC07	*Df(2R)BSC699/ CyO GFP*	CyO GFP balancer. CG8878 deletion.	Canham
LC08	*w; 1a27a*	CG8878 mutant from screen	McCracken
LC09	*w; 3a22a*	CG8878 mutant from screen	McCracken
LC10	*w; 3a52a*	CG8878 mutant from screen	McCracken
LC11	*w; 3a66a*	CG8878 mutant from screen	McCracken
LC12	*w; 3a90a*	CG8878 mutant from screen	McCracken
LC13	*w; 1a27a / Cyo GFP*	CG8878 mutant balanced over CyO GFP	Canham
LC14	*w; 3a22a / Cyo GFP*	CG8878 mutant balanced over CyO GFP	Canham
LC15	*w; 3a52a / Cyo GFP*	CG8878 mutant balanced over CyO GFP	Canham
LC16	*w; 3a66a / Cyo GFP*	CG8878 mutant balanced over CyO GFP	Canham
LC17	*w; 3a90a / Cyo GFP*	CG8878 mutant balanced over CyO GFP	Canham
100985		VDRC. KK Library. Viable *UAS-CG8878* stock.	VDRC
28970		VDRC. GD library. Viable *UAS-CG8878* stock.	VDRC

28971		VDRC. GD library. Viable *UAS-CG8878* stock.	VDRC
108630		VDRC. KK Library. Lethal *UAS-ballchen* stock.	VDRC
35571	*y[1] sc[*] v[1]; P{y[+t7.7] v[+t1.8]=TRiP.GL00068}attP2*	Germline RNAi *UAS-ballchen*. Vector: VALIUM22	Bloomington
31350	*y^1 sc^* v^1; P{TRiP.GL00068}attP2*	Germline RNAi *UAS-ballchen*. Vector: VALIUM1	Bloomington
35175	*y[1] sc[*] v[1]; P{y[+t7.7] v[+t1.8]=TRiP.GL00045}attP2*	Germline RNAi *UAS-CG8878*. Vector: VALIUM22	Bloomington
42483	*y[1] sc[*] v[1]; P{y[+t1.8]=TRiPGL01342}attP2*	Germline RNAi *UAS-CG8878*. Vector: Valium23	Bloomington
	w^- ; ey-GAL4 ; p^p atm^8 e / T(2;3) SM5a - TM6b	eye specific GAL4 driver	Campbell Lab
	neur-GAL4 P72 / TM6B	neural GAL4 driver	Campbell Lab
	w; elav-GAL4	neural GAL4 driver. Homozygous 3rd chromosome	Campbell Lab

Table 2.2. Summary of bioinformatics programs and their purpose. N/A means that the program name is not an acronym.

Program Name	Program Full Name	URL	Summary
BLAST	Basic Local Alignment Search Tool	http://blast.ncbi.nlm.nih.gov/Blast.cgi	Compares sequences to databases to find similarity
HMMER	N/A	http://hmmer.janelia.org/	Compares sequences to databases to find similarity. Uses profile hidden Markov models to detect homologs more accurately, even if the relation is distant.
MUSCLE	MUltiple Sequence Comparison by Log-Expectation	http://www.drive5.com/muscle/	Multiple sequence alignment program. More robust than CLUSTALW
BEAUTi / BEAST	Bayesian Evolutionary Analysis Utility / Bayesian Evolutionary Analysis Sampling Trees	http://beast.bio.ed.ac.uk/	BEAST is a Bayesian tree builder using Markov Chain Monte Carlo, creating rooted time-measured phylogenies. BEAUTi is the graphical user interphase for BEAST.
FigTree	N/A	http://tree.bio.ed.ac.uk/software/figtree/	Used to visualize the phylogenetic tree file produced by BEAST.
jDotter	N/A	http://athena.bioc.uvic.ca/virology-ca-tools/jdotter/	jDotter creates dotplot comparisons between two or more sequences
I-TASSER	Iterative Threading ASSEmbly Refinement	http://zhanglab.ccmb.med.umich.edu/I-TASSER/	Protein structure and function prediction based on comparing to structures and functions of known proteins.
Swiss PDB viewer	N/A	http://spdbv.vital-it.ch/	.pdb protein structure file viewer.

Table 2.3. List of sequences removed from phylogenetic alignment and tree analysis. GI number of the protein, species and reason for removal are listed. *Drosophila* species, except *melanogaster* and *virilis* were removed to simplify data. For all others, incomplete sequences and multiple isoforms were removed. Note this table spans four pages.

GI Number	Species	Reason for removal
194745075	*Drosophila ananassae*	Drosophila
194753325	*Drosophila ananassae*	Drosophila
194765063	*Drosophila ananassae*	Drosophila
194744777	*Drosophila ananassae*	Drosophila
194763983	*Drosophila ananassae*	Drosophila
194907816	*Drosophila erecta*	Drosophila
194883796	*Drosophila erecta*	Drosophila
194905093	*Drosophila erecta*	Drosophila
194901248	*Drosophila erecta*	Drosophila
194895817	*Drosophila erecta*	Drosophila
194880411	*Drosophila erecta*	Drosophila
195055167	*Drosophila grimshawi*	Drosophila
195030033	*Drosophila grimshawi*	Drosophila
195062248	*Drosophila grimshawi*	Drosophila
195038635	*Drosophila grimshawi*	Drosophila
195041888	*Drosophila grimshawi*	Drosophila
195041883	*Drosophila grimshawi*	Drosophila
195064397	*Drosophila grimshawi*	Drosophila
95981790	*Drosophila mauritiana*	Drosophila
195113115	*Drosophila mojavensis*	Drosophila
195120640	*Drosophila mojavensis*	Drosophila
195110213	*Drosophila mojavensis*	Drosophila
195133230	*Drosophila mojavensis*	Drosophila
195133232	*Drosophila mojavensis*	Drosophila
195117868	*Drosophila mojavensis*	Drosophila
195165908	*Drosophila persimilis*	Drosophila
195148962	*Drosophila persimilis*	Drosophila
195159045	*Drosophila persimilis*	Drosophila
195152792	*Drosophila persimilis*	Drosophila
195174911	*Drosophila persimilis*	Drosophila
195159832	*Drosophila persimilis*	Drosophila
198450387	*Drosophila pseudoobscura pseudoobscura*	Drosophila
198455746	*Drosophila pseudoobscura pseudoobscura*	Drosophila
390176783	*Drosophila pseudoobscura pseudoobscura*	Drosophila
390178937	*Drosophila pseudoobscura pseudoobscura*	Drosophila
390178935	*Drosophila pseudoobscura pseudoobscura*	Drosophila
125983232	*Drosophila pseudoobscura pseudoobscura*	Drosophila

198462129	*Drosophila pseudoobscura pseudoobscura*	Drosophila
198475501	*Drosophila pseudoobscura pseudoobscura*	Drosophila
195349776	*Drosophila sechellia*	Drosophila
195352508	*Drosophila sechellia*	Drosophila
195333614	*Drosophila sechellia*	Drosophila
195341678	*Drosophila sechellia*	Drosophila
195349418	*Drosophila sechellia*	Drosophila
195352686	*Drosophila sechellia*	Drosophila
195344728	*Drosophila sechellia*	Drosophila
95981826	*Drosophila simulans*	Drosophila
95981832	*Drosophila simulans*	Drosophila
95981830	*Drosophila simulans*	Drosophila
95981800	*Drosophila simulans*	Drosophila
95981808	*Drosophila simulans*	Drosophila
95981806	*Drosophila simulans*	Drosophila
95981802	*Drosophila simulans*	Drosophila
95981798	*Drosophila simulans*	Drosophila
95981804	*Drosophila simulans*	Drosophila
195566668	*Drosophila simulans*	Drosophila
95981828	*Drosophila simulans*	Drosophila
95981812	*Drosophila simulans*	Drosophila
195574224	*Drosophila simulans*	Drosophila
95981818	*Drosophila simulans*	Drosophila
95981824	*Drosophila simulans*	Drosophila
95981796	*Drosophila simulans*	Drosophila
95981820	*Drosophila simulans*	Drosophila
95981822	*Drosophila simulans*	Drosophila
95981834	*Drosophila simulans*	Drosophila
95981816	*Drosophila simulans*	Drosophila
95981814	*Drosophila simulans*	Drosophila
95981810	*Drosophila simulans*	Drosophila
195551825	*Drosophila simulans*	Drosophila
195575229	*Drosophila simulans*	Drosophila
195554866	*Drosophila simulans*	Drosophila
195450947	*Drosophila willistoni*	Drosophila
195455456	*Drosophila willistoni*	Drosophila
195449244	*Drosophila willistoni*	Drosophila
195451079	*Drosophila willistoni*	Drosophila
195446804	*Drosophila willistoni*	Drosophila
195450715	*Drosophila willistoni*	Drosophila
195503956	*Drosophila yakuba*	Drosophila

195485526	*Drosophila yakuba*	Drosophila
195501031	*Drosophila yakuba*	Drosophila
195483827	*Drosophila yakuba*	Drosophila
28571749	*Drosophila melanogaster*	Gish isoforms
386765894	*Drosophila melanogaster*	Gish isoforms
62472622	*Drosophila melanogaster*	Gish isoforms
281361900	*Drosophila melanogaster*	Gish isoforms
28571746	*Drosophila melanogaster*	Gish isoforms
386765896	*Drosophila melanogaster*	Gish isoforms
78706449	*Drosophila melanogaster*	Gish isoforms
28571751	*Drosophila melanogaster*	Gish isoforms
24647391	*Drosophila melanogaster*	Gish isoforms
429892242	*Drosophila melanogaster*	CG8878 Partial
429892222	*Drosophila melanogaster*	CG8878 Partial
429892230	*Drosophila melanogaster*	CG8878 Partial
429892236	*Drosophila melanogaster*	CG8878 Partial
429892240	*Drosophila melanogaster*	CG8878 Partial
429892244	*Drosophila melanogaster*	CG8878 Partial
429892226	*Drosophila melanogaster*	CG8878 Partial
429892246	*Drosophila melanogaster*	CG8878 Partial
429892234	*Drosophila melanogaster*	CG8878 Partial
429892232	*Drosophila melanogaster*	CG8878 Partial
429892252	*Drosophila melanogaster*	CG8878 Partial
429892224	*Drosophila melanogaster*	CG8878 Partial
429892254	*Drosophila melanogaster*	CG8878 Partial
429892250	*Drosophila melanogaster*	CG8878 Partial
429892238	*Drosophila melanogaster*	CG8878 Partial
429892248	*Drosophila melanogaster*	CG8878 Partial
429892228	*Drosophila melanogaster*	CG8878 Partial
378744222	*Drosophila melanogaster*	CG8878 Duplicate
28317155	*Drosophila melanogaster*	ballchen partial
66771647	*Drosophila melanogaster*	asator partial
281359551	*Drosophila melanogaster*	asator partial
442614391	*Drosophila melanogaster*	asator partial
157816797	*Drosophila melanogaster*	asator isoforms
281359549	*Drosophila melanogaster*	asator isoforms
442614397	*Drosophila melanogaster*	asator isoforms
442614399	*Drosophila melanogaster*	asator isoforms
442614393	*Drosophila melanogaster*	asator isoforms
442614395	*Drosophila melanogaster*	asator isoforms
3335146	*Drosophila melanogaster*	disc duplicate

1502306	*Drosophila melanogaster*	CK1a partial
18446996	*Drosophila melanogaster*	ck1? duplicate
328725791	*Acyrthosiphon pisum*	asator isoforms
328725793	*Acyrthosiphon pisum*	asator isoforms
328701995	*Acyrthosiphon pisum*	CK1a duplicate
328704611	*Acyrthosiphon pisum*	Gish isoforms
157141863	*Aedes aegypti*	ballchen isoforms
157116475	*Aedes aegypti*	ballchen isoforms
157130002	*Aedes aegypti*	CG8878 Partial
157105690	*Aedes aegypti*	Gish isoforms
157105686	*Aedes aegypti*	Gish isoforms
347971046	*Anopheles gambiae*	Gish isoforms
347971050	*Anopheles gambiae*	Gish isoforms
347971048	*Anopheles gambiae*	Gish isoforms
350404213	*Bombus impatiens*	disc isoform
112983860	*Bombyx mori*	disc isoform
112983854	*Bombyx mori*	ck1a isoform
498930617	*Ceratitis capitata*	asator isoforms
498969029	*Ceratitis capitata*	CG8878 isoform
498933773	*Ceratitis capitata*	Gish isoforms
156118308	*Danaus plexippus*	disc isoform
478256805	*Dendroctonus ponderosae*	ck1a isoform
195402231	*Drosophila virilis*	asator isoforms
195399039	*Drosophila virilis*	ck1a isoform
241558619	*Ixodes scapularis*	ck1a isoform
345486235	*Nasonia vitripennis*	asator isoforms
345493765	*Nasonia vitripennis*	ballchen partial
270009353	*Tribolium castaneum*	shorter asator
189241127	*Tribolium castaneum*	ck1a isoform
91088549	*Tribolium castaneum*	disc isoform
270014464	*Tribolium castaneum*	Gish isoforms
270011569	*Tribolium castaneum*	Gish isoforms
End		

Table 2.4. A summary of the antibodies used for the Western Blots and Immunofluorescence assay. Antibody 1, 2 and 3 were predicted to bind to the protein BSHE. β-Tubulin and PH3 were used as positive controls.

Antibody	**Antibody Type**	**Species**	**Concentration (mg/mL)**	**Polypeptide Derivation**	**Location in polypeptide**
Antibody 1	Polyclonal Affinity Purified IgG	New Zealand Rabbit	1.200	MGKRLQLERPTTDRC	N-terminus
Antibody 2	Polyclonal Affinity Purified IgG	New Zealand Rabbit	1.063	CRGRPKGTSRKQTTS	C-terminus
Antibody 3	Polyclonal Affinity Purified IgG	New Zealand Rabbit	0.431	CATGEGERKLKSGRT	C-terminus
B-Tubulin	Monoclonal Affinity Purified IgG	Mouse	-	-	-
PH3	Polyclonal Affinity Purified IgG	Rabbit	-	-	-
Goat Anti-Rabbit IgG	Polyclonal HRP-Linked	Goat	-	-	-
Sheep Anti-Mouse IgG	Monoclonal HRP-Linked	Sheep	-	-	-
Anti-Rabbit IgG	Conjugated-Fluorophore Alexa Fluor® 488	-	-	-	-

References

1. McCracken A, Locke J. Mutations in CG8878, a novel putative protein kinase, enhance P element dependent silencing (PDS) and position effect variegation (PEV) in Drosophila melanogaster. PLoS ONE. 2014;9(3):e71695.

2. Ashburner M. Drosophila: A laboratory manual. Cold Spring Harbor Laboratory Press; 1989. 1 p.

3. Eddy SR. Profile hidden Markov models. Bioinformatics. 1998.

4. Edgar RC. MUSCLE: multiple sequence alignment with high accuracy and high throughput. Nucleic Acids Res. 2004;32(5):1792–7.

5. Yang Z. Maximum likelihood phylogenetic estimation from DNA sequences with variable rates over sites: approximate methods. J Mol Evol. 1994 Mar 9;39(3):306–14.

6. Zhang Y. I-TASSER server for protein 3D structure prediction. BMC Bioinformatics. 2008;9:40.

7. Roy A, Kucukural A, Zhang Y. I-TASSER: a unified platform for automated protein structure and function prediction : Abstract : Nature Protocols. Nat Protoc. 2010.

8. Guex N, Peitsch MC. SWISS-MODEL and the Swiss-PdbViewer: an environment for comparative protein modeling. Electrophoresis. 1997 Dec;18(15):2714–23.

9. Brodie R, Roper RL, Upton C. JDotter: a Java interface to multiple dotplots generated by dotter. Bioinformatics. 2004.

3. Chapter 3: *Banshee* phylogenetics and protein structure shows it as an insect specific protein with a probable functioning kinase domain.

Introduction

Protein kinases are one of the most abundant groups of proteins, cumulatively comprising 1.5-2.5% of all eukaryotic genes. Typically they have a common catalytic core structure consisting mostly of a beta-sheet N-lobe and a alpha-helix C-lobe(1,2), along with a catalytic ATP domain and phosphotransfer domain located within the C-lobe. The protein kinase family is split into two major groups: typical and atypical. Atypical kinases (AK) share homology with the typical kinases (TK) at the catalytic domain, but are not conserved across the other motifs (3-7).

Casein Kinase 1 family protein structure

The gene *banshee* is part of the Casein Kinase 1 family (6). The Casein Kinase 1 (CK1) family of protein kinases is considered a TK, but it has some peculiarities that distinguish itself from all other TKs. Specifically, the APE amino acid motif found in the activation loop is replaced with an SIN amino acid motif (1,8-12). The APE motif is found within the substrate recognition pocket. The CK1 family also has amino-acid substitutions that affect linkage between different regions of the C-terminal domain. For example, E208-R280 ion pairs are highly conserved in other TKs, but they are not present in CK1 (3,5,7,10,13-16). The overall structure of CK1 remains the same as other TKs. CK1 also exhibits similarities to tyrosine kinase structures for helix 1, despite being a serine/threonine kinase (8-12,17). The intermediate helix 1 designation, as well as the APE-SIN motif change, suggests that CK1 is possibly an intermediate between TKs and AKs. Since the CK1 group is found widely in eukaryotes (6,18), the formation of the CK1 group must have occurred soon after the origin of eukaryotes. This evidence indicates the CK1 family is an ancient group of TK.

Within the CK1 kinase group thus far described there are 12 human proteins, 10 *Drosophila melanogaster* proteins, 4 *Saccharomyces cerevisiae* proteins and 85 *Caenorhabditis elegans* proteins (6). Within humans and *Drosophila*, this includes the sub-families: *casein kinase 1*α (*ck1α*), *casein kinase 1*γ (*ck1γ*), *casein kinase 1*δ/ε (*ck1δ/ε*), *tau-tubulin kinase* (*ttbk*) and *vaccinia-related kinase* (*vrk*).

Roles of human Casein Kinase 1 genes

In humans, CK1 family members have a wide variety of roles. Of most interest to my research is VRK1, because of *banshee* is a part of the VRK subgroup. VRK1 has been implicated in various cell cycle functions, chromatin condensation, golgi fragmentation and DNA damage response(19-22). It co-localizes with heterochromatin during interphase, but is dispersed throughout the nucleus during mitosis (4,6). It also is found in the cytosol, colocalizing with the golgi (1,10). VRK-2 is part of signaling pathways that are involved in apoptosis and tumor growth (23,24). Gene variants are associated with schizophrenia (25). Not much in known of human VRK3, though it appears to have lost its phosphorylation activity (26,27). It still appears able to bind with substrate though. In particular, it can bind and activate an Erk phosphatase, and localizes to the nucleus (28,29).

There are six Casein Kinase 1 isoforms in humans (α, δ, ε, γ1, γ2, and γ3). They play a variety of roles, including Wnt signaling, membrane trafficking, circadian rhythm and DNA damage response (3,5,7,10). CK1 members can be found associated with various membranes, in the nucleus or cytoplasm, depending on the type of CK1 and the splice variants that occur (8-12). TTBK1 and TTBK2 phosphorylate tau and tubulin proteins (6,13-16). Mutations in the TTBK genes have been implicated in neurodegenerative phenotypes like Alzheimer's Disease (6,17). The *Drosophila* ortholog *asator* also localizes with the mitotic spindle during cell division (18-22).

Drosophila Casein Kinase 1 family

Drosophila melanogaster contains orthologs to the human CK1 family genes described above. These include *ck1α*, *disc* (*hCK1γ*), *gish* (*hCK1ε*), *asator* (*hTTBK1/2*) and *ballchen* (*hVRK1/2*). The gene I am interested in, *banshee (bshe)*, has also been shown to be a part of the VRK subfamily, along with *ballchen (ball* is also known as *nuclear histone kinase 1* or *nhk1* in some literature*)* (6). The prevalence of *bshe* found in other organisms is not known.

BSHE's protein domains have only been briefly described (30). We know that it has a putative kinase domain, with a large interruption in the centre of it. It also has a nuclear localization signal and three regions containing a high number of acidic amino acids (30). It is unknown whether the interruption in the kinase domain causes a

significant enough change in the protein structure to render the kinase activity non-functional.

Research objectives

Bioinformatics analysis is the first step I have taken to investigate the function of BSHE. Through creating a phylogenetic tree and finding the prevalence of the gene in other organisms we can understand its origins. Knowing which species do and don't have it will lead to knowledge of its function. In the kinomen of the model organisms, all other genes in the *VRK* subfamily more closely relate to *ball*, with nothing that aligns more closely to *bshe* (6). This is coupled with previous observations that *bshe* is seen in mosquitos and *Bombyx mori* (the silkworm moth) suggesting that *bshe* may be more confined to Arthropods (30). With this in mind, I chose insect species to be the in-group, and species from the subphyla Arachnida, which are still Arthropods, to be the out-group. If *bshe* were to be found within the Arachnid group, a further expansion of my search criteria would have been the next step but this did not prove necessary.

A molecular structure prediction can begin to confirm how the interruption in the kinase domain affects the folding of the protein.

Results and Discussion

Building a phylogenetic tree

Initial amino acid sequence comparison suggested that BSHE is a putative histone kinase and an initial BLAST search found evidence of BSHE homologs within other Dipterans (30). Here I have confirmed BSHE orthologs within Dipterans and have extended my search to determine the extent of its prevalence in other species.

A phylogenetic tree was built based around Arthropoda of the CK1 family proteins (Figure 3.1. Figure 3.2 is a simplified version of Figure 3.1 that will be used for analysis). The steps for how the tree was made are as follows. First, an alignment was made of previously identified BSHE proteins within *Drosophila*, and other mosquito and moth species (30). Specifically the kinase domains were aligned to create a HMMER profile to search for other proteins with similar kinase domains. HMMER uses profile hidden Markov models (HMM) to statistically describe consensus sequences (31). By providing a statistical score for the consensus sequence of an already aligned group of proteins, it

allows a more robust search of the Genbank database to find distantly related proteins. Those proteins were then aligned with MUSCLE, which is a robust and accurate multiple sequence alignment program (32). Then the amino-acid sequences were converted to their original DNA sequences, in order to note the fine changes that lead to the different proteins. When aligning many different proteins there will be gaps where sequences don't align. Where more than 10% of the alignment is gaps, that nucleotide is removed. This allows comparison of only of the most conserved parts of the protein to see the finest changes in the functional areas; in this situation, the kinase domain. A Bayesian maximum sum of clade credibility tree was built using this alignment using the Baysian Markov chain Monte Carlo (MCMC) algorithm program BEAST. To define this better, one must understand Bayesian posterior probability, which put simply is the probability of event A occurring given that event B occurred. Posterior probability shows how well the model agrees with the observed data. Each clade in a tree is given a score based on the fraction of times it appears in the sampled posterior trees, and the product of that score is the overall tree score. The tree with the highest is the maximum clade credibility. The maximum sum of clade credibilities tree then sums all of the clade posteriors.

Phylogenetic analysis shows *bshe* as an insect specific kinase

There are six distinct groups within the tree: *Drosophila bshe, ballchen* (*hVRK-1*), *asator* (*hTTBK*), *CK1α* (*hCK1α*), *gish* (*hCK1γ*) and *disc* (*hCK1ε*). There is also a single *Drosophila* specific casein-kinase-like protein (gi:24584859) that is similar, but does not assort with any casein kinase group specifically. All the expected *Drosophila* genes were found based on the known *Drosophila* kinome (6). A kinome is the collective group of all known or possible kinases within a species.

Representatives of each Order were found within each gene group, except *bshe*, which is missing in the Arachnida outgroup. Completely sequenced species were also found within all groups. When not found, they were either a species not completely sequenced, or appeared to have a miscalled protein sequence that highly deviated from expected and so was removed (See Chapter 2). Based on this collection of sequences, *bshe* is found within all Insecta Orders, but is not found within the representatives of the Arachnida outgroup. This does not necessarily mean that there is no *bshe* found outside

of insects, and declarations can only be made as far as the data is presented. When first creating the tree, the Crustacea subphylum was removed due to an incorrect understanding of Arthropod evolution. Crustaceans are more related to insects than Arachnids, and so should have been included. There may be a possibility that a *bshe* gene could be found within the Crustacea subphylum members. A rough exploration into CK1 family proteins within Crustaceans so far is presented within the Appendix, and shows no protein is similar to BSHE. This exploration was not as robust as the phylogenetics performed here though.

Hypothesis for the origin of *ball* and *bshe*

These observations could be accounted for in multiple ways. Either the divergence of *ball* and *bshe* occurred at the origin of Insecta, or the divergence occurred prior to the formation of Insecta but was only retained within Insecta and lost from all other phyla. Based on the branch lengths of the tree (Figure 3.2), the *ball*/*bshe* lineage is a more ancient clade than *asator* and the *casein kinases*. The latter groups have diverged more recently as evidence by their shorter branch lengths and similar sequences.

bshe is an essential gene within *Drosophila melanogaster*, and based upon its similarity and prevalence throughout insects it is reasonable to assume it to be essential within the other Insect species. This leads us to the question of why this protein appears essential within Insecta, yet appears to be lost in other groups, like Arachnida and all other phyla. The following are three hypotheses that could explain this.

Firstly, the origin of the *ball*/*bshe* divergence could have occurred before insect divergence, but was then lost from other phyla. This could be explained by *bshe* retaining its function in Insects, while being lost through disuse in other organisms. The role of *bshe* in other organisms could be replaced by other genes, making *bshe* unnecessary. A problem with this hypothesis is that it is not very parsimonious to assume that this ancient group of proteins has been so far removed that one cannot find traces of it in non-coding DNA of any other phyla, especially those organisms closely related to insects, like other Arthropods.

The next hypothesis is that the divergence of *bshe* and *ball* occurred near the origin of Insecta. This helps to account for the ancientness of those branches of the tree,

as well as the long divergence from *ball*. A possible explanation of why this is specific to insects is that it is involved in an insect specific function, like metamorphosis. It has been recently shown that *bshe* is involved in development of imaginal discs (33), which further supports an insect-specific role, as imaginal discs are the precursors to adult tissues that develop during metamorphosis. A problem with this hypothesis is that according to our tree the *CK1* kinases (*CK1α, gish, disc*) and *asator* are also ancient. CK1 subgroups are found across many phyla, from yeast to humans (6). Because VRK's are not found in as many phyla, it would appear that CK1 would be more ancient, and therefore should have longer branch lengths. Since the branches are longer in the *bshe/ball* clade, then this hypothesis does not completely account for the data provided.

Lastly, is the hypothesis that branch length is more indicative of selective pressures than of time scale. The faster a gene evolves, the more changes are seen in the sequence, and so the more divergent they appear in a phylogenetic tree. It could be that at some time, *ball* and *bshe* were placed under a large amount of selective pressure, leading to more apparent changes than what is seen with other CK1 family members like the *CK1* genes. These selective pressures could have occurred at the point of divergence, some other point in time, or ongoing since the point of divergence. You can see, that even within the Orders (Figure 3.2) there is much more divergence in the *ball*/*bshe* lineage than from the CK1 family groups. This helps solve the problem of the shorter branch lengths seen in the other CK1 kinases, despite evidence that they are ancient. This could make it more difficult to predict function through comparison to *ball*, if even between Orders there are many changes.

All of the above hypothesis have their potential pros and cons, but can begin to explain the unique phylogenetics seen with *bshe*.

Relation of *bshe* to *ball*

Within the *D. melanogaster* genome, *bshe*'s sequence is most similar to *ball*. As a homolog of human *VRK1*, *ball* is fairly well characterized. BALL has been shown specifically to phosphorylate threonine 119 in histone H2A, and also has a localization pattern based upon cell cycle (34). During S-phase in Cycle 7-12 embryos, BALL is localized to the cytoplasm. Starting in prophase and continuing to the end of mitosis, BALL localizes to the chromatin (34). It, as well as other VRKs, was also found to

phosphorylate Barrier-to-Autointegration Factor (BAF), which untethers BAF from the nuclear envelope, allowing karyosome formation (35). It is required for proper chromatin organization and meiotic progression within oocytes (36). Null *ball* mutants also have defects in proliferating tissues in larvae, showing brain and imaginal disc developmental delays (37). This was later explained through BALL being required for self-renewal and prevention of differentiation of stem cells, as well as having a similar role with germ line stem cells (38,39).

We know, from the genetic screen where *bshe* was identified, that *bshe* is involved with chromatin (30). This suggests a similar role to that of *ball*. The similarity could indicate that *ball* and *bshe* have similar functions, but possibly localized to different tissues or expressed at different stages of development. This phylogenetic similarity is how I will begin to address the possible functions of *bshe* in the rest of my thesis, through comparison to *ball*.

Molecular structure of BSHE shows possible kinase function

The phylogenetic tree was built through aligning the kinase domains. But BSHE has a unique feature: its kinase domain is not continuous, but instead has a large 238 amino acid insertion in the middle. Analysis of the location of this insert within the kinase domain shows that it occurs right in the middle of the main catalytic region. Specifically between the catalytic loop and the Mg^{2+} binding loop (Figure 3.3B). The catalytic loop, Mg^{2+} binding loop and the Activation/P+1 loop all require close proximity in order for kinase function to occur. This would appear to affect the function of this kinase domain. This wouldn't be unprecedented, because VRK3 is in the same kinome group and also is lacking catalytic activity based on subtitutions of a few key amino acids (27). To address this question through bioinformatics I chose to look into the predicted structure of the BSHE protein, with the assumption that if the kinase domain is capable of keeping its normal conformation then there is a higher likelihood that BSHE's kinase domain remains catalytic.

The I-TASSER program (Iterative Threading ASSEmbly Refinement) predicts the structure and function of proteins based on amino acid sequence. It does this through comparing the submitted sequence to other protein sequences with known molecular

structures, and through a variety of other predictive measures and clean up methods provides you with a predicted protein structure.

The structure predicted by I-TASSER for BSHE is shown in Figure 3.3A. The most notable thing is that the insertion appears to loop out away from the kinase domain of the folded polypeptide keeping the kinase domain apparently intact. The most important regions, the catalytic kinase domains, are all in the conformation that is expected for a functional kinase domain.

A confidence score (C-score) was generated for the overall structure and for the five sub-regions I designated as: N-terminus, the kinase domain pre-insert, the insert, the kinase domain post-insert, and the C-terminus. The C-score is a way to estimate accuracy of the structure predictions and ranges from -5 to 2. A higher C-score signifies a model with high confidence, with a C-score higher than -1.5 having a false-positive and false-negative rate of 0.05 and 0.09 respectively (40). The C-score for the entire protein is low at -2.37. The five sub-regions, described above, have C-scores of -3.67 (N-terminus), -0.02 (kinase pre-insert), -2.96 (insert), 0.77 (kinase post insert) and -2.65 (C-terminus) respectively. The kinase domains each have sufficiently high C-scores suggesting that their structure is correct. This is likely because VRK1, the human ortholog of BALL, has a known structure, allowing I-TASSER to confidently predict its structure. The other regions have lower confidence values, which means we cannot be completely confident that the structure is as it says, as there were no significant regions of similarity to other known proteins. These structures are still, at best, a prediction based upon only their sequences.

Based upon the information provided by I-TASSER it appears that the kinase domain should stay in appropriate conformation, despite the large insert. The insert loops away from the kinase domain. Predictive structure for the insert does not contain many higher order structures, with only a few sparsely placed alpha-helices. This does not suggest a defined function at this time, except that it probably doesn't impede BSHE kinase activity. Showing BSHE has a functional kinase domain would be to do a kinase activity assay is the next step for future research.

Conservation of the insert region across Orders

The insert seen in the *melanogaster* BSHE kinase domain is present in all insects observed in this phylogenetic analysis. The location within the kinase domain is also the same. This suggests the region has functional significance. However, the lengths and sequences of each of the insert regions are not conserved. Within Dipterans, the flies have the largest with a range from 238-256, mosquitos with a range of 176-177, Lepidoptera (butterflies/moths) ranging from 164-173, Coeloptera (beetles) ranging from 79-84, Hymenoptera (bees/wasps/ants) ranging from 10-14 and the louse (Phthiraptera) with the smallest insert of 9 amino acids. (Figure 3.4C). The size and also sequence are similar within orders, but have no similarity across orders.

Despite the dissimilarity of the insert, the kinase domain is very similar across all insect orders (Figure 3.4B). For the N- and C- terminus, the louse, hymenoptera, coleoptera and lepidoptera for the most part all have a similar length ranging from 34-50 and 89-383 (Figure 3.4A and D). The dipterans appear more spread out, with the mosquitos and flies clustering together, overall having larger domains that the other orders. This could all be evidence of the more distant time of divergence, or high selective pressures on the *bshe* lineage.

While the dissimilarity across orders can be explained by the divergence and apparent selective pressure upon *bshe*, it makes it difficult to predict any sort of function for the inserted region. The sequence and size may not be tightly influential on the protein's function, but rather there is a structural or regulatory function to the region, since it is present in the same place. An example of this may be if the insert allows the kinase domain to hinge away and stop kinase activity at certain times. Alternatively, it just may be a spandrel, or byproduct of evolution, with the fluctuating size and sequence showing that this region is not being selected for or against in any fashion.

jDotter was used to compare *Drosophila melanogaster* BSHE with other CK1 kinase family proteins. Dot plots show regions of similarity when comparing two proteins, where the similarity is seen by dark shading in an X- and Y-axis. This can most easily be seen across all panels of Figure 3.5. The kinase domain, which is similar no matter which protein you are looking at, is seen as a diagonal line. With BSHE compared to other protein, a gap can be seen in that diagonal line where the insert in the kinase

domain is found. When comparing *Drosophila* BSHE to *Drosophila* BSHE, a complete diagonal line across can be seen which shows that it is the same protein being compared. Other dark spots highlight similar domains found in multiple regions of the protein.

When comparing *Drosophila* BSHE to other species BSHE, you can see how the gap size is different. In the *P. humanus* section there is a large vertical gap while a very small horizontal gap from the strong diagonal line of the kinase domain. This shows that *Drosophila*'s gap is much larger than *P. humanus*. When comparing the insert region across all organisms you can also see that, with the exception of the other Dipteran, there isn't a strong association of sequence similarity in the insert region.

BSHE has three acid-rich amino acid regions within its sequence, two within the insert, and one within the C-terminal part of the protein. The acidic regions of BSHE are not conserved across BSHE proteins in other organisms, as seen in dot plot analysis (Figure 3.5A). Since the acid rich regions have many aspartic acid and glutamic acid amino acids, they will identify regions in other proteins that are also rich in those amino acids and show up as dark shading on the dot plots. These acid rich regions are seen in mosquito, but no other *bshe* orthologs appears to have major acidic regions. This does not rule out it possibly having a function in Dipteran BSHE, but it does not show it being a conserved trait common to all Insecta.

Other proteins in the CK1 family have been identified to have acidic or basic regions, though no function has been associated with them at this time. Notably, in the VRK-1 family from *Caenorhabditis elegans* to humans, all have a base-acid-base motif (34). This can also be seen in dot plot analysis (Figure 3.5B). ASATOR orthologs also have some acidic regions within its sequences (Figure 3.5C), while CK1α does not (Figure 3.5D)

After BALL, comparing BSHE to ASATOR (Figure 3.5C) and to CK1α (Figure 3.5D), shows less and less similarities between the proteins, within even the related kinase domain. In terms of comparing *D. melanogaster* ASATOR to other ASATORs, it appears that ASATOR has much more repetitive sequences, as evidenced

by the amount of black dots (Figure 3.5C). A similar comparison of CK1A shows a lack of repetitive sequences from its fairly clean dot plot (Figure 3.5D).

Conclusion

Through my bioinformatics investigation into *bshe* I have found and explored several of its unique features. *Bshe* is an insect specific gene found within the CK1 kinase family. It, and its closest homolog *ball*, appear to be a more ancient protein or are under higher selective pressure than other members of the CK1 kinase family.

The *D. melanogaster* BSHE has a large insert within the kinase domain, but through structural analysis it does not appear to affect the conformation of the kinase domain. This insert is found across all BSHE orthologs.

Because of these ancient or selective differences from *ball*, it may be more difficult to declare a common function based upon sequence similarity. Nonetheless it provides a starting point in order to begin to understand *bshe*'s role in *Drosophila*. Next I will be comparing the mutant phenotype of *bshe* to *ball* to compare the functional differences from that mutant phenotype. I will then later be exploring protein function and localization through antibody analysis.

Figures and Tables

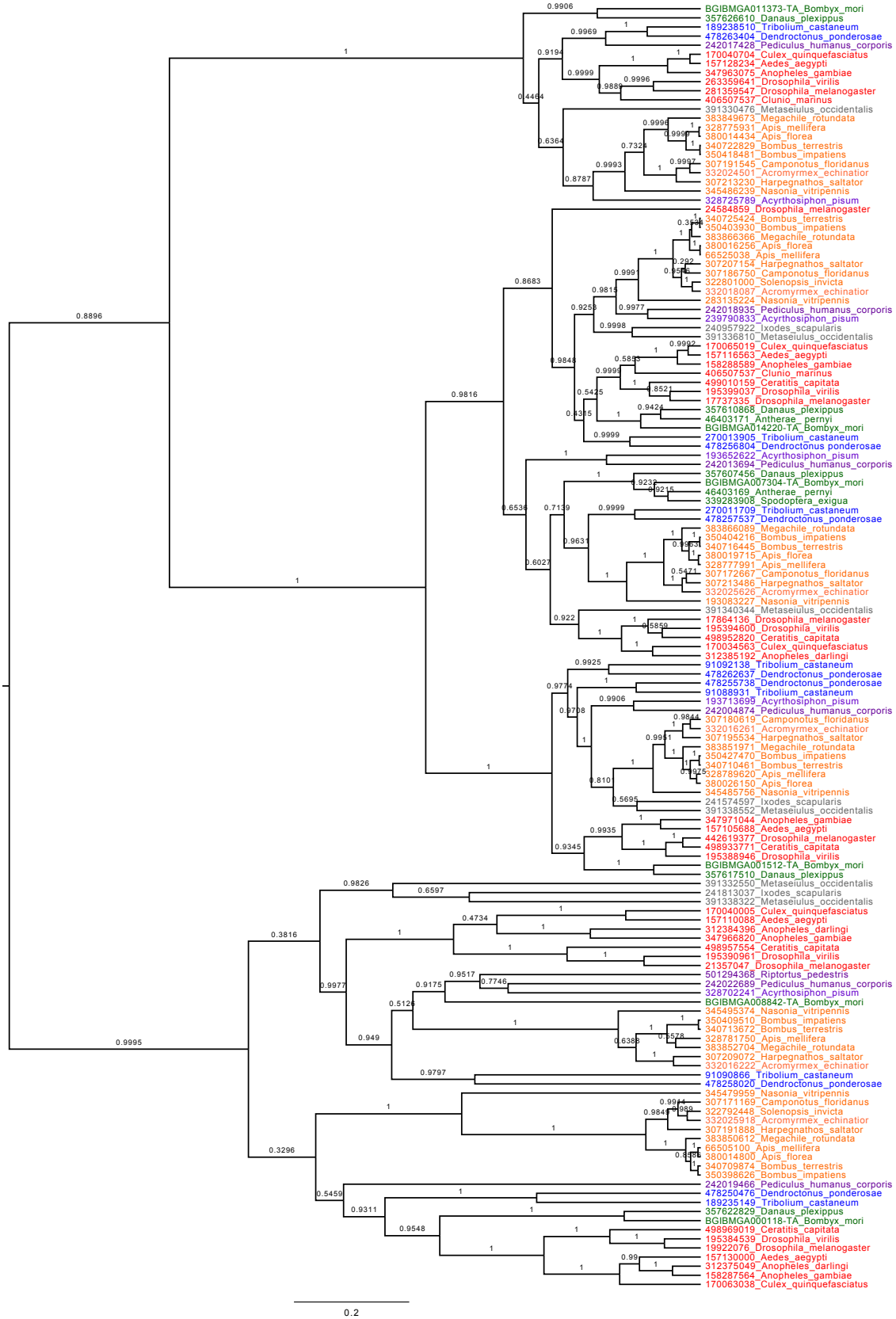

Figure 3.1. Uncollapsed Maximum Sum Clade Credibility tree of CK1 family proteins within select Arthropoda. Built based on the nucleotide sequence found from the proteins that came up through the HMMER search. GI protein numbers and species listed along the right. Branch values are the posterior probability. Tree branches are not necessarily flipped in the same orientation as Figure 3.2.

Colours designate the species Class, Order or Superorder.

Class: Arachnida (grey).
Superorder: Paraneoptera (purple).
Order: Hymenoptera (orange),
Lepidoptera (green),
Coleoptera (blue),
Diptera (red).

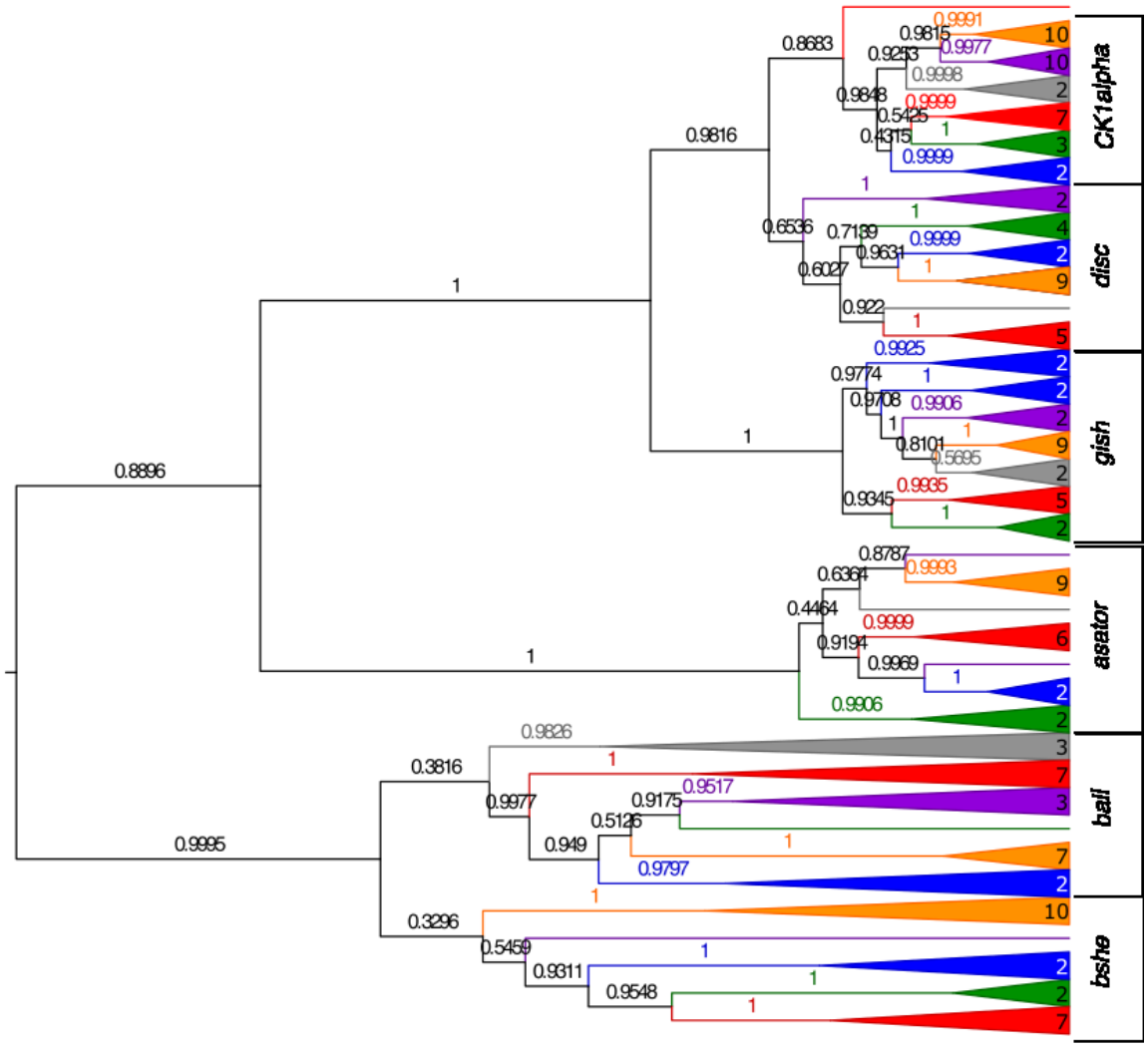

Figure 3.2. Maximum Sum Clade Credibility tree of CK1 family proteins within select Arthropoda. Built based on the nucleotide sequence found from the proteins that came up through the BLAST search. Branch values are the posterior probability. Numbers within the coloured triangular branches indicate the number of branches held within each collapsed clade. Single lines indicate only one species was found in that branch.

Colours designate the species Class, Order or Superorder.
Class: Arachnida (grey).
Superorder: Paraneoptera (purple).
Order: Hymenoptera (orange),
Lepidoptera (green),
Coleoptera (blue),
Diptera (red).

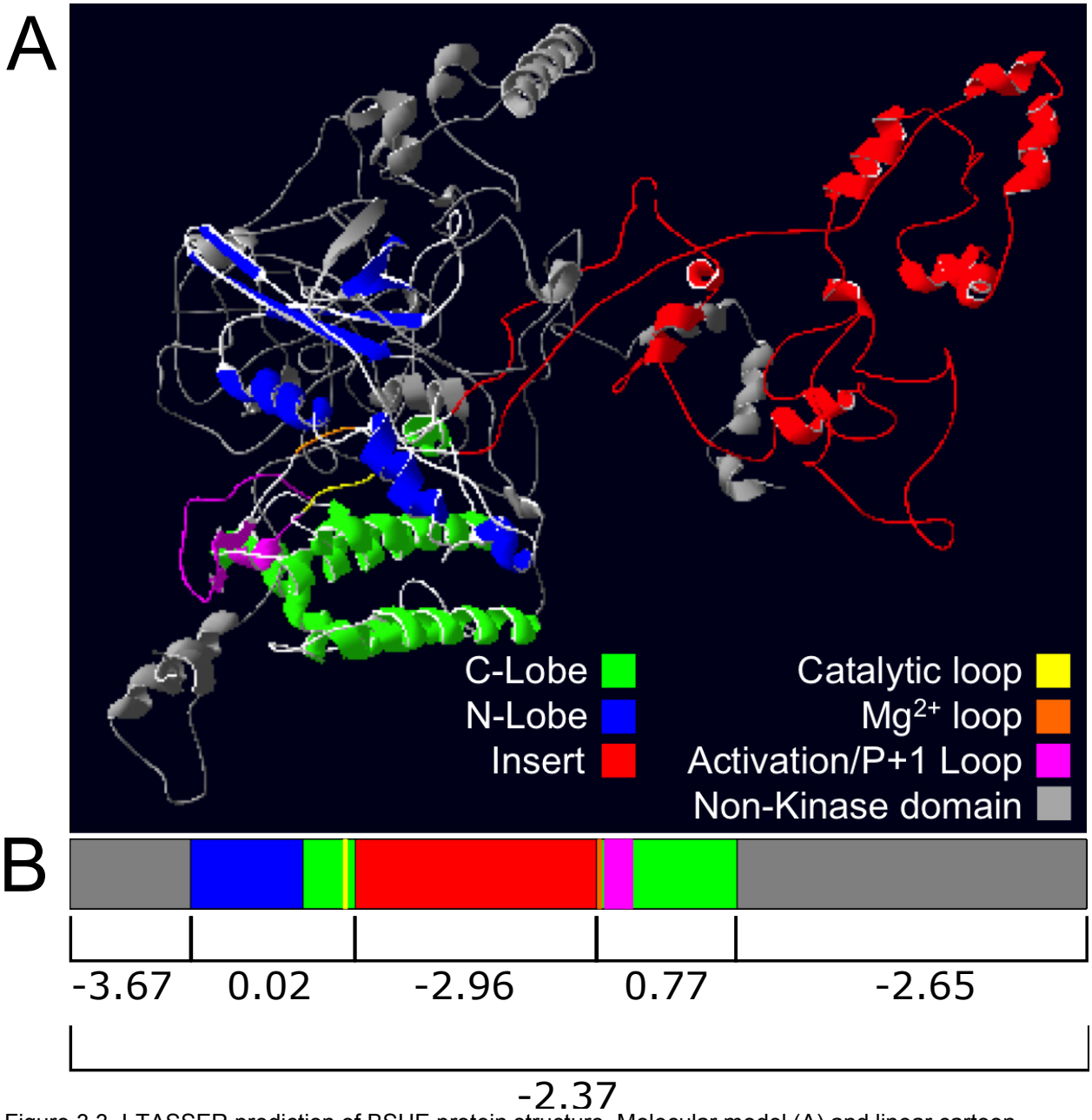

Figure 3.3. I-TASSER prediction of BSHE protein structure. Molecular model (A) and linear cartoon schematic (B) to orient to the specific features. Confidence value for entire protein and individual regions marked under (B). The features of the model include the kinase domain's N-Lobe (Blue), C-Lobe (Green), Insert (Red), Catalytic loop (yellow), Mg^{2+} binding loop (orange), Activation and P+1 loop (Pink) and N- and C- terminal domains (grey)

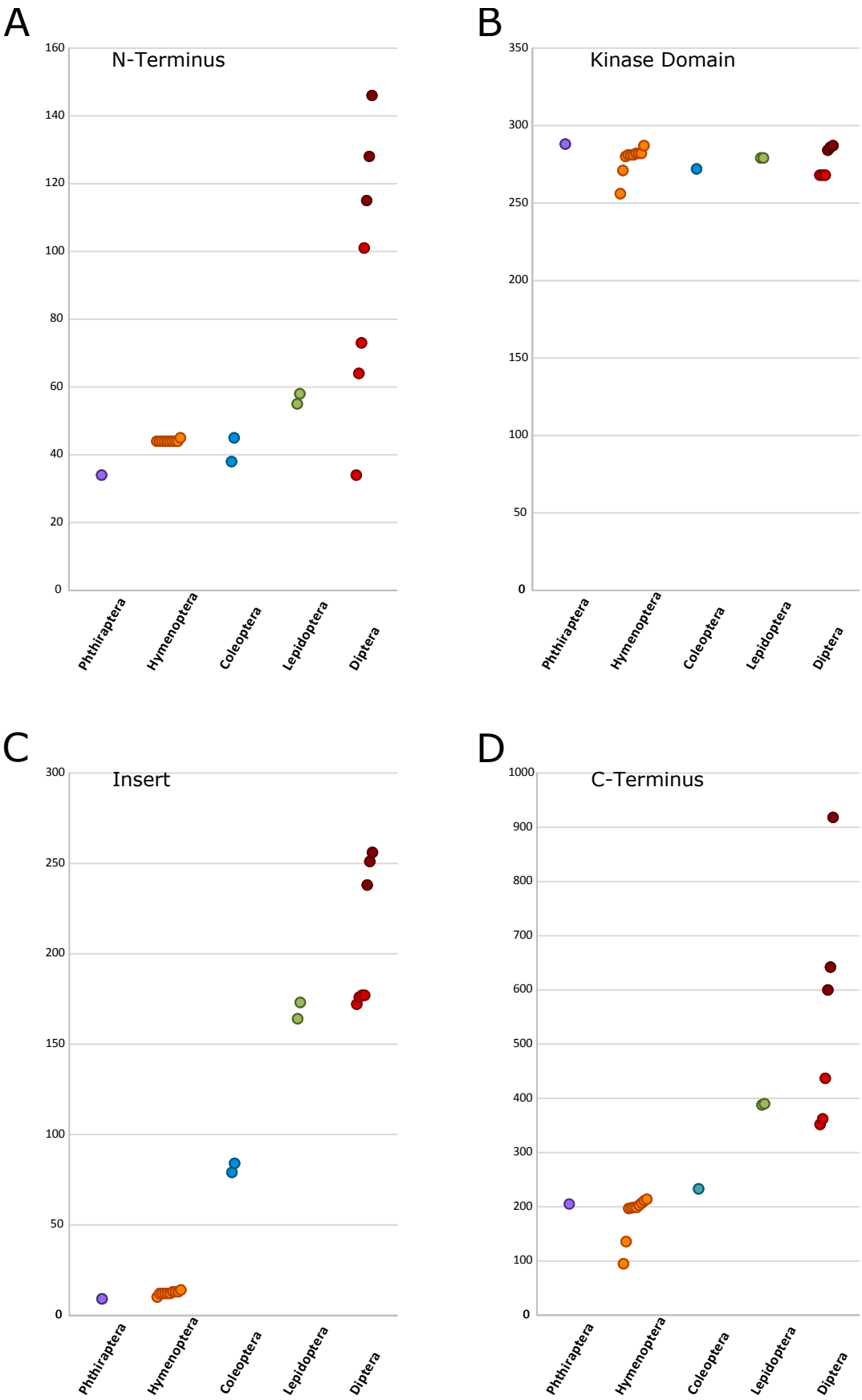
A
N-Terminus
160
140
120
100
80
60
40
20
0
Phthiraptera
Hymenoptera
Coleoptera
Lepidoptera
Diptera
B
Kinase Domain
350
300
250
200
150
100
50
0
Phthiraptera
Hymenoptera
Coleoptera
Lepidoptera
Diptera
C
Insert
300
250
200
150
100
50
0
Phthiraptera
Hymenoptera
Coleoptera
Lepidoptera
Diptera
D
C-Terminus
1000
900
800
700
600
500
400
300
200
100
0
Phthiraptera
Hymenoptera
Coleoptera
Lepidoptera
Diptera

Figure 3.4. Graphical representation of the length in amino acids of each of the distinct regions of BSHE across Orders. Each individual dot represents the size of that region for the one species in that order. The distinct regions include the
(A) N-Terminus,
(B) Kinase Domian,
(C) Insert within kinase domain and
(D) the C-Terminus.

Maroon = Diptera - Flies.
Red = Diptera - Mosquitos
Green = Lepidoptera. (butterflies/moths)
Blue = Coleoptera. (beetles)
Orange = Hymenoptera. (bees/wasps/ants)
Purple = Phtheraptera. (louse)

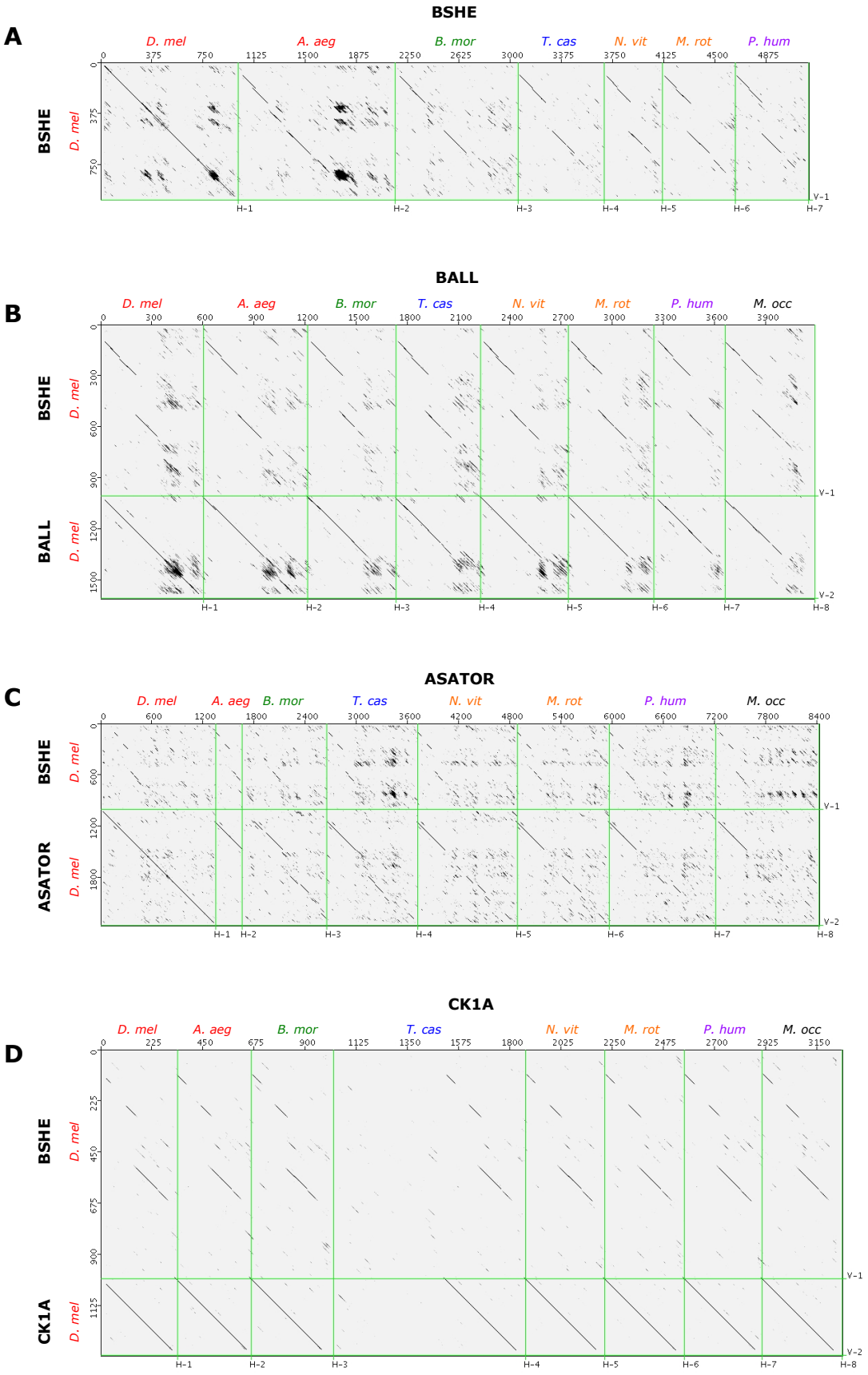
A
BSHE
D. mel
A. aeg
B. mor
T. cas
N. vit
M. rot
P. hum
BSHE
D. mel
V-1
H-1
H-2
H-3
H-4
H-5
H-6
H-7
B
BALL
D. mel
A. aeg
B. mor
T. cas
N. vit
M. rot
P. hum
M. occ
BSHE
D. mel
BALL
D. mel
V-1
V-2
H-1
H-2
H-3
H-4
H-5
H-6
H-7
H-8
C
ASATOR
D. mel
A. aeg
B. mor
T. cas
N. vit
M. rot
P. hum
M. occ
BSHE
D. mel
ASATOR
D. mel
V-1
V-2
H-1
H-2
H-3
H-4
H-5
H-6
H-7
H-8
D
CK1A
D. mel
A. aeg
B. mor
T. cas
N. vit
M. rot
P. hum
M. occ
BSHE
D. mel
CK1A
D. mel
V-1
V-2
H-1
H-2
H-3
H-4
H-5
H-6
H-7
H-8

Figure 3.5. Dot plot analysis highlighting sequence similarity of CK1A family across species. Along the vertical axis are the sequences of *Drosophila melanogaster* BSHE and the specified Drosophila melanogaster protein. Across the horizontal axis is the sequence of one or two members of each insect order for the specified protein. A dot occurs when sequences are similar at the intersection the horizontal and vertical sequence. A clean diagonal line across the entire horizontal and vertical sequences indicates sequence identity. A gap in the horizontal line of the kinase domains in the figure above shows where the BSHE insert is found. A 'smudge' indicates a larger region of similarity, like repetitive sequences or groups of similar amino acids.
(A) Comparing *D. melanogaster* BSHE to other species BSHE. Zoom factor 5 bases/pixel, pixel factor 49.
(B) Comparing *D. melanogaster* BSHE to other species BALL. Zoom factor 4 bases/pixel, pixel factor 46.
(C) Comparing *D. melanogaster* BSHE to other species ASATOR. Zoom factor 8 bases/pixel, pixel factor 48.
(D) Comparing *D. melanogaster* BSHE to other species CK1A. Zoom factor 3 bases per pixel, pixel factor 41.

Legend:

D.mel = Drosphila melanogaster.
A. aeg = Aedes aegypti.
B. mor = Bombyx mori.
T. cas = Tribolium castaneum.
N. vit = Nasonia vitripennis.
M. rot = Megachile rotundata.
P. hum = Pediculus humanus corporis.
M. occ = Metaseiulus occidentalis.

Red = Diptera. (flies/mosquitos)
Green = Lepidoptera. (butterflies/moths)
Blue = Coleoptera. (beetles)
Orange = Hymenoptera. (bees/wasps/ants)
Purple = Phtheraptera. (louse)
Black = Arachnida. (mites/ticks)

References

1. Valbuena A, López-Sánchez I, Vega FM, Sevilla A, Sanz-García M, Blanco S, et al. Identification of a dominant epitope in human vaccinia-related kinase 1 (VRK1) and detection of different intracellular subpopulations. Arch Biochem Biophys. 2007 Sep;465(1):219–26.

2. Taylor SS, Radzio-Andzelm E. Three protein kinase structures define a common motif. Structure. 1994.

3. Knippschild U, Gocht A, Wolff S, Huber N, Löhler J, Stöter M. The casein kinase 1 family: participation in multiple cellular processes in eukaryotes. Cell Signal. Elsevier; 2005;17(6):675–89.

4. Valbuena A, Sanz-García M, López-Sánchez I, Vega FM, Lazo PA. Roles of VRK1 as a new player in the control of biological processes required for cell division. Cell Signal. 2011 Aug;23(8):1267–72.

5. Gallego M, Virshup DM. Post-translational modifications regulate the ticking of the circadian clock. Nat Rev Mol Cell Biol. 2007 Feb;8(2):139–48.

6. Manning G, Plowman GD, Hunter T, Sudarsanam S. Evolution of protein kinase signaling from yeast to man. Trends Biochem Sci. 2002 Oct;27(10):514–20.

7. Price MA. CKI, there's more than one: casein kinase I family members in Wnt and Hedgehog signaling. Genes Dev. 2006 Feb 15;20(4):399–410.

8. Gross SD. A phosphatidylinositol 4,5-bisphosphate-sensitive casein kinase I alpha associates with synaptic vesicles and phosphorylates a subset of vesicle proteins. J Cell Biol. 1995 Aug 1;130(3):711–24.

9. Milne D. Catalytic Activity of Protein Kinase CK1δ (Casein Kinase 1δ) Is Essential for Its Normal Subcellular Localization. Exp Cell Res. 2001 Feb 1;263(1):43–54.

10. Scheeff ED, Bourne PE. Structural Evolution of the Protein Kinase–Like Superfamily. PLoS Comput Biol. Public Library of Science; 2005 Oct 21;1(5):e49.

11. Behrend L, Stöter M, Kurth M, Rutter G, Heukeshoven J, Deppert W, et al. Interaction of casein kinase 1 delta (CK1delta) with post-Golgi structures, microtubules and the spindle apparatus. Eur J Cell Biol. 2000 Apr;79(4):240–51.

12. Sillibourne JE, Milne DM, Takahashi M, Ono Y, Meek DW. Centrosomal Anchoring of the Protein Kinase CK1δ Mediated by Attachment to the Large, Coiled-coil Scaffolding Protein CG-NAP/AKAP450. J Mol Biol. 2002 Sep;322(4):785–97.

13. Sato S, Cerny RL, Buescher JL, Ikezu T. Tau-tubulin kinase 1 (TTBK1), a neuron-specific tau kinase candidate, is involved in tau phosphorylation and aggregation. J Neurochem. 2006 Sep;98(5):1573–84.

14. Houlden H, Johnson J, Gardner-Thorpe C, Lashley T, Hernandez D, Worth P, et al. Mutations in TTBK2, encoding a kinase implicated in tau phosphorylation, segregate with spinocerebellar ataxia type 11. Nat Genet. 2007 Dec;39(12):1434–6.

15. Takahashi M, Tomizawa K, Sato K, Ohtake A, Omori A. A novel tau-tubulin kinase from bovine brain. FEBS Lett. 1995 Sep;372(1):59–64.

16. Tomizawa K, Omori A, Ohtake A, Sato K, Takahashi M. Tau-tubulin kinase phosphorylates tau at Ser-208 and Ser-210, sites found in paired helical filament-tau. FEBS Lett. 2001 Mar;492(3):221–7.

17. Lund H, Cowburn RF, Gustafsson E, Strömberg K, Svensson A, Dahllund L, et al. Tau-Tubulin Kinase 1 Expression, Phosphorylation and Co-Localization with Phospho-Ser422 Tau in the Alzheimer's Disease Brain. Brain Pathol. 2012 Nov 20;23(4):378–89.

18. Qi H, Yao C, Cai W, Girton J, Johansen KM, Johansen JR. Asator, a tau-tubulin kinase homolog in Drosophilalocalizes to the mitotic spindle. Dev Dyn. 2009 Dec;238(12):3248–56.

19. Sanz-Garcia M, Lopez-Sanchez I, Lazo PA. Proteomics Identification of Nuclear Ran GTPase as an Inhibitor of Human VRK1 and VRK2 (Vaccinia-related Kinase) Activities. Mol Cell Proteomics. 2008 Nov 6;7(11):2199–214.

20. Kang T-H, Park D-Y, Choi YH, Kim K-J, Yoon HS, Kim K-T. Mitotic Histone H3 Phosphorylation by Vaccinia-Related Kinase 1 in Mammalian Cells. Mol Cell Biol. 2007.

21. Lopez-Sanchez I, Sanz-Garcia M, Lazo PA. Plk3 Interacts with and Specifically Phosphorylates VRK1 in Ser342, a Downstream Target in a Pathway That Induces Golgi Fragmentation. Mol Cell Biol. 2009 Feb 11;29(5):1189–201.

22. Valbuena A, Castro-Obregón S, Lazo PA. Downregulation of VRK1 by p53 in Response to DNA Damage Is Mediated by the Autophagic Pathway. PLoS ONE. Public Library of Science; 2011 Feb 28;6(2):e17320.

23. Monsalve DM, Merced T, Fernández IF, Blanco S, Vázquez-Cedeira M, Lazo PA. Human VRK2 modulates apoptosis by interaction with Bcl-xL and regulation of BAX gene expression. Cell Death Dis. 2013;4:e513.

24. Vázquez-Cedeira M, Lazo PA. Human VRK2 (vaccinia-related kinase 2) modulates tumor cell invasion by hyperactivation of NFAT1 and expression of cyclooxygenase-2. Journal of Biological Chemistry. 2012 Dec 14;287(51):42739–50.

25. Steinberg S, de Jong S, Andreassen OA, Werge T, Børglum AD, Mors O, et al. Common variants at VRK2 and TCF4 conferring risk of schizophrenia. Hum Mol Gen. 2011.

26. Nichols RJ, Traktman P. Characterization of three paralogous members of the Mammalian vaccinia related kinase family. J Biol Chem. 2004 Feb 27;279(9):7934–46.

27. Scheeff ED, Eswaran J, Bunkoczi G, Knapp S, Manning G. Structure of the pseudokinase VRK3 reveals a degraded catalytic site, a highly conserved kinase fold, and a putative regulatory binding site. Structure. 2009 Jan 14;17(1):128–38.

28. Kang T-H, Kim K-T. Negative regulation of ERK activity by VRK3-mediated activation of VHR phosphatase. Nat Cell Biol. 2006 Jul 16;8(8):863–9.

29. Kang T-H, Kim K-T. VRK3-mediated inactivation of ERK signaling in adult and embryonic rodent tissues. Biochim Biophys Acta. 2008 Jan;1783(1):49–58.

30. McCracken A, Locke J. Mutations in CG8878, a novel putative protein kinase, enhance P element dependent silencing (PDS) and position effect variegation (PEV) in Drosophila melanogaster. PLoS ONE. 2014;9(3):e71695.

31. Eddy SR. Profile hidden Markov models. Bioinformatics. 1998.

32. Edgar RC. MUSCLE: multiple sequence alignment with high accuracy and high throughput. Nucleic Acids Res. 2004;32(5):1792–7.

33. Swarup S, Pradhan-Sundd T, Verheyen EM. Genome-wide identification of phospho-regulators of Wnt signaling in Drosophila. Development. 2015 Apr 15;142(8):1502–15.

34. Aihara H, Nakagawa T, Yasui K, Ohta T, Hirose S, Dhomae N, et al. Nucleosomal histone kinase-1 phosphorylates H2A Thr 119 during mitosis in the early Drosophila embryo. Genes Dev. 2004 Apr 15;18(8):877–88.

35. Lancaster OM, Cullen CF, Ohkura H. NHK-1 phosphorylates BAF to allow karyosome formation in the Drosophila oocyte nucleus. J Cell Biol. Rockefeller Univ Press; 2007;179(5):817–24.

36. Ivanovska I. A histone code in meiosis: the histone kinase, NHK-1, is required for proper chromosomal architecture in Drosophila oocytes. Genes Dev. 2005 Nov 1;19(21):2571–82.

37. Cullen CF. The conserved kinase NHK-1 is essential for mitotic progression and unifying acentrosomal meiotic spindles in Drosophila melanogaster. J Cell Biol. 2005 Nov 14;171(4):593–602.

38. Herzig B, Yakulov TA, Klinge K, Günesdogan U, Jäckle H, Herzig A. Bällchen is required for self-renewal of germline stem cells in Drosophila melanogaster. Biol Open. 2014 May 29.

39. Yakulov T, Günesdogan U, Jäckle H, Herzig A. Bällchen participates in proliferation

control and prevents the differentiation of Drosophila melanogaster neuronal stem cells. Biol Open. 2014;3(10):881–6.

40. Zhang Y. I-TASSER server for protein 3D structure prediction. BMC Bioinformatics. 2008;9:40.

4. Chapter 4: *Banshee* mutants have lethality in early development

Introduction

A forward genetic screen found *banshee* (*bshe*) was an *Enhancer of variegation* (*E(var)*) and an essential gene (1). This suggests that it has a role in maintaining chromatin in a euchromatic state or setting up the heterochromatin/euchromatin boundaries, since the mutant phenotype in this screen results in spread of silencing heterochromatin. Its lethal phenotype suggests that it has an essential role, probably in development. By learning more about the nature of *bshe*'s mutant phenotype, we can understand more about its biological role.

Available *bshe* mutants

A former PhD student, Allen McCracken obtained seven independent mutations in a mutagenic screen (1). Of those seven mutations two were the same mutagenic lesion, so there are five unique lesions (Figure 4.1). Four of them are found within the coding region of the gene. The fifth is a four base pair deletion within the E-box of the promoter. Of the four within the coding sequence, two of them had a GC to AT transition mutation leading to a premature stop codon. One had a single base pair deletion leading to a frame shift and stop codon. The last has a GC to AT transition, abolishing the intron donor splice site, leading to a stop codon. All coding sequence mutants have some or the entire kinase domain truncated.

Function and mutant phenotype of *ballchen*

Based on the previous chapter we now know that the most similar gene to *bshe* in Drosophila is *ballchen (ball)*. BALL is a histone kinase with roles in neurogenesis and neuronal stem cell maintenance, male and female stem cell maintenance, female meiosis, and karyosome formation (2-7). It phosphorylates histone H2A Thr119, only in the presence of chromatin (8). *Ball* is an essential gene. When observing *ball* mutants, all larvae hatch normally and proceed through all larval stages behaving and growing normally, but die in early pupation (3). Upon dissection, third instar larvae were missing or had degenerated imaginal discs and a poorly developed central nervous system (3). The reason for the degenerate mitotic tissues was shown to be that *ball* is required for proper spindle organization in somatic mitosis (3). Hypomorphic alleles, which reduce but not abolish the expression of *ball* are not lethal, but show female fertility defects or

sterility. This was later shown to also be due to spindle defects during female meiosis (3). *ball* is also required for the self-renewal of germ line stem cells in both males and female, which can contribute to fertility defects (6).

Research goals

Exploration of *ball* mutant phenotype lead to greater understanding of its function in development. Similarly, characterizing *bshe* mutant phenotype could lead to a greater understanding of its role. *Bshe* mutants have already been identified as lethal prior to adulthood, so further characterization of the timing, morphology and behaviour of the lethal individuals will elucidate the developmental time and potential tissues where *bshe* is required.

The lethality of *bshe* mutants prevents investigation of its role in adult tissues. In order to observe the adult phenotypes of *bshe*, I looked for phenotypes using an RNAi strain with a *bshe* knockdown responder transgene in combination with four tissue specific drivers. The goal of this is to observe the potential phenotype of the knockdown to determine *bshe*'s role in individual tissues, without killing the fly.

Once the time of lethality is known, this will provide clues for when and where *bshe* is necessary for development. Knowing the developmental time points and some tissue candidates will help further elucidate the function of *bshe* in the cell and in development. If RNAi knockdowns provide strong and consistent phenotypes, they could be useful in future experiments to isolate *bshe*'s role in specific cells and tissues, without risk of affecting the whole organism.

Results and Discussion

Mutant Lethality Experimental Setup

To begin my experiment to determine the lethal stage of the mutants, I had to develop a way to determine whether individuals had the mutation or not. To do this, I used a second chromosome *CyO* balancer that had a *P* element insert carrying an *act-GFP* gene (this chromosome will be called *CyO-GFP*), balancing the mutant *bshe* genes. This will allow identification under a fluorescent microscope of the balancer chromosome. A cross involving two individuals with this balancer will generate: 25% of the offspring with a homozygous balancer that should have double fluorescence as an

embryo, but are also embryonic lethal; 50% heterozygous with fluorescence; and 25% homozygous mutant that lack fluorescence, which will be the object of study. Fluorescent heterozygote siblings were used as controls in the length experiment (Figure 4.3, described later).

An initial observation was done to roughly determine when the homozygous mutants died. Three mutants were chosen: the earliest stop codon *3a52a*, a middle stop codon *3a66a*, and the E-box deletion *3a90a* (Figure 4.1). All were tested with the *CyO-GFP* balancer described above. Mass larvae collections were done, where *bshe / CyO-GFP* flies of each mutant strain were crossed to themselves (eg. *3a52a* x *3a52a*), allowed to continuously lay eggs for 3-5 days and then larvae were collected and scored for presence or absence of GFP. These collections were done multiple times and the data compiled. Note: this is not the ideal way to measure survivability of each mutant strain, as the lethal phenotype may be affected by other mutations on the chromosome becoming homozygous. Laying for 3-5 days also causes crowding which can further affect larvae, particularly sick larvae. Therefore this is only an initial look into the survivability of each mutant.

If the mutant larvae were not lethal, we would expect 33% to not have GFP. Any percentage lower than 33% of non-GFP larvae would show that larvae were dying before that stage. The three different mutants all had different levels of survivability (Figure 4.2A). *3a52a* (early stop) has the 33% non-GFP 1st instar larvae, but they are reduced by 2nd instar and completely lacking in 3rd instar larvae. *3a66a* (middle stop) mutants are decreased by the first instar and thus appear not to hatch, or if they do they die early. Despite this, those that do survive hatching persist until 3rd instar. *3a90a* (E-box deletion) has more than expected at 1st instar (a sampling error). None appear to survive past the first instar.

Despite lethality, it appears that some *bshe* mutants have the ability to survive into the larval stages. Because of this observation, I chose to look at the larvae in more detail.

Mutant *bshe* larvae have delayed molting

After finding that some homozygous *bshe* mutants survive into the larval stages, I wanted to observe the health and growth rates of larvae until they died. Initially I began this experiment with crossing the mutant with the earliest stop codon, *3a52a*/*CyO-GFP*, to itself (Figure 4.1). The mutants were generated through EMS, and so there are likely multiple lesions on the chromosome, some of which could affect the mutant phenotype when homozygous. Because of this, these initial results are possibly not an accurate portrayal of the mutant phenotype, and so will be presented in the Appendix. Larvae in this test did survive for a certain period of time, and will be discussed later in this chapter for that trend of surviving a portion of larvalhood.

I repeated this protocol again, this time crossing female *3a52a/CyO-GFP* to male *Df(2R)BSC699/CyO-GFP*. *Df(2R)BSC699* is a deficiency that deletes the *bshe* gene region, so non-fluorescent offspring will be hemizygous for the mutant allele. I collected larvae within an hour of hatching and scored for presence or absence of GFP. I then monitored and measured each individual larvae every 12 hours until they died or pupated (full methods can be found in Chapter 2). A total of 8 hemizygous mutant and 8 control larvae were observed in this way. While the initial round with homozygous chromosomes showed a difference in growth rate of larvae (Appendix), this round with hemizygous mutants showed the growth rate was not significantly different (Figure 4.3A). Larvae were typically smaller when close to death, and so affected the curves of both hemizygous mutants and controls that died. When separating the mutant and control larvae into cohorts by whether they died or survived to pupae did not show a difference in length (Figure 4.3B). In fact, many controls died during this experiment, suggesting that my handling of the larvae could have contributed to their deaths, or that this small sample size included control larvae that would have naturally died anyway (Figure 4.3D).

There was a difference between mutant and control where molting was concerned (Figure 4.3C). Comparing the control to the hemizygous mutants at the first molt, the control molted at around 41 hours while the mutants molted at around 49 hours. While the molting times from first to second instar are not significantly different, for the molting from second to third instar, and the time of pupation is significantly later in the

hemizygous mutants that survived that long. Controls completed their second molt at around 90 hours, and mutants at around 117 hours; and controls pupated at 179 hours, with surviving mutants pupating at 231 hours. This could suggest that there is some checkpoint event that allows for molting or pupation that is delayed. It is not possible to make many conclusions on this, as so few mutants and controls were used, and many controls died in this experiment. Repeating this experiment to obtain higher numbers for both mutants and wildtype would provide more substantial support for the trend that was seen.

Early lethality in reciprocal cross

Attempting to repeat the experiment to get a higher n-value for both mutants and controls, proved difficult. The crosses were set up with the male *3a66a/CyO*-GFP or *3a52a/CyO-GFP* crossed to female *Df(2R)BSC699/CyO-GFP*. Previously the male and female parents were opposite. From these embryo cages I was unable to find any non-fluorescent hemizygous mutant larvae after hatching.

Since I only wanted to observe molting times, in my next attempt to repeat the experiment the method of collecting and analyzing larvae was changed. Because the process of picking larvae and measuring individual larvae is time intensive and to try and observe a larger number of larvae, I chose to instead do 5-10 hour egg lays, wait a period of time, and score for fluorescence and molting stage. Enough embryo plates were collected to cover the entire larval development. This was done to get a large number of larvae and observe them for delayed molting. The larvae were all from the same parental cages, just different cohorts. This was done for both *3a66a* and *3a52a* mutants, which was the original experiment. Similarly to the last attempt, little to no mutant larvae were found at any stage of development (Table 4.2).

Discussion of early lethality

For clarity, the four different experiments will be labeled as follows: Initial trial discussed in Appendix (Trial #1), individual embryo collection from Figure 4.3 (Trial #2), individual embryo collection with no hemizygous mutants seen (Trial #3), and mass larvae collection with no hemizygous mutants seen from Table 4.2 (Trial #4).

This discrepancy between the first two results (Trial #1 and Trial #2) and the latter two results (Trial #3 and Trial #4) was unexpected. Embryo collections were done from the same stock parents, with the exception of also using *3a66a* in Trial #3 and #4. They were kept on the same media, in the same style of cages, in similar densities. They were all raised in the same 25ºC incubator. Upon further inspection, only one difference is seen between the different trials: the male and female parents were reversed. In Trial #2 the cross was the male deficiency line crossed to the female mutant line, and Trial #3 and Trial #4 had male mutant line crossed to the female deficiency line. Trial #1 had both male and female parents as mutants (no deficiency). This suggests either a maternal or paternal effect on the early viability of the offspring.

Trial #1 was a cross in which both parents were *3a52a*, and Trial #2, with the males as the deletion and the females as *3a52a bshe* mutants showed a less severe phenotype where the majority of the offspring survived at least till the larval stages. Trials #3 and #4 both had males, which were *3a52a* or *3a66a bshe* mutants and females of the deletion strain had a more severe phenotype with little to no hemizygous larval seen, so the hemizygous mutant progeny died during embryogenesis.

Trial #3 and #4 which both had two different *bshe* alleles (*3a52a* and *3a66a*) as males showed a stronger lethality. This suggests that the lethality likely is not because of a second site mutation caused by EMS, since the likelihood of both alleles independently having a mutation in the same gene is low. Also Trial #1 in which both parents were the *3a52a bshe* mutant shows longer viability (Appendix), which suggests that it is not the male *bshe* mutant that causes the increased lethality. Additionally, this observation fails to support the hypothesis that a second EMS mutation is causing the early lethality.

This does support the hypothesis that the deficiency chromosome, when it is used as a female parent, causes a more severe lethality. The deficiency *BSC699* spans 36 genes, 11 of which (*bshe* excluded) have listed lethality or decreased viability (Table 4.3), along with many unstudied genes. This stock is healthy as a balanced stock, so possibly a combination with *bshe* mutant leads to a maternal affect lethal haploinsufficency. A maternal effect lethal is supported by the RNA-seq and microarray

data on Flybase.org. There is moderate to high expression in the ovaries and early embryo respectively (9). This could suggest that a threshold amount of BSHE protein may be required to support the delayed lethality, which the mutant mother can supply but the deficiency mother cannot.

There may be other explanations for the cause of the differences in lethality of larvae and embryos, but based upon the information known so far, this appears the most reasonable. The reason for the discrepancy with the stage of lethality has to be addressed. Once found, the results should be repeated to take into account the cause of this discrepancy, to find the true timing of lethality.

Differences in mutants from *ballchen*

When comparing the results observed in *ball* mutants to my *bshe* mutants, we see differences. The *ball* mutants hatch and appear normal in growth and behaviour up until pupation, when they die at a discrete point. Dissections of third instar larvae show that they have degenerated or missing imaginal discs, and similarly degenerated central nervous system (3). This shows that *ball* is essential for growth of the mitotic tissues, as the endoreplicative larval tissues grow normally. With *bshe*, the results suggest either that it is an embryonic lethal mutant, or that the gene is involved in some system that affects the molting and ability to thrive as larvae, which could be many. Because of the conflicting results seen in repetitions of experiments, no conclusive explanations can be made at this time. The experiment needs to be repeated and the discrepancy resolved. Whichever phenotype represents the true mutant however, neither appears to be similar to *ball*. This suggests that *bshe* is involved in something that is required earlier in development, as opposed to just involved in mitotic cells of larvae.

Some roles of BSHE have recently been identified in multiple screens. In an RNAi cell culture screen looking for factors impacting RAS-mediated MAPK activation in the RAS/MAPK signaling pathway, *bshe* is found to be a positive regulator of RAS signaling (10). Through epistasis experiments they found that *bshe* acts downstream of RAF and upstream of MEK in the pathway. Also *bshe* was found in an *in vivo* RNAi screen looking for kinases and phosphatases that regulate the WNT pathway within the wing disc. Note that *bshe* was identified as a kinase here because it has previously been characterized as a part of the Casein Kinase 1 family, not because it has been shown to have kinase

activity (11). In this screen, *bshe* was identified as a positive Wnt pathway regulator that functions downstream of the ligand-receptor interaction in the cells receiving the signal, and this interaction does not involve Notch (12). While neither of these screens point to a possibility of *bshe* being a histone kinase as predicted, they do show a major involvement in developmental processes that might explain the failure to thrive and lethality seen in the *bshe* mutants.

RNAi knockdown experimental setup

The RNAi system was set up using the *Drosophila* GAL4/UAS system (13). Initial crosses were unsuccessful upon discovering that the UAS-driven inverted repeat transgene lines from Bloomington Stock Center (Stock numbers: 35571,31350,35175,42483) were made for expression in the germline only, so no phenotype was seen (results not shown). The experiment was repeated with three *UAS-bshe* lines and one *UAS-ball* line from Vienna Drosophila Resource Center (VDRC). One *UAS-bshe* line was made from the VDRC KK library (100985) and will be referred to as *UAS-bshe* KK, and two *UAS-bshe* lines are from the VDRC GD library (28970 and 28971) and will be referred to as *UAS-bshe* GD1 and *UAS-bshe* GD2 respectively. All *UAS-bshe* RNAi lines are homozygous viable. The *UAS-ball* line is from the KK library, and is a balanced lethal over *CyO*. Four GAL4 driver lines were used: *eyeless* (*ey*), *embryonic lethal abnormal vision* (*elav*), *neuralized* (*neur*), and *actin* (*act*). The ubiquitous *act-GAL4* driver was chosen to observe if there are threshold effects of BSHE. The neural drivers *elav-GAL4* and *neur-GAL4* were chosen as a comparison to *ball* and other *VRK* genes, as they are usually found within neural tissues. The *ey-GAL4* driver was chosen as an easily scored developmental tissue.

Each line of both GAL4 and UAS has different balancers, so for each I will note the expected proportions of each progeny class.

Elav-GAL4

The *elav-GAL4* line is a homozygous line, and because all the *UAS-bshe* lines are homozygous as well, all the progeny should have an RNAi knockdown. The *UAS-ball* line (*CyO/UAS-ball*) will have 50% RNAi knockdown and 50% *CyO* balancer phenotype.

All *elav-GAL4* crosses showed no discernable phenotype morphologically, behaviorally or in developmental timing with any of the UAS lines (Table 4.1). This suggests that either *bshe* doesn't have a significant role in tissues expressing *elav*, which include developing and differentiated peripheral and central nervous system from embryos right through to adulthood (14), or the knockdown was not strong enough in those tissues to produce a noticeable affect.

Neur-GAL4

The *neur* gene is expressed in embryogenesis in the neurogenic ectoderm and in neuroblasts, and also seen in the sensory precursor cells on imaginal discs (15). If *bshe* has a function in these tissues, we expect to see some sort of mutant neural phenotype, or possibly lethality if a knockdown has a major negative effect in these tissues.

Because of the balancers present in the *neur-GAL4* strain, for the *UAS-bshe* crosses I expect 50% of the progeny to be *TM6b* balancer and 50% to be RNAi knockdown. For the same GAL4 driver with the *UAS-ball* crosses I expect 25% to be *CyO* balancer, 25% to be *TM6b* balancer, 25% to be both *CyO* and *TM6b* and 25% to be RNAi knockdown.

Actual ratios of balancer are less than expected for all three *UAS-bshe* crosses, and the *CyO TM6b* combined class is completely missing from the *UAS-ball* cross (Figure 4.4A). Discussion of expected and actual ratios of all RNAi lines together is found after all RNAi experiments are discussed.

Bristle defects were seen in the *bshe* knockdown with the *neur-GAL4* driver, but in low frequencies (Figure 4.4A). The highest frequency was seen in *UAS-bshe KK*, though still over half (62%) of the non-balancer flies had no visible phenotype. There were a variety of bristle defects seen, mostly in the humeral and scutellar bristles. In the humeral region, there was a variable loss of both major and minor bristles. This ranged from losing one of the two major bristles (Figure 4.5B and D), losing both major bristles but still having minor bristles (Figure 4.5C), or a complete loss of all bristles in the humeral region (Figure 4.5A). In the scutellar region, where typically there are four major bristles, there was some loss or gain of bristles (Figure 4.5E and F). Also, in only two cases there was a cluster of steurnopleural and notopleural bristles, respectively

(Figure 4.5G and H). This was a rare event, and as Figure 4.4 shows, the majority of the time in all *bshe* and *ball* knockdowns, the flies looked normal.

The control balancer flies were unable to be scored for loss of bristles, as the balancer had the *humeral* mutation, causing excess humeral bristles. No abnormal scutellar bristles were seen. A better control would be outcrossing the *neur-GAL4* driver to observe it alone, but this cross was not performed.

ey-GAL4

The *eyeless* (*ey*) gene is one of the *Drosophila Pax6* genes involved in eye development (16,17). It also has expression in central nervous system development, including the ventral nerve cord and the brain (18,19). A mutant phenotype would be expected in the eye or nervous system.

Expected ratios of the *UAS-bshe* to the *ey-GAL4* crosses are as follows: 50% will be *TM6b* balancer and 50% will be RNAi knockdown. For the same GAL4 driver and the *UAS-ball* cross the expected ratios are 33% *CyO* balancer, 33% *TM6b* balancer and 33% RNAi knockdown.

The actual ratios of the *UAS-bshe* cross progeny show lower than expected for the *TM6b* balancers. For the *UAS-ball* cross the ratios are as expected (Figure 4.4B). Discussion of expected and actual ratios of all RNAi lines together is found after all RNAi experiments are discussed.

The *ey-GAL4* tissue knockdown of *bshe* or *ball* show a disorganization or reduction in the ommatidia of the eye, ranging from minor disorganization (Figure 4.6A) to partial reduction with disorganization (Figure 4.6B and C) to a dramatic reduction in the eye (Figure 4.6D). The most dramatic reduction observed was an eye with less than 10 ommatidia (no photograph taken). Like in the *neur-GAL4* driver, penetrance was poor, particularly in *UAS-bshe* GD1 and GD2 and *UAS-ball* KK (Figure 4.4B). The percentage of non-balancer progeny with eye defects in the *UAS-bshe* KK*, UAS-bshe* GD1*, UAS-bshe* GD2*,* and *UAS-ball* KK lines respectively are: 53%, 13%, 6% and 3%. The defects were also not consistent in both eyes of an affected fly. One eye may be normal, while the other was disorganized or reduced.

A phenotype like this suggests *bshe* has a role in maintaining the survival of cells forming eye structures. During larval development the eye goes through a wave of differentiation called the morphogenetic furrow. The ability to observe expression and localization of normal or knockdown *bshe* with antibodies in these tissues could have an insight into its role in the eye, or possibly broader tissues overall. The lack of penetrance of this phenotype may cause difficulty in obtaining definitive results if this experiment was repeated.

Act-GAL4

Actin is a major structural protein that is expressed in high amounts in all cells. With this driver I would expect knockdown of *bshe* and *ball* in all tissues, possibly giving a similar lethal phenotype as in the mutant. Because RNAi is never a complete knockdown there may be some survival, if a threshold of protein is sufficient for survival.

The expected ratios of the progeny when *act-GAL4* is crossed to the *UAS-bshe* strains are 50% with a *CyO* balancer phenotype and 50% RNAi knockdown. With the same GAL4 crossed to the *UAS-ball* strain, 66% should be *CyO* balancer and 33% should be RNAi knockdown.

The actual ratios of the progeny for the *UAS-bshe* KK line, show 93% of the progeny is *CyO* balancer phenotype (Figure 4.4C). This higher proportion of balancer shows that the RNAi knockdown has lethality before adulthood. The *UAS-bshe* GD1 and GD2 lines both show expected ratios (46% *CyO* balancer, and 51% *CyO* balancer, respectively) (Figure 4.4C). For the *UAS-ball* line, 25% have no balancer and 75% have the *CyO* phenotype (Figure 4.4C). This is statistically different from the expected 33% : 66% (X^2 P value: 0.0227). So, similar to the *UAS-bshe* KK cross, a higher ratio of balancer indicates that the RNAi knockdown is partially lethal.

Of those adult flies that survived and were not a balancer, some looked normal and healthy. Looking at non-balancer progeny, for *UAS-bshe* KK 63% were normal, for *UAS-bshe* GD1 64% were normal, for *UAS-bshe* GD2 36% were normal and for *UAS-ball* KK 62% were normal. The others, while otherwise healthy, did have some abnormal bristle phenotypes. These include similar loss of humeral bristles as seen in the *neur-GAL4*

driver. There was also either a loss or gain of scutellar bristles, or a normal amount of scutellar bristles, but with abnormal morphology (Figure 4.7).

Observing the *act*-GAL4 driver can also serve as a control for the extent of knockdown with other drivers. It appears that the *UAS-bshe* KK line has a much stronger knockdown effect compared to the two *UAS-bshe* GD lines used, with only 8 out of 126 flies scored surviving to adulthood, while ratio of balancer flies surviving in the two GD lines is expected showing no lethality.

Act-GAL4 UAS-bshe knockdown shows pupal lethality

Because most of the *UAS-bshe KK* line with the *act* driver died before adulthood, I wanted to observe when in development this cross died, and if it was similar to the survivability seen with the initial mutant cross. By setting up the cross in a similar way to the mutant survivability, with the parent *act-GAL4/CyO-GFP* crossed with the homozygous *UAS-bshe* KK line, doing 5-7 day long egg lays and then scoring for the presence or absence of GFP. In this cross, 50% will not be a knockdown and have GFP, while 50% will have the RNAi knockdown and be lacking GFP. Figure 4.2B shows that the larvae appear in normal ratios from 1st instar through to pupae. A decrease in survivability was observed at the adult stage. This suggests that the critical point with this knockdown is sometime during pupal development. This knockdown strain could prove useful in studying larval tissues in late 3rd instar or pupa to see what the critical defect is that prevents survivability of this knockdown cross.

Discussion of RNAi progeny ratios

Many of the RNAi results show unexpected ratios of balancer progeny. A summary of expected and actual ratios that have been described previously for all crosses is listed in Table 4.4. Both *UAS-bshe* and *UAS-ball* crossed to the *act-GAL4* lines showed a lethal or expected phenotype ratio, and the *UAS-ball* crossed to *ey-GAL4* showed an expected phenotype ratio. The rest have unexpected ratios that point to missing balancer progeny. This could mean that the dominant balancer phenotypes were subtle enough that they were mistaken for normal, increasing that class of progeny. This could also suggest that some balancer progeny were dying.

At this time the RNAi experiments did not provide anything strong and consistent, with decent enough penetrance to allow for easy further experiments. Once the *bshe* antibody is optimized, exploring protein localization and overall morphology of the eye imaginal discs in the *ey-GAL4* driver RNAi could show some useful results.

Conclusions

Analysis of the *bshe* mutations is still ongoing. Reciprocal crosses of mutants to deficiency show a likely maternal effect change to survivability. One has survivability into larvalhood, while the other is embryonic lethal. The results suggest a maternal effect on the survivability of hemizygous mutant offspring. This could either be due to another mutation in the region of the deficiency compounding the already mutant offspring, or that the deficiency female does not provide enough maternal *bshe* mRNA or protein for survivability past embryogenesis. Further research is required to explore the lethality of *bshe* mutants in order to more completely understand its function and necessity for development.

RNAi knockdowns of *bshe* produced variable results. At this time the *act-GAL4* driver with the *UAS-bshe KK* responder is the most hopeful for future research. It has a near complete lethality, but survives to pupation. This could be used to study larval development of a *bshe* knockdown in a way that could not be done in the mutants because they do not survive that long. This would be a useful endeavor in the future for understanding the role of *bshe*.

Figures and Tables

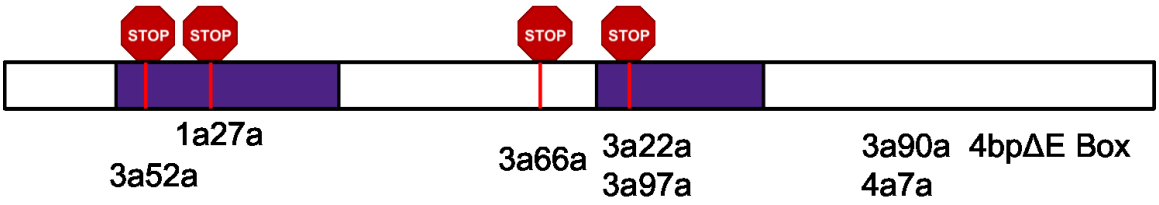

Figure 4.1. Location of *bshe* mutations.
Seven independent mutations were recovered from a genetic screen for *Enhancers of variegation* with PDS previously done in our lab (1). Two recovered mutants had the same mutagenic lesions as two other mutations, making five unique mutations. The five mutations separate into four with premature stop codons (*3a22a* and *3a97a* had the same change) and one pair (*3a90a* and *4a7a*) with a four base pair deletion in the enhancer box (E-box) of the promoter region. The purple sections show where the interrupted kinase domain is.

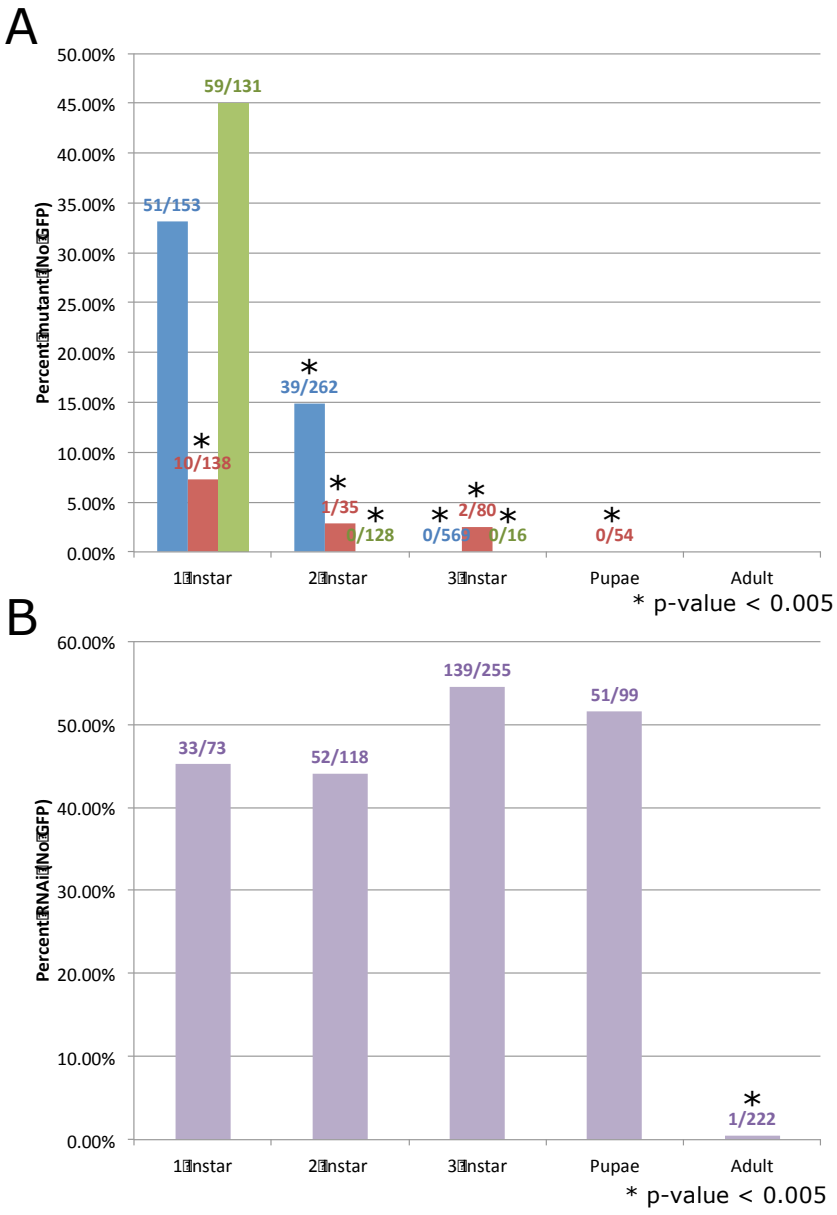

Figure 4.2. Survival of *bshe* mutant and RNAi larvae.
(A) Crosses were set up and larvae were collected from mutants *3a52a* (blue), *3a66a* (red) and *3a90a* (green). The outcome of these crosses expect that one-third of the larvae should be homozygous mutant and lack GFP if the larvae survive, with any number significantly less indicating lethality. Numbers above each bar indicate the number of non-GFP larvae scored out of the total number scored for each larval stage and mutant respectively.
(B) Crosses were set up between *bshe* KK UAS and *act-GAL4 / CyO-GFP*. Larvae were scored similarly to the mutants, with the expectation that one half of the larvae will be a *bshe* RNAi knockdown and lack GFP if the larvae survive. Numbers above each bar indicate the number of non-GFP larvae scored out of the total number scored for each larval stage.
Statistical significance for both was calculated using a chi-squared (X^2) test. Expect 1/3 non-fluorescent in (A) and ½ non-fluorescent in (B).

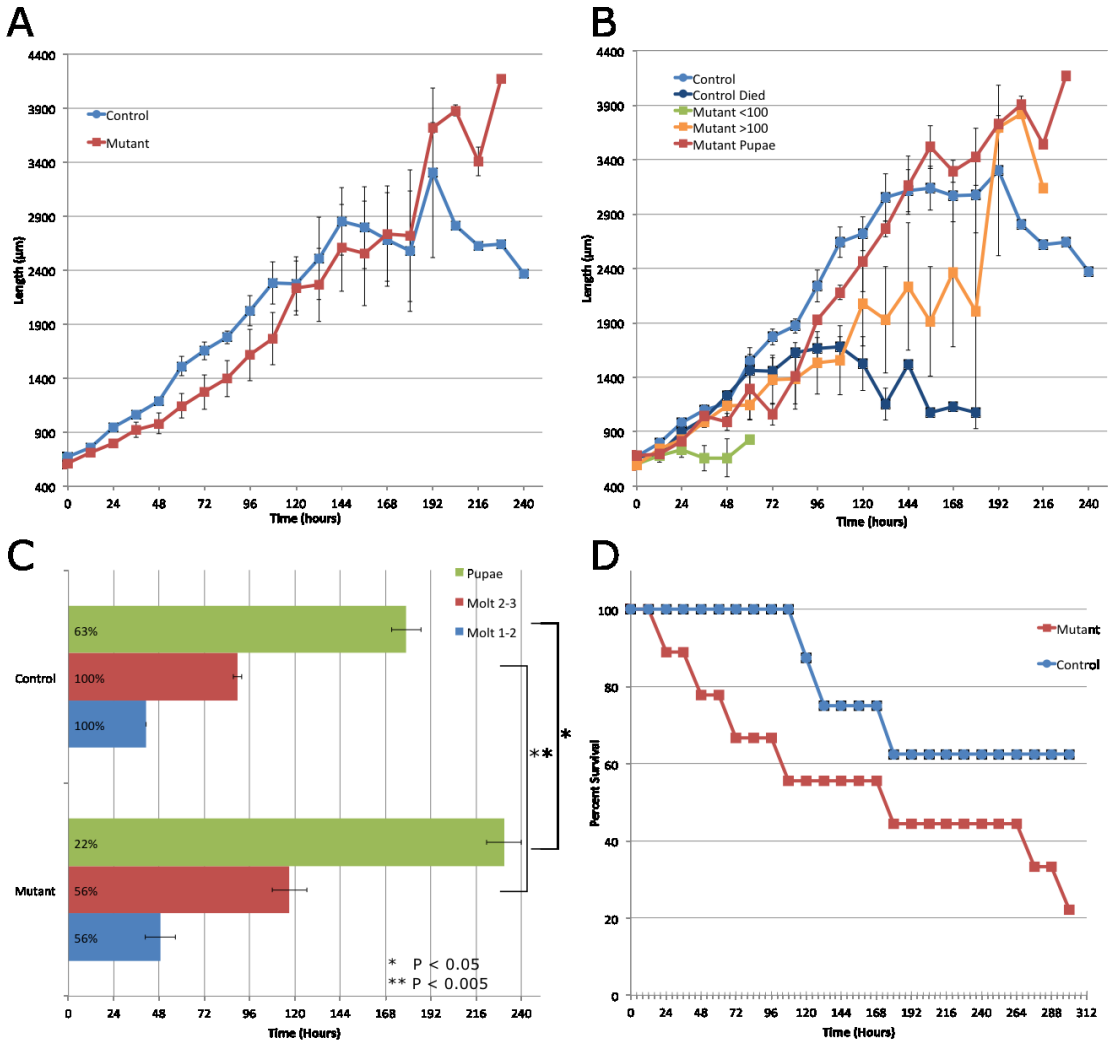

Figure 4.3 Mutant larval growth rates, molting and survivability over time. *Bshe* mutant *3a52a/CyO-GFP* crossed to *Df(BSC699)/CyO-GFP* parents were crossed and eight GFP positive (control) larvae and eight GFP negative (mutant larvae) were observed individually till pupation or death. (A) Control (blue circle) and mutant (red square) larvae length over time.
(B) Larvae length were divided into cohorts representing control that lived (light blue circle), controls that died (dark blue circle), mutants that lived less than 100 hours (green square), mutants that lived more than 100 hours but died before pupation (orange square) and mutants that died after pupation (red square).
(C) Average time when larvae molted from 1st to 2nd instar (blue), 2nd to 3rd instar (red) or pupated (green) between mutants and controls. Numbers within the bars represent the percentage of larvae that survived that molt. Two-tailed two-sample homoscedastic t-test to determine the significance of the molting times.
(D) Survival curve of mutant (red square) and control (blue circle) larvae over time.

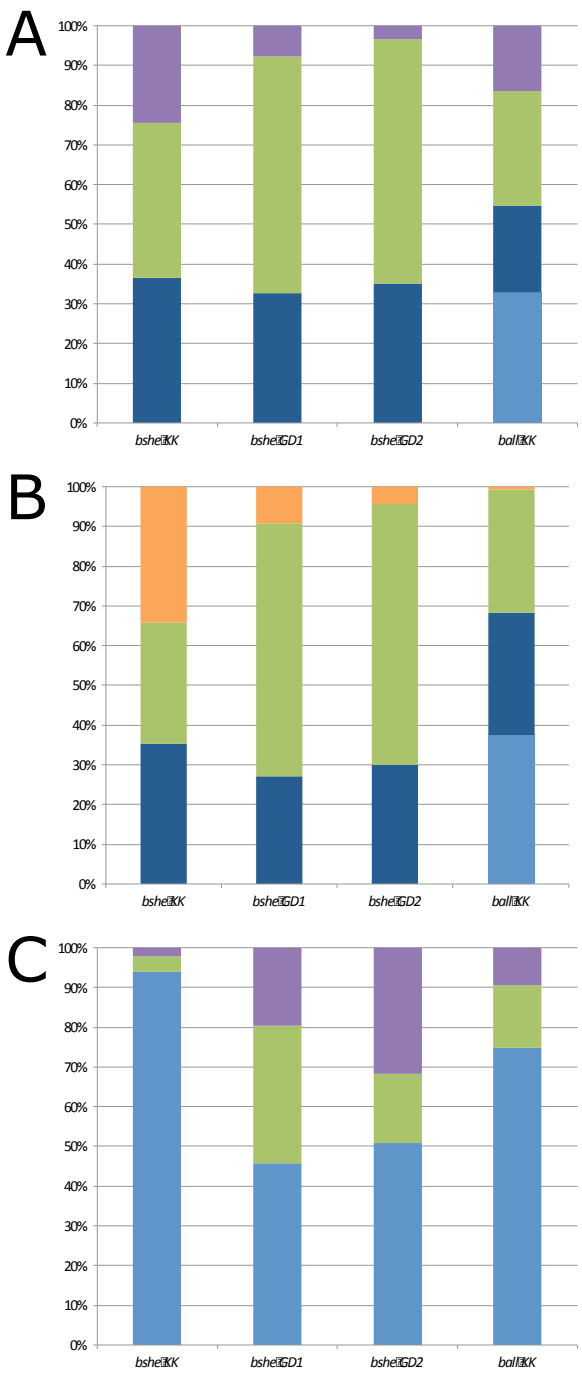

Figure 4.4. Results of RNAi knockdown experiment. Each cross was done with the UAS lines from VRDC: *UAS-bshe* KK, *UAS-bshe* GD1, *UAS-bshe* GD2 and *UAS-ball* KK. The GAL4 driver lines used were
(A)*neur-GAL4*
(B) *ey-GAL4* or
(C) *act-GAL4* .
Each cross is set up differently, and so has different proportions of balancers. *CyO/SM6a* (Curly phenotype) balancers are light blue. *TM6b* (Humeral phenotype) balancers are dark blue. Normal, or no noticeable phenotypes are green. Abnormal bristle phenotypes are purple. Abnormal eye phenotypes are orange.

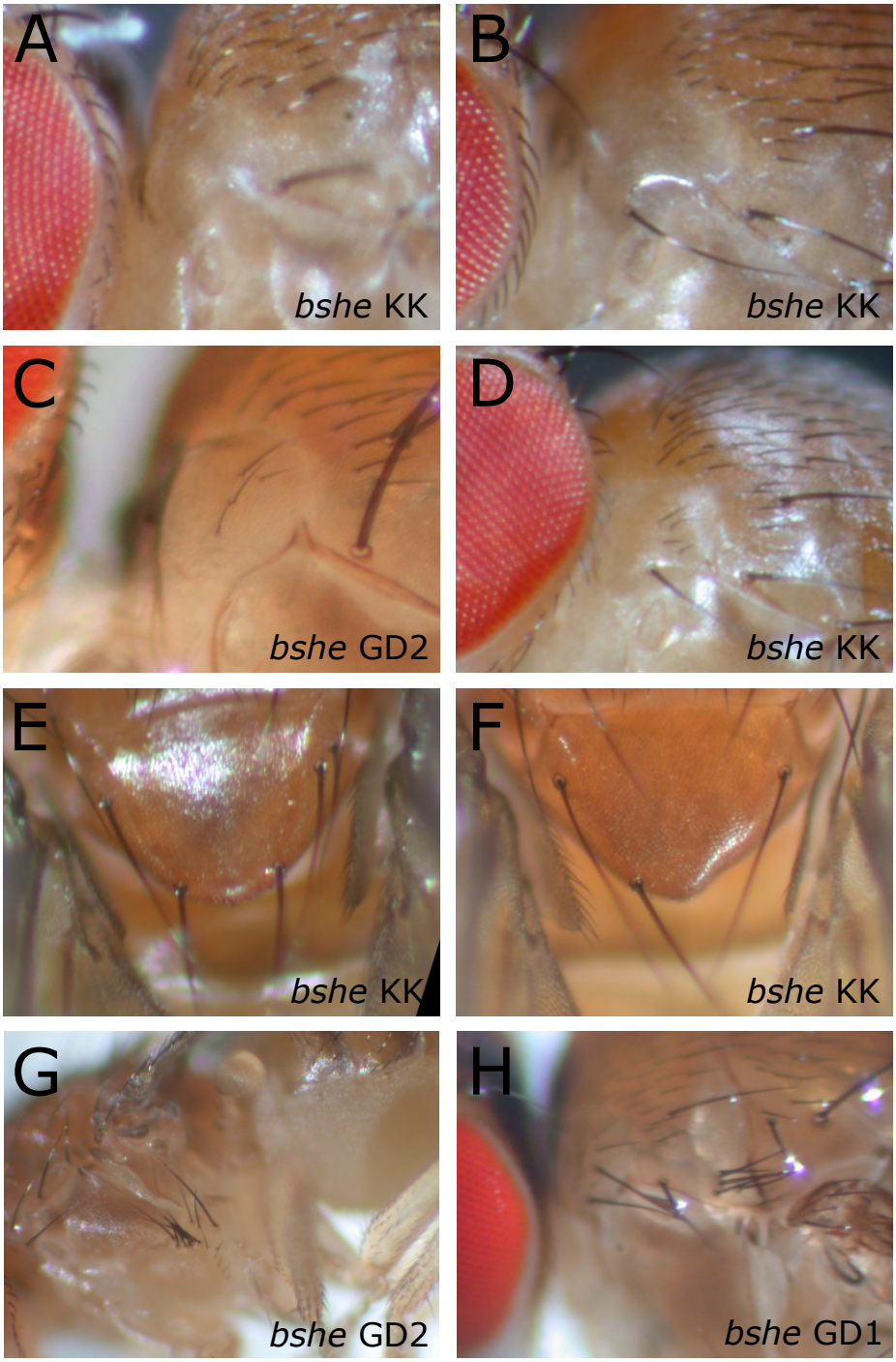

Figure 4.5. Abnormal bristle phenotypes seen with the *neur-GAL4* driver and *UAS-bshe* responder.
(A-D) Different abnormal humeral bristles. Humeral bristles normally have two major bristles and approximately 10 minor bristles.
(E-F) Gain or loss of scutellar bristles. There are normally four scutellar bristles.
(G-H) Clustered bristles seen in sternopleural region (G) and notopleural region (H).

Name in the bottom right corner shows the UAS stock represented in the picture.

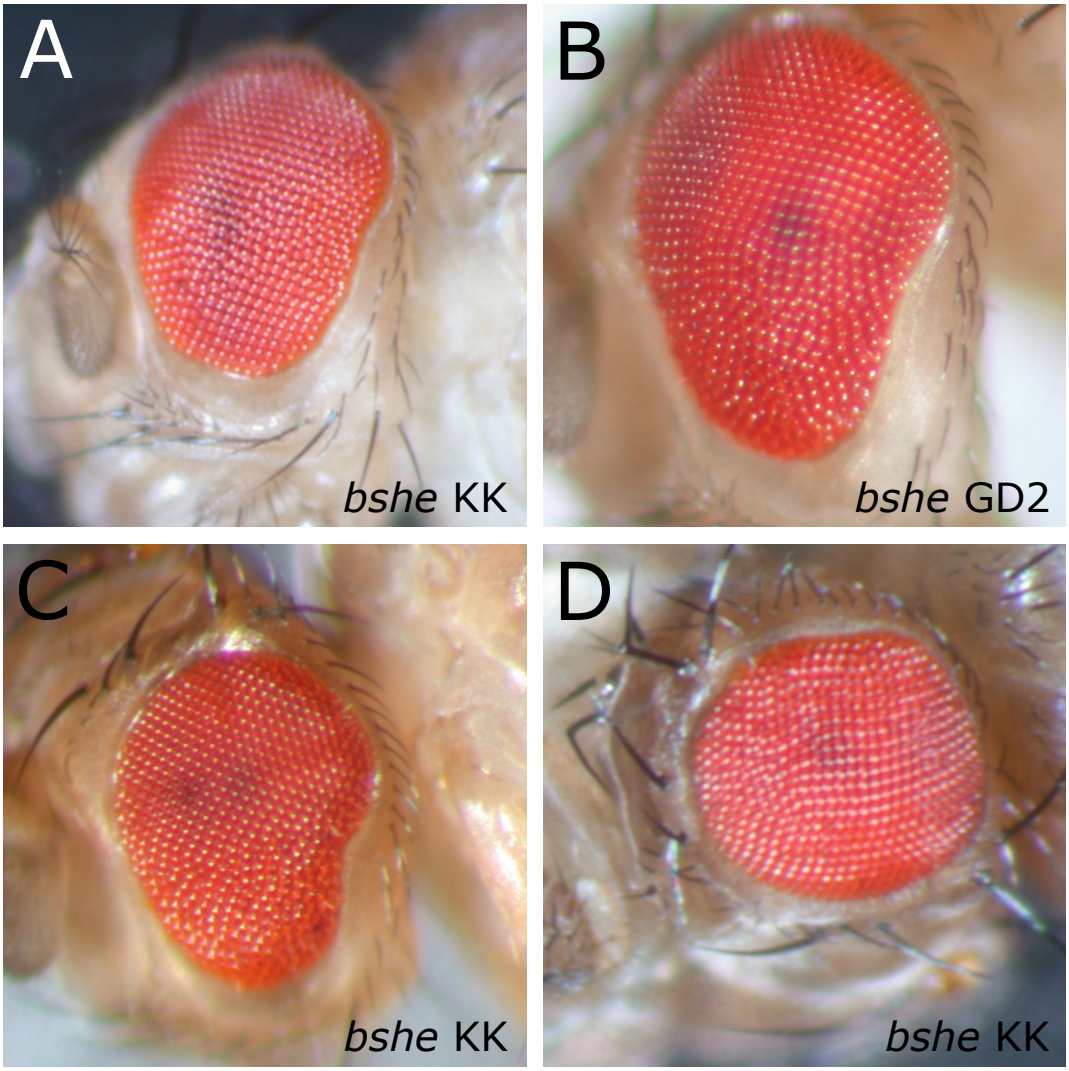

Figure 4.6. Abnormal ommatidia patterning phenotypes seen with the *ey-GAL4* driver and *UAS-bshe* responder. Phenotypes range from
(A)disorganized ommatidia with no noticeable loss of eye size,
(B-C) Disorganized ventral eye with reduction in size in the disorganized region, to
(D) substantial reduction of eye size with disorganization throughout.

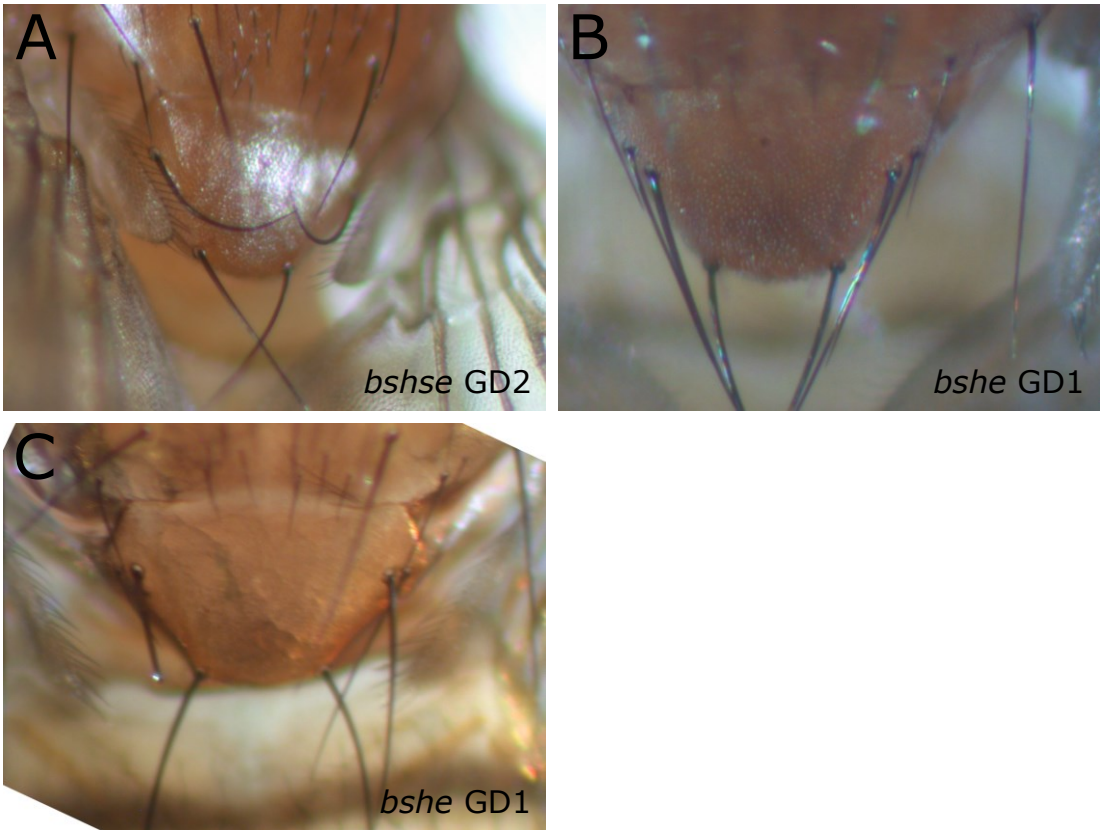

Figure 4.7. Abnormal bristle phenotypes seen in the *act-GAL4* driver and *bshe-UAS* responder, The majority of progeny of the *UAS-bshe KK* x *act-GAL4* cross caused lethal phenotype, so bristle phenotypes were mostly seen in the two *bshe GD UAS* crosses. Phenotypes were only seen in the scutellar region. Abnormalities ranged from
(A) curved or bent scutellar bristles,
(B) gain of scutellar bristles or
(C) shows both extra scutellar bristles, with one shortened.

Table 4.1. *elav-GAL4* RNAi results. Crosses of homozygous *UAS-bshe* or balanced *UAS-ball* to homozygous *elav-GAL4*. Two control crosses were done between two of the UAS lines and wildtype flies for comparison. No abnormal flies in morphology, behaviour or development seen.

Stocks	Normal flies	Abnormal flies	Balancer flies
UAS-bshe KK	144	0	-
UAS-bshe GD1	187	0	-
UAS-bshe GD2	158	0	-
UAS-ball KK	90	0	50
UAS-bshe KK non-RNAi Control	167	0	-
UAS-ball KK non-RNAi Control	114	0	-

Table 4.2. Results observing larval lethality with mass collection of larvae. Male parents were either *3a52a* or *3a66a* mutants balanced over *CyO-GFP*, and female parents were the *bshe* deficiency. Parents were allowed to lay in embryo cages with yeast cornstarch media for a period of time and then the plates were removed and allowed to grow before collecting and scoring larvae for molt stage and presence or absence of GFP.

Cross	**Age (hours)**	**1st instar**		**2nd instar**		**3rd instar**	
		GFP+	**GFP-**	**GFP+**	**GFP-**	**GFP+**	**GFP-**
3a66a/ CyO-GFP x *Df(2R)BSC699/ CyO-GFP*	23.7 - 38.5	65	0	0	0	0	0
	40.0 - 48.0	103	0	17	0	0	0
	49.8 - 64.0	2	0	36	0	0	0
	66.0 - 78.5	3	0	214	0	8	0
	95.3 - 111.8	1	0	55	0	162	0
	112.0 - 119.2	0	0	10	0	598	0
3a52a/ CyO-GFP x *Df(2R)BSC699/ CyO-GFP*	26.5 - 34.0	90	3	0	0	0	0
	34.0 - 50.3	35	1	4	0	0	0
	48.5 - 63.0	7	6	41	0	0	0
	65.7 - 72.8	2	0	118	0	6	0
	103.5 - 120.3	0	0	7	0	241	0
	118.3 - 125.7	0	0	7	3	585	1

Table 4.3. Genes with lethal mutant phenotypes within the second chromosome deletion *BSC699*. Lethality description from summary section of each gene in FlyBase.org, describes lethality seen in some alleles. This doesn't necessarily mean all alleles are lethal.

Gene name	**Gene shorthand**	**Lethality description**
off-track	*otk*	partially lethal - majority die
off-track2	*otk2*	some die during pupal stage, lethal - all die before end of pupal stage
pds5	*pds5*	lethal, increased mortality during development
RNA polymerase III 128kD subunit	*RPIII128*	lethal - all die before end of pupal stage
DNA fragmentation factor-related protein 3	*Drep3*	lethal - neuroanatomy defective
jelly belly	*jeb*	lethal - all die before end of P-stage, increased cell death
washout	*wash*	increased mortality during development
t-complex chaperonin 5	*Cct5*	lethal - neuroanatomy defective
ornithine decarboxylase antizyme	*oda*	lethal - all die before end of larval stage
small ribonucleoprotein particle protein SmD3	*SmD3*	increased mortality during development
pre-mRNA processing factor 8	*Prp8*	increased mortality during development.

Table 4.4. Expected ratios from RNAi crosses. *Elav-GAL4* not included because results did not show any change. In the approximate actual ratio column, lethal shows that all or a portion of the adult progeny died, and so the ratios will be different from expected. Expected shows that the ratios seen are as stated in the expected column.

Crosses	Expected Ratio	Approx. Actual Ratio
bshe-UAS / neur-GAL4	1 RNAi : 1 TM6b	2 RNAi : 1 TM6b
bshe-UAS / ey-GAL4	1 RNAi : 1 TM6b	5 RNAi : 2 TM6b
bshe-UAS / act-GAL4	1 RNAi : 1 CyO	Lethal / expected
ball-UAS / neur-GAL4	1 RNAi : 1 CyO : 1 TM6b : 1 TM6b+CyO	4 RNAi : 3 CyO : 2 TM6b : 0 TM6b+CyO
ball-UAS / ey-GAL4	1 RNAi : 1 CyO : 1 TM6b	1 RNAi : 1 CyO : 1 Tm6b expected
ball-UAS / act-GAL4	1 RNAi : 2 CyO	lethal

References

1. McCracken A, Locke J. Mutations in CG8878, a novel putative protein kinase, enhance P element dependent silencing (PDS) and position effect variegation (PEV) in Drosophila melanogaster. PLoS ONE. 2014;9(3):e71695.

2. Ivanovska I. A histone code in meiosis: the histone kinase, NHK-1, is required for proper chromosomal architecture in Drosophila oocytes. Genes Dev. 2005 Nov 1;19(21):2571–82.

3. Cullen CF. The conserved kinase NHK-1 is essential for mitotic progression and unifying acentrosomal meiotic spindles in Drosophila melanogaster. J Cell Biol. 2005 Nov 14;171(4):593–602.

4. Lancaster OM, Cullen CF, Ohkura H. NHK-1 phosphorylates BAF to allow karyosome formation in the Drosophila oocyte nucleus. J Cell Biol. Rockefeller Univ Press; 2007;179(5):817–24.

5. Lancaster OM, Breuer M, Cullen CF, Ito T, Ohkura H. The Meiotic Recombination Checkpoint Suppresses NHK-1 Kinase to Prevent Reorganisation of the Oocyte Nucleus in Drosophila. PLoS Genet. Public Library of Science; 2010 Oct 28;6(10):e1001179.

6. Herzig B, Yakulov TA, Klinge K, Günesdogan U, Jäckle H, Herzig A. Bällchen is required for self-renewal of germline stem cells in Drosophila melanogaster. Biol Open. 2014 May 29.

7. Yakulov T, Günesdogan U, Jäckle H, Herzig A. Bällchen participates in proliferation control and prevents the differentiation of Drosophila melanogaster neuronal stem cells. Biol Open. 2014;3(10):881–6.

8. Aihara H, Nakagawa T, Yasui K, Ohta T, Hirose S, Dhomae N, et al. Nucleosomal histone kinase-1 phosphorylates H2A Thr 119 during mitosis in the early Drosophila embryo. Genes Dev. 2004 Apr 15;18(8):877–88.

9. Gelbart WM, Emmert DB. FlyBase High Throughput Expression Pattern Data. 2013.

10. Ashton-Beaucage D, Udell CM, Gendron P, Sahmi M, Lefrançois M, Baril C, et al. A Functional Screen Reveals an Extensive Layer of Transcriptional and Splicing Control Underlying RAS/MAPK Signaling in Drosophila. PLoS Biol. Public Library of Science; 2014;12(3):e1001809.

11. Manning G, Plowman GD, Hunter T, Sudarsanam S. Evolution of protein kinase signaling from yeast to man. Trends Biochem Sci. 2002 Oct;27(10):514–20.

12. Swarup S, Pradhan-Sundd T, Verheyen EM. Genome-wide identification of phospho-regulators of Wnt signaling in Drosophila. Development. 2015 Apr 15;142(8):1502–15.

13. Brand AH, Perrimon N. Targeted gene expression as a means of altering cell fates and generating dominant phenotypes. 1993.

14. Robinow S, White K. Characterization and spatial distribution of the ELAV protein during Drosophila melanogaster development. J Neurobiol. 1991 Jul;22(5):443–61.

15. Boulianne GL, la Concha de A, Campos-Ortega JA, Jan LY, Jan YN. The Drosophila neurogenic gene neuralized encodes a novel protein and is expressed in precursors of larval and adult neurons. EMBO J. 1991 Oct;10(10):2975–83.

16. Halder G, Callaerts P, Gehring WJ. Induction of ectopic eyes by targeted expression of the eyeless gene in Drosophila. Science. 1995 Mar 24;267(5205):1788–92.

17. Halder G, Callaerts P, Gehring WJ. New perspectives on eye evolution. Curr Opin Genet Dev. 1995 Oct;5(5):602–9.

18. Kammermeier L, Leemans R, Hirth F, Flister S, Wenger U, Walldorf U, et al. Differential expression and function of the Drosophila Pax6 genes eyeless and twin of eyeless in embryonic central nervous system development. Mech Dev. 2001 May;103(1-2):71–8.

19. Quiring R, Walldorf U, Kloter U, Gehring WJ. Homology of the eyeless gene of drosophila to the small eye gene in mice and aniridia in humans. Science. 1994. 785 p.

5. Chapter 5: *banshee* antibody optimization

Banshee (bshe) was found through a genetic screen looking for dominant (dose dependent) enhancers of *Pci* variegation (1). This means that when *bshe* is mutant, there is increased silencing of the mini-*white* gene on the *P* element inserted near *ci* on the fourth chromosome. This suggests that reductions in *bshe*'s molecular function (two normal doses to one normal dose) results in more silencing of the mini-*white* gene at *ci.* This increased silencing, suggests that BSHE's normal function is to maintain the heterochromatin-euchromatin boundary on the fourth chromosome, or maintain the euchromatic chromatin in the region. Another possibility that cannot be excluded is that *bshe* is an indirect effector, and that it modifies or regulates other proteins involved in maintaining the heterochromatin/euchromatin organization in the *ci* region.

Function and localization of BALL

Chapter 3 suggests that despite the insertion within the kinase domain it may still be possible that the kinase domain is still functional. Determining whether *bshe* is a kinase or not is an important first step in understanding its function. The homology searches I performed revealed that *bshe* is related to *ball*. Therefore understanding some of what *ball* does would be an important to give us the first steps to understanding *bshe*'s role, and how it has changed since the evolutionary split from *ball*. Remember that the split appeared to have happened long ago (Figure 3.2), or have been under high selective pressure causing significant changes, at least in terms of base pair changes in the kinase domain.

Ballchen's secondary name is *nuclear histone kinase 1*, which describes its role. It was found in a search for novel histone kinases (2). It was first shown to phosphorylate histone H2A threonine 119, but only in chromatin (2-4). It does not phosphorylate purified histone H2A-H2B dimers. Phosphorylation of this residue, or the equivalent histone H2A threonine 120 in humans is has been shown to cause transcriptional repression through repressive chromatin (5), and is phosphorylated in the kinetochore proximal region of the centromere (6). Also a loss of *ballchen* activity, and so loss of phosphorylation at H2A(T119), is associated with a loss of acetylation at H3(K14) and H4(K5), all of which are likely required for karyosome formation (4).

BALL is not solely found within the nucleus, but moves into the cytoplasm depending on the stage of the cell cycle. In early S phase, BALL is seen in the cytoplasm, and localizes to condensing chromatin from prophase to metaphase, and then localizes back to the cytoplasm after completion of mitosis (2). BALL has a role specifically with chromatin in mitosis (2,7). So as a form of regulation it is extruded from the nucleus to prevent untimely action on chromatin during interphase. This does not exclude it from also having targets in the cytoplasm, as VRK-1 has also shown to have phosphorylation targets in the golgi that contribute to its fragmentation during G2/M phase of mitosis (8). Evidence of BALL's importance in mitosis show in that mutants have normal larval structures, but the mitotic cells are less developed and irregular (9,10).

Overall it appears that BALL's main action, in terms of chromosome condensation, is through suppression of barrier-to-autointergration factor (BAF) activity through phosphorylation (11-13). One role of BAF is establishing higher order chromatin structure (14). Orthologs of *ball* in other species also regulate BAF through phosphorylation. (15-17).

Research Goals

BALL's role in phosphorylating histones, and the close relationship of BALL and BSHE's kinase domain coupled with of BSHE's apparent role in chromatin, provides support for looking for histone kinase activity in BSHE.

The next step in understanding BSHE's molecular function is to examine its protein distribution and level. Firstly, I must generate an antibody for the protein, followed by optimization of their binding in various assays. Once optimized, they can be used for purification, immunoprecipitation assays and immunohistochemistry. With the help of an undergraduate BIOL 398 student, Brian McNish, we were able to begin antibody optimization as a start to understanding BSHE's function. Brian McNish completed all the Western blot and immunofluorescence experiments in this chapter with my oversight.

Results and Discussion

Generation of antibodies

Three antibodies were obtained from the company GenScript USA Inc (Piscataway, NJ, USA). Antibody#1 used a sequence from the N-terminus of the polypeptide, while antibodies #2 and #3 used different sequences from the C-terminus as shown in Figure 5.1. Making three antibodies provides a greater chance of finding an antibody that are specific to BSHE, and having both termini would be useful to detect truncated proteins.

A BLAST search of each of the peptides shows that BSHE is the most similar protein. The e-values of the next most similar protein for each peptide range from 0.045 to 5.2 (Table 5.1). These results suggest the antibodies to be unique and should not have any obvious non-specific bands. Based on BSHE's 1004 amino acid sequence, the predicted protein size should be 113.8 kDa.

Western blot experimental setup

Western blots must be optimized for each antibody used, with proper controls to ensure that the antibody is specific. Variables used in optimization include: number of embryos per sample, protease inhibitor, blocking agent (BSA or skim milk powder), and primary and secondary antibody concentration. A monoclonal β-tubulin antibody was used as a loading control and was tested under the same conditions as each individual experiment.

Five different experimental trials were completed selectively changing the variables above. Electrophoresis and fixation protocols were never changed across all trials.

Trial #1 was blocked with 5% BSA in TBST buffer. 1µg/ml for all primary antibody and 1/25000 secondary antibody dilution was used. Antibody 2 and β-tubulin probing was done on a stripped membrane for this trial. Embryo sample size was 1 embryo, 3 embryos, 5 embryos and 7 embryos per 10µl sample loaded.

Trial #2 was blocked 5% BSA in TBST buffer. 0.2µg/ml for all primary antibody and 1/5000 secondary antibody dilution was used. Embryo sample size was 1 embryo, 2 embryos, 3 embryos and 5 embryos per 10µl sample loaded. Every trial after this also used this sample size.

Trial #3 stripped the membranes from trial #2. Trial #3 was blocked in 5% skim milk powder (SMP) in TBST. 0.2µg/ml for all primary antibody and 1/5000 secondary antibody dilution was used.

Trial #4 used a protease inhibitor during sample preparation. The membrane was blocked in 5% BSA in TBST buffer. For primary antibodies dilutions, Antibody 1 was diluted to 0.1µg/ml, and Antibody 2 and 3 were diluted to 0.2µg/ml. A 1/5000 dilution was used for the secondary antibody.

Trial #5 stripped the membrane from trial #4. Membrane was blocked in 5% SMP in TBST. Antibody 1 was diluted to 0.02µg/ml and Antibody 2 was diluted to 0.1µg/ml. Antibody 3 was probed in two dilutions 0.1µg/ml and 0.02µg/ml. Secondary antibody dilution was 1/5000.

Optimization of antibodies for Western blots

For Antibody 1 probing, Trial #3 and Trial #4 produced the best blots to date. Trial #3 produced many bands, most prominently seen in the 5 embryo lane (Figure 5.2A). Major bands are seen at approximately 15 kDa, 30 kDa, 40kDa, 60 kDa, with a smear from 70kDa to 120kDa. Trial #4 was smearier at 5 embryos, but at 3 embryos produced strong bands (Figure 5.2B). Here, major bands are seen at approximately 23kDa, 40kDa, 60kDa, 70kDa and 110 kDa. Bands were not consistent across the two trials, but this could be due to the introduction of a protease inhibitor for trial #4, causing less degradation products. The band at approximately 110kDa Figure 5.2B looks promising for a possible BSHE band.

For Antibody 2 probing, Trial #1 and Trial #4 produced the best blots. Trial #1 was fairly smudgy but did have some promising bands (Figure 5.2C). The clearest lane with the best definition appears to be the 5 embryos lane. Major bands seen are at approximately 30kDa, 40kDa, 70kDa and 120kDa. Trial #4 produced more defined bands than trial #1 (Figure 5.2D). 3 embryos appear to be the optimum lane in this blot. The major bands here are at approximately 40kDa, 55kDa, 80kDa and 120kDa. Like in Antibody 1, Trial #4 produces the cleanest bands, likely because of the addition of the protease inhibitor. There is also a band of the approximate right size to possibly be BSHE seen in both trial #1 and trial #4.

For Antibody 3 probing, Trial #1 and Trial #3 produced the best results. Like in Antibody 2, Trial #1 produced a smudgy blot, and the 5 embryos lane appears to give the most usable results (Figure 5.2E) Major bands are seen at approximately 30kDa, 40kDa, a smudge from 55 to 70kDa and a smudge at approximately 130-140kDa. The trial #3 blot produced slightly less smudginess, but is not as defined as the best blots seen in the previous two antibodies (Figure 5.2F). There does not appear to be much difference between the 3 and 5 embryo lane. The major bands seen here are at approximately 16kDa, 25kDa, 28-33kDa, 40kDa, and a smudge from 70-140kDa. There are bands in the approximate size range for BSHE, which is around 114kDa, but there also appears to be a lot of background bands. Unlike the other two antibodies, the protease inhibitor did not provide a strong signal (results not shown).

Trial #2 and #5 did not produce clear or distinct bands for any of the antibodies, so the results are not presented.

Discussion of Western blot trials

Bands of approximately 114 kDa are seen in each antibody (Figure 5.2B,D,F), though always with many other bands, and not always the most prominent band. When comparing each blot together, some of the major background bands are seen across all three of the antibodies, particularly at approximately 40kDa. This band is not in the β-tubulin positive control or a control with no primary antibody (results not shown). Because these three antibodies are for completely different peptides at different positions in the protein, this suggests that it is not degradation products, but likely there is something in the antibody prep itself that all these antibodies are binding in common. Another possibility may be post-transcriptional or post-translational modification that would change the size of the final protein. A protein null control would be necessary to confirm or refute this.

Upon further discussion of these results, after experiments were completed, it became apparent that I did not follow the standard protocols for protein preparation for Western blots. In all trials I fixed the embryos with 4% formaldehyde in PBS prior to solubilization in SDS sample preparation buffer. Formaldehyde treatment would result in polypeptide crosslinking and thus prevent linearization of the polypeptide. Consequently the polypeptide may show abberant mobility in the SDS-polyacrylamide gel. This might

account for the 40kDa band seen across all trials, as it may be specific to BSHE. Experiments will need to be repeated, without fixing embryos, to resolve if the apparent non-specific bands from the trials I completed are actually consistent with the BSHE polypeptide.

The β-tubulin loading control should produce a band at around 50kDa. The band found in the tubulin loading control for Figure 5.2A and F are this correct size, but the band in Figure 5.2B-E are smaller at around 37kDa. It is uncertain at this time why these bands are at the incorrect size, though it may be because of the problems with using fixed embryos in the sample prep, as described previously.

Western blot analysis of protein negative control

The next step is a negative control using a *bshe* deficient stock. If there is a specific band that is missing from the deficient stock, this will help to further optimize the antibody to remove the background and non-specific bands. This experiment was only done once with Antibody 1 and 2, and did not include Antibody 3. *Bshe* deficient embryos are difficult to reliably collect, and so there were limited embryos available. Because of this, only the two cleanest antibodies were chosen.

Negative control embryos were collected using *Df(2R)BSC699/ CyO P{act-GFP}* strain described in a previous chapter. This was chosen as opposed to the mutant because with the mutant there might be a chance of truncated protein present, whereas in the deficiency strain there should be no protein produced at all. They were scored at 17-21 hours for absence of GFP, and then immediately fixed and prepared for Western blot analysis. Ability to select for GFP negative embryos was difficult to concretely define, and labor intensive, so it only allowed for a few sample preps to be made. Embryos still showed gut autofluorescence, and at times it was difficult to discern GFP negative embryos (Figure 5.4A) from GFP positive embryos (Figure 5.4B). Note in Figure 5.4B that some embryos have comparable amount of fluorescence to Figure 5.4A, but were removed because there was a small amount of distinctly green fluorescence seen. Because of the difficulty concretely deducing GFP negative embryos, some of the samples may still have the balancer (and are thus $bshe^{+}$), but the sample should still have a lowered expression level compared to wild type of a similar stage. To attempt to control for this, multiple protein preps were made using different

embryos with using three embryos in each, to try and improve the chances of having at least one sample that is a true protein null. Since Trial #4 produced the best results for both Antibody 1 and 2, this protocol was used for this protein null experiment.

Expected results for this experiment would be the positive control wild type embryos showing similar bands to the 3 embryo lane for Antibody 1 and 2 in Figure 5.2B and D, respectively. The three BSHE deletion lanes are expected to still have the background bands, but be missing a single band, representing the BSHE protein. Because of the possibility of collecting an improper embryo, the deletion lanes may still have a band, but fainter than the positive control lane. Actual results seen did not follow these expected trends (Figure 5.5)

First, the wild type embryos, which should have BSHE and serve as a positive control, did not show the same banding pattern as was seen in the wild type optimization done previously (Figure 5.2B and D). This suggests that either some part of the protocol changed, or possibly the batch of primary antibody has been reused too many times and so does not bind effectively anymore. The expected 113.8kDa band was not seen and a faint band, the non-specific 40kDa band as described previously, is seen across all antibodies. Two other faint bands are seen in Antibody 1 across both wildtype and deletion samples at approximately 80 and 90kDa (Figure 5.3A). Another faint band was seen across all samples at 16kDa in the Antibody 2 probing (Figure 5.3B).

Second, the β-tubulin positive control antibody, which was the third probing of that membrane, showed no bands across all samples (Figure 5.3C). This could be due to a poor sample prep, or to the fact that this was a product of the membrane being stripped twice, possibly stripping off the β-tubulin protein and other protein products. A combination of the failure in both positive and loading controls suggests that any banding or lack of it seen in the experimental lanes is inconclusive.

These results do not completely discount these antibodies, but suggests the experiment should at least be repeated with attention to quality controls to be sure that they are still treated similarly to prevent any possible false positives or negatives in these results. Optimization of western blots has not been completed and is still ongoing.

Immunohistochemistry experimental setup

When *ball* was first discovered, the localization of the BALL protein in embryos was explored (2). In embryonic cycle 10-12, BALL protein had variable localization depending on the stage of the cell cycle, moving from the cytoplasm into the nucleus from metaphase to the end of mitosis (2). Since *ball* is the most similar *Drosophila* gene to *bshe*, a similar experiment was performed using our BSHE antibodies on early embryos.

A first test was done using a PH3 antibody, which is well known to cause consistent staining at the stage we were testing. This is a control to make sure the protocol will produce results with a well-tested antibody. PH3 is a phosphorylated form of Histone 3 that is only present in mitotic nuclei. In this test, non-mitotic cells within the embryo should have no fluorescence, while the nuclei of mitotic cells within the embryo will show fluorescent staining. Hoechst staining was used to identify DNA in these embryos. Hoechst staining was not applied correctly for this test, and so nuclei are not visible in the embryos observed (Figure 5.5B). Despite this, distinct nuclei are seen in mitotic embryos, showing that staining for PH3 was as expected (Figure 5.5A). Optimization for secondary antibody concentration was completed on these PH3 embryos from a 1/1000 to 1/5000 dilution (results not shown). 1/5000 showed the cleanest results, and will be used for the experimental immunofluorescence.

BSHE immunohistochemistry of *Drosophila* embryos

Now that the control shows our technique is correct, the next step is analyzing the BSHE antibody. Antibody 2 is chosen as the first antibody to be optimized; as it has the least amount of background bands seen in the Western blots (Figure 5.2D). Two samples of embryos were collected for the *bshe* antibody staining. The positive control sample was of a $w^- y^-$ fly strain, which was chosen because it lays eggs better than our lab stock of OregonR, and still is wildtype at the *bshe* locus. The deletion strain *Df(2R)BSC699/CyO-GFP* was also chosen as a BSHE null negative control. If Antibody 2 is binding to BSHE, then we expected 25% of the embryos from this stock should have no BSHE protein produced and thus 75% should show staining. A range in primary antibody concentrations were used, 1/1000, 1/2500, 1/5000 and 1/10000 (results not

shown). 1/2500 is chosen because it shows the strongest fluorescence without too much background.

Every embryo on the wild type slides had fluorescent antibody staining (Figure 5.6). This is in contrast with PH3, for example, which only has staining in embryos undergoing mitosis. Staining in every embryo suggests that BSHE is a more ubiquitous protein at this stage of development. Interphase embryos consistently show cytoplasmic staining, with no staining in the nucleus (Figure 5.6D-L). This is similar to BALL staining at this stage (2). This cytoplasmic staining is even seen in older embryos (Figure 5.6J-L). In mitosis, BSHE staining is no longer similar to BALL. No discernable pattern is seen in mitotic embryos (Figure 5.6A-C).

Based upon BSHE's discovery in an *E(var)* screen, it is presumed to be a putative histone kinase (1). No localization to the nucleus at any part of the cell cycle in these early embryos draws to question if BSHE is truly a histone kinase. Its role may be in a more upstream regulatory or modifying position. Another hypothesis could be that it does not directly interact with chromatin until a later stage of development.

Immunohistochemistry of protein negative control

In the deletion preparations, we are expecting ¼ of embryos to be BSHE null and thus lacking antibody staining entirely, if Antibody 2 is specific. What are seen in the deletion preparations are embryos that completely lacked staining (Figure 5.7C). These preparations still had embryos with staining in the same localization as seen in the wild type embryo preparations (Figure 5.7C), suggesting that the non-stained embryos have the *bshe*. On a slide of 115 embryos, 21 did not show staining. This is not significantly different from the expected 25% for *bshe* deficient embryos ($\chi^2 = 2.786$, degrees of freedom = 1, p=0.0951).

The lack of staining in presumed BSHE null embryos suggests that Antibody 2 is specific to BSHE and the protocol used for immunofluorescence does not produce any noticeable background. To completely confirm that the non-fluorescent embryos are truly the *bshe* deficient embryos, those lacking staining should be collected and PCRed to determine that they are actually a *bshe* deficiency. The lack of staining also suggests

that these embryos were analyzed at a point that maternal protein is no longer present, and that these embryos were correctly collected after the maternal to zygotic transition.

Occasionally, brightly fluorescing foci were seen. The clearest picture is seen in a fluorescing embryo on the *bshe* deficiency preparation (Figure 5.7D). These foci were seen in multiple embryos that had BSHE antibody staining in both wildtype and deletion slides. Hoechst staining failed in these embryos (data not shown), so what stage or part of the cell cycle is not known, but the pattern looks very similar to Figure 5.6A, where there is no discernable pattern during mitosis. Without any other markers to suggest other cellular structures, these foci cannot be further identified at this time.

This was the first experiment into immunofluorescence with this antibody, and it has not been properly optimized yet. With further optimization to reduce background (in any), this antibody can be used at more stages of development to learn more about BSHE's localization and role.

Conclusion

I have begun preliminary optimization of BSHE antibodies. Further optimization is still required for Western blots. There are potential ~114kDa bands in all antibodies that could show specificity to BSHE, but appropriate controls have not been conclusive at this time to support any one band as the BSHE specific band. Inappropriate fixing of sample embryos may be the cause of this.

Initial immunofluorescence using Antibody 2 provides more conclusive results than the Western blots. Cytoplasmic specific staining is seen in all wild type embryos, and apparent *bshe* deletion embryos have no fluorescence at all. These presumed deletion embryos still need to be confirmed, but at this time the evidence suggests they are BSHE null.

My hypothesis that *bshe* is a histone kinase is not well supported by these cytoplasmic results. BSHE's cytoplasmic localization in early embryos does not completely refute its possible histone kinase role. Further analysis in different points of development is required to observe if this cytoplasmic location is consistent, or differs depending on developmental timing or tissue type.

The question arises from these results, what could BSHE's role be in the cytoplasm? A recent genetic screen for factors impacting RAS-mediated MAPK activation found *bshe* to be a positive regulator of RAS signaling (18). Epistasis experiments put *bshe* downstream of RAF and upstream of MEK in the pathway. Both RAF and MEK are cytoplasmic proteins, and BSHE's cytoplasmic localization is supported. BSHE has also recently been found in a screen for regulators of WNT signaling (19). In the Wnt pathway, BSHE is in the signal-receiving cells downstream of the ligand-receptor interaction, and regulates Wnt pathway targets independently of the Notch pathway. If BSHE is also part of the Wnt signaling cascade, it could have roles in the cytoplasm as well.

As discussed in previous chapters, *bshe* is an insect specific protein. A role in such conserved pathways as the MAPK pathway and Wnt pathway is interesting, and may fill a niche that another protein fills in another organism. It may also be involved in signaling in insect specific processes. These questions may begin to be answered once antibody optimization is complete and more direct assays against the protein can be performed.

Figures and Tables

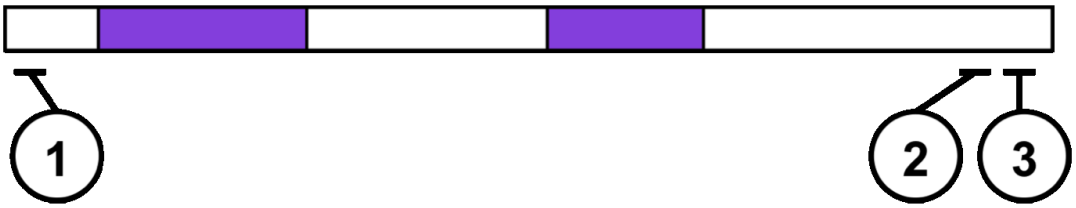

Antibody	Peptide sequence
1	MGKRLQLERPTTDRC
2	CRGRPKGTSRKQTTS
3	CATGEGERKLKSGRT

Figure 5.1. Location and sequence of peptides used for generating antibodies for BSHE. A linear representation of the BSHE protein, with the purple regions showing the interrupted kinase domain. Antibodies 1, 2 and 3 are each created from 15 amino acid peptide sequences in unique regions of the protein.

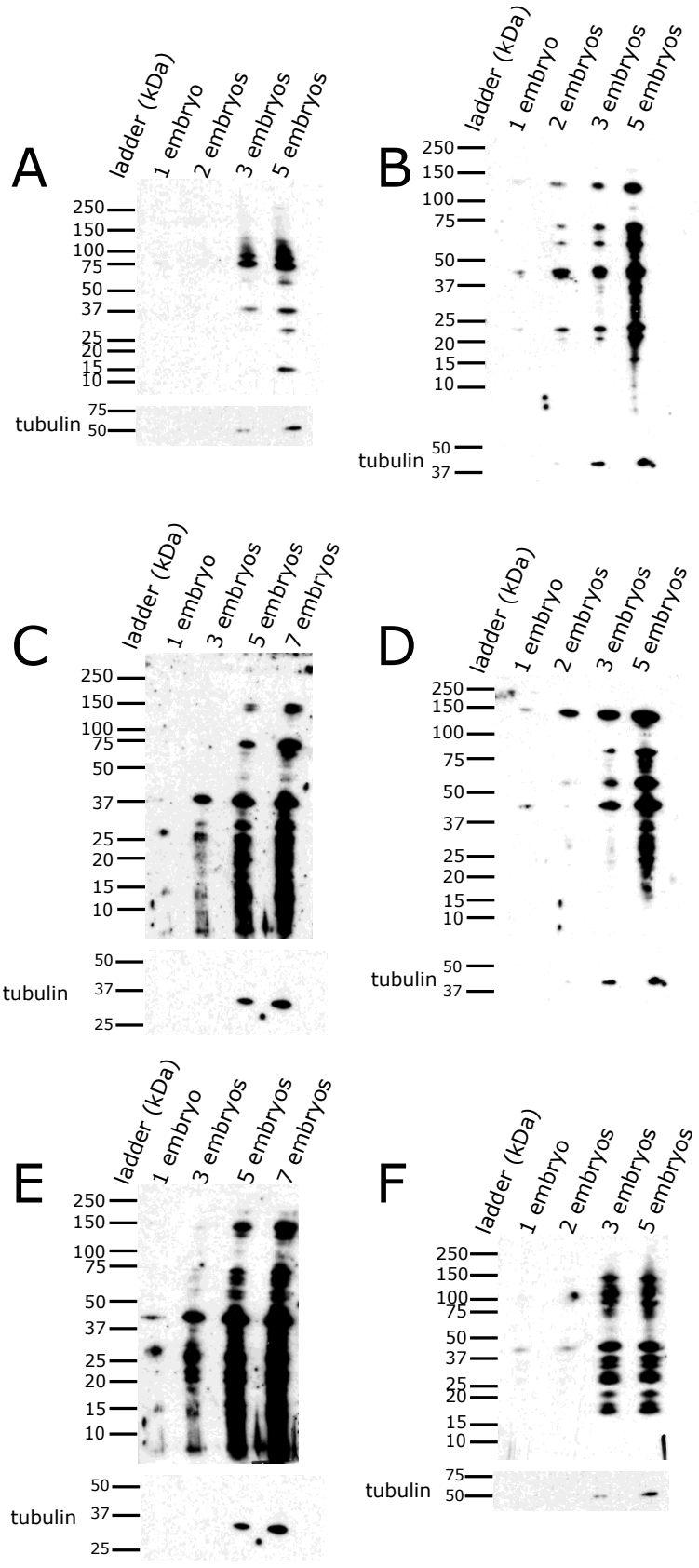
A
ladder (kDa)
1 embryo
2 embryos
3 embryos
5 embryos
250
150
100
75
50
37
25
20
15
10
tubulin
75
50
B
ladder (kDa)
1 embryo
2 embryos
3 embryos
5 embryos
250
150
100
75
50
37
25
20
15
10
tubulin
50
37
C
ladder (kDa)
1 embryo
3 embryos
5 embryos
7 embryos
250
150
100
75
50
37
25
20
15
10
tubulin
50
37
25
D
ladder (kDa)
1 embryo
2 embryos
3 embryos
5 embryos
250
150
100
75
50
37
25
20
15
10
tubulin
50
37
E
ladder (kDa)
1 embryo
3 embryos
5 embryos
7 embryos
250
150
100
75
50
37
25
20
15
10
tubulin
50
37
25
F
ladder (kDa)
1 embryo
2 embryos
3 embryos
5 embryos
250
150
100
75
50
37
25
20
15
10
tubulin
75
50

Figure 5.2. Western blot analysis of antibody 1 (A,B), antibody 2 (C,D) and antibody 3 (E,F). A tubulin antibody was used as a loading control, depicted under each figure. The results were generated from three different trials, which followed the protocol presented in the materials and methods with the following changes.

Trial #1 (C and E) were blocked in 5% bovine serum albumin (BSA) and had 1.0µg/ml primary antibody with a three minute film exposure.

Trial #3 (A and F) were blocked in 5% skim milk powder had a 0.2µg/ml dilution of the primary antibody with a five minute film exposure. These membranes have been previously used, stripped and reprobed.

Trial #4 (B and D) had a protease inhibitor added during sample preparation, blocked in 5% BSA and had a 0.1µg/ml primary antibody dilution for antibody 1 and a 0.2µg/ml dilution for antibody 2, with a five minute film exposure.

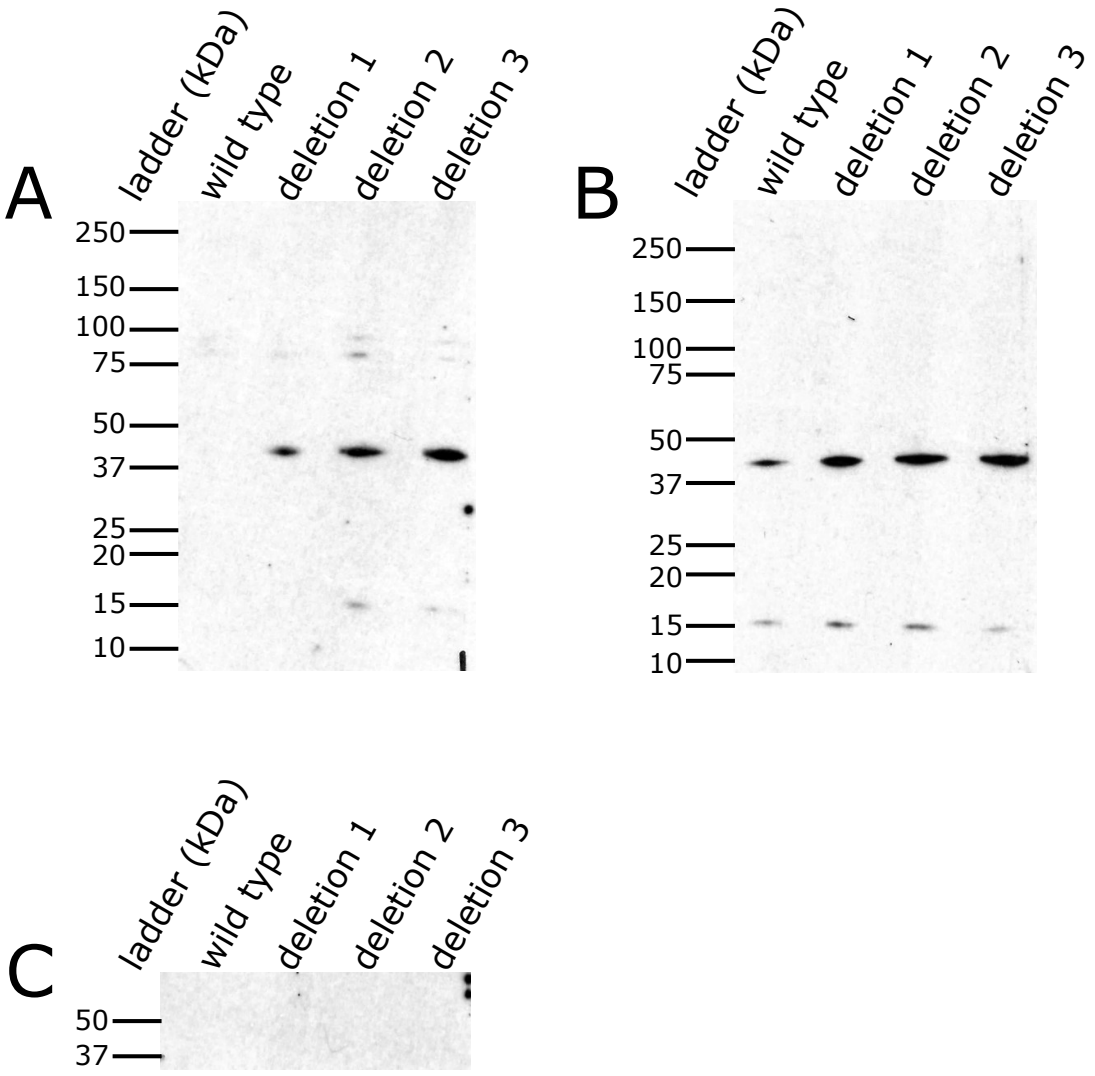

Figure 5.3. Western blot analysis of *bshe* null embryos using
(A) BSHE antibody 1,
(B) antibody 2 or
(C) β-tubulin loading control.

Deletion embryos were collected from GFP negative embryos of the deficiency stock Df(2L)BSC699/CyO-GFP, and wild type embryos from w^{-} $y^{=}$ stock with wildtype *bshe*. Samples were blocked in 5% BSA and had a primary antibody dilution of 1/5,000 and with a 30 minute film exposure.
(A) was the first probing of the membrane,
(B) was the same membrane as A but stripped and re-probed, and
(C) was from a second stripping of the same membrane.

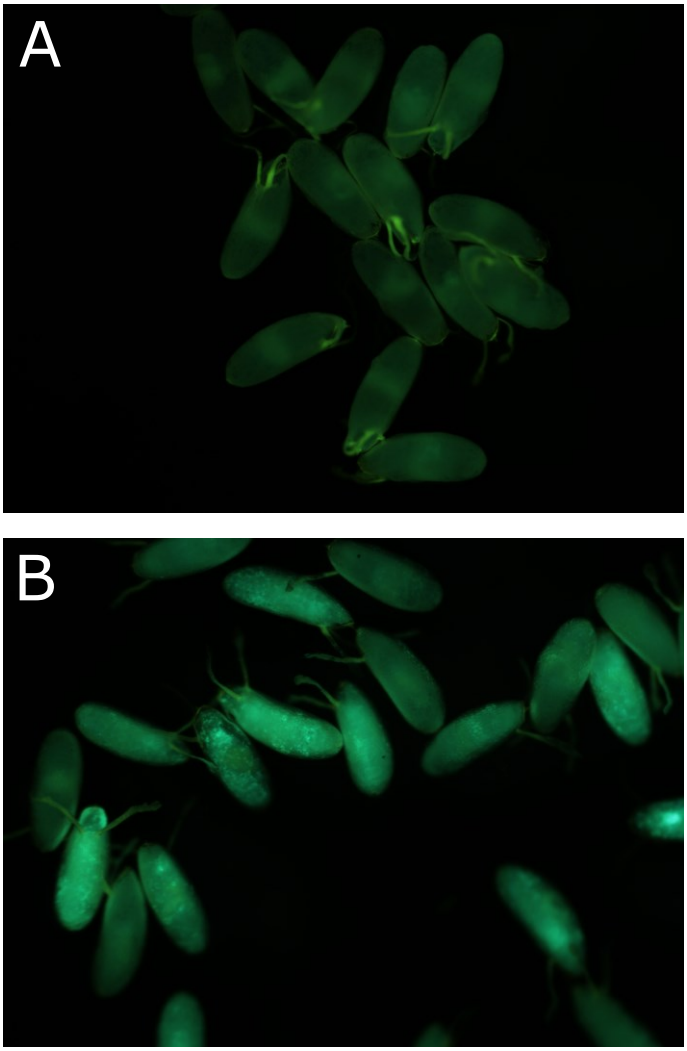

Figure 5.4. Fluorescent sorting of embryos from stock Df(2L)BSC699/CyO-GFP with
(A) GFP negative embryos and
(B) GFP positive embryos.

17-21 hour embryos collected and scored with their chorion still intact. Embryos were placed in 40% glycerol to be sorted. GFP negative embryos were then washed with water before proceeding with fixation.

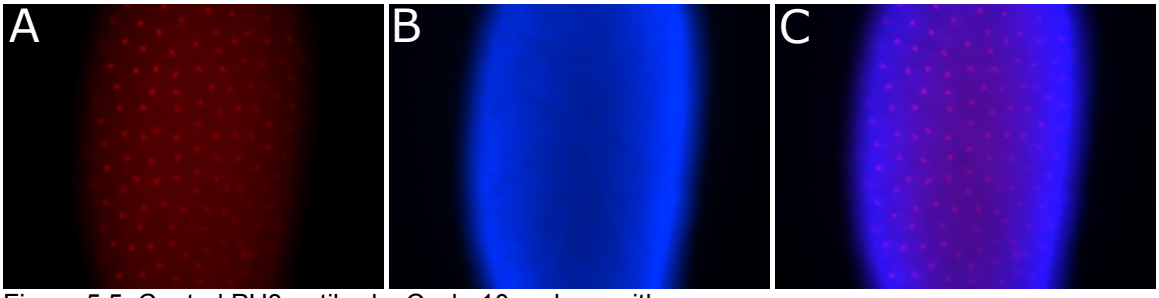

Figure 5.5. Control PH3 antibody. Cycle 10 embryo with
(A) PH3 staining
(B) Hoechst DNA staining
(C) and merged.

Fixed 1-2 hour old embryos blocked in 5% BSA and incubated with PH3 primary antibody at 1/1000 dilution and a red fluorophore conjugated secondary dilution at 1/2000. Images are 200X magnification.

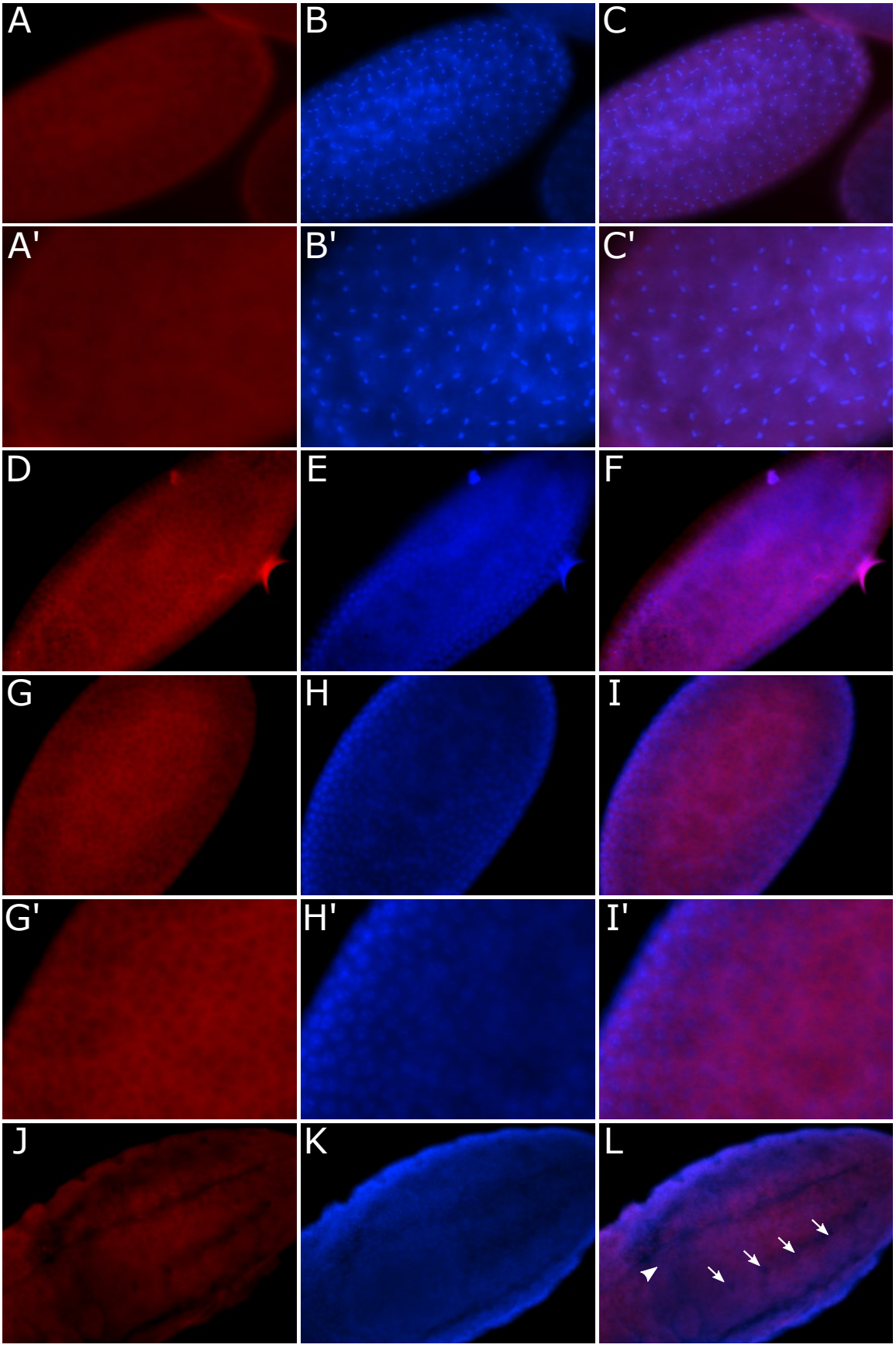
A
B
C
A'
B'
C'
D
E
F
G
H
I
G'
H'
I'
J
K
L

Figure 5.6. Wild type BSHE antibody 2 staining of 1-2 hour old embryos
(A,D,G,J) BSHE antibody,
(B,F,H,K) Hoechst staining
(C,E,I,L) merge.

(A-C) Embryo in anaphase of cycle 10.
(A'-C') is a zoom of A-C
(D-I) Embryo in cycle 12
(G'-H') is a zoom of G-H
(J-L) approximately stage 11 embryo dorsal view, with extended germ band (arrowhead) and parasegmental furrows (arrows).

Embryos were blocked in 5% BSA, and probed with BSHE antibody to at a dilution of 1/2500 and a red fluorophore conjugated secondary concentration of 1/5000. Images are 200X magnification.

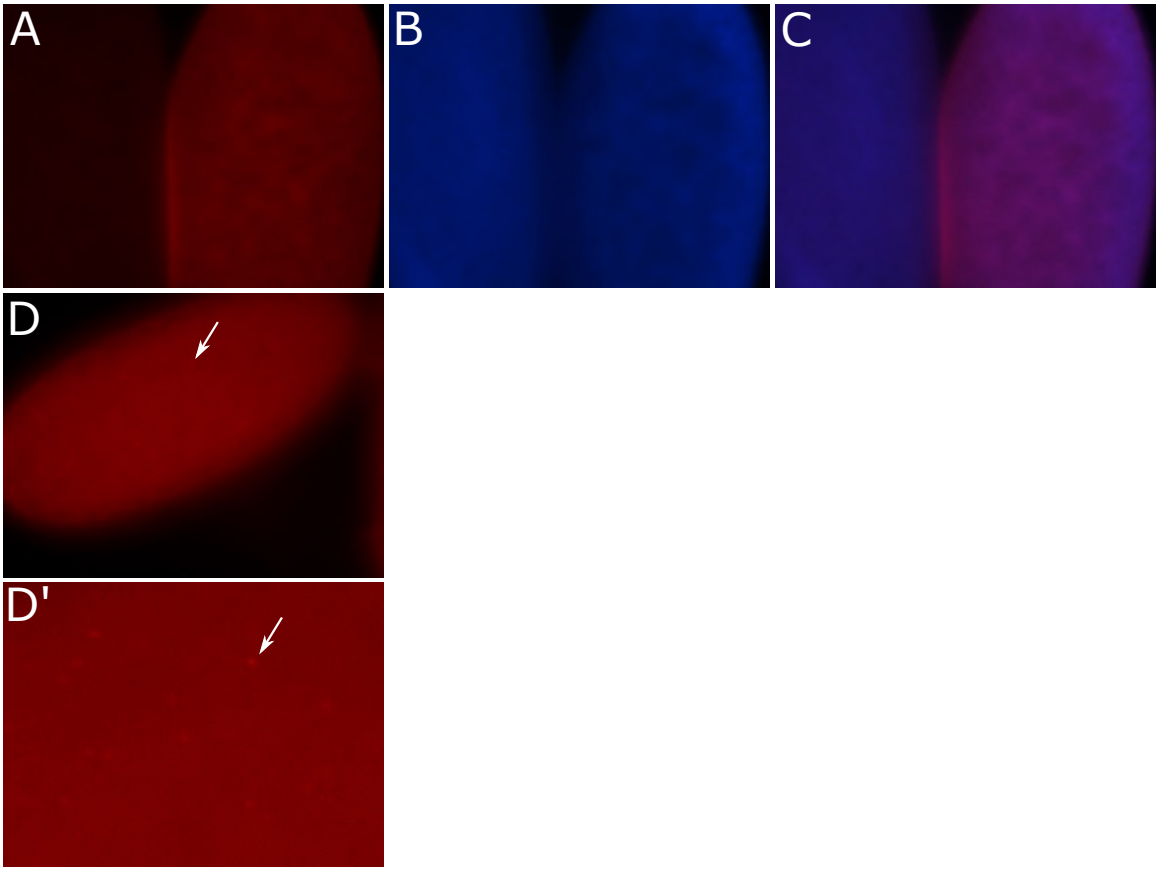

Figure 5.7. Immunofluorescence negative control with *bshe* deletion embryos. This is the offspring of Df(2L)BSC699/CyO-GFP parents, of which 25% of the offspring are expected to be *bshe* deficient.
(A,D,D') *bshe* antibody 2,
(B) Hoechst
(C) merge.

Improper Hoechst stain prevents staging the embryo (A-C)

(D) *bshe* embryo with heavily stained foci seen (arrow identifies one of many).
(D') is a zoom of panel D

Embryos were blocked in 5% BSA, probed with BSHE primary antibody 2 at 1/1000 dilution and probed with the red fluorophore conjugated secondary antibody at a 1/5000 dilution. Images are 200x maginification.

Table 5.1. The top four results from a BLAST search for each peptide used to create the three antibodies. The four lowest e-values are presented here for each peptide. Peptide sequences are in Figure 5.1.

Antibody 1		Antibody 2		Antibody 3	
protein	e-value	protein	e-value	protein	e-value
CG8878	3e-08	CG8878	3e-06	CG8878	1e-06
CG3290	1.4	CG1024	0.045	Ance-5	5.2
jean-baptiste	2.6	weckle	10	CG42553	29
pickpocket 3	3.7	CG7372	14	Tudor-SN	29

References

1. McCracken A, Locke J. Mutations in CG8878, a novel putative protein kinase, enhance P element dependent silencing (PDS) and position effect variegation (PEV) in Drosophila melanogaster. PLoS ONE. 2014;9(3):e71695.

2. Aihara H, Nakagawa T, Yasui K, Ohta T, Hirose S, Dhomae N, et al. Nucleosomal histone kinase-1 phosphorylates H2A Thr 119 during mitosis in the early Drosophila embryo. Genes Dev. 2004 Apr 15;18(8):877–88.

3. Ivanovska I. A histone code in meiosis: the histone kinase, NHK-1, is required for proper chromosomal architecture in Drosophila oocytes. Genes Dev. 2005 Nov 1;19(21):2571–82.

4. Ivanovska I, Orr-Weaver TL. Histone modifications and the chromatin scaffold for meiotic chromosome architecture. Cell Cycle. Landes Bioscience; 2006;5(18):2064–71.

5. Kim K, Kim J-M, Kim J-S, Choi J, Lee YS, Neamati N, et al. VprBP has intrinsic kinase activity targeting histone H2A and represses gene transcription. Mol Cell. 2013 Nov 7;52(3):459–67.

6. Carmena M, Wheelock M, Funabiki H, Earnshaw WC. The chromosomal passenger complex (CPC): from easy rider to the godfather of mitosis. Nat Rev Mol Cell Biol. 2012 Dec;13(12):789–803.

7. Brittle AL, Nanba Y, Ito T, Ohkura H. Concerted action of Aurora B, Polo and NHK-1 kinases in centromere-specific histone 2A phosphorylation. Exp Cell Res. 2007 Aug;313(13):2780–5.

8. Lopez-Sanchez I, Sanz-Garcia M, Lazo PA. Plk3 Interacts with and Specifically Phosphorylates VRK1 in Ser342, a Downstream Target in a Pathway That Induces Golgi Fragmentation. Mol Cell Biol. 2009 Feb 11;29(5):1189–201.

9. Cullen CF. The conserved kinase NHK-1 is essential for mitotic progression and unifying acentrosomal meiotic spindles in Drosophila melanogaster. J Cell Biol. 2005 Nov 14;171(4):593–602.

10. Yakulov T, Günesdogan U, Jäckle H, Herzig A. Bällchen participates in proliferation control and prevents the differentiation of Drosophila melanogaster neuronal stem cells. Biol Open. 2014;3(10):881–6.

11. Lancaster OM, Cullen CF, Ohkura H. NHK-1 phosphorylates BAF to allow karyosome formation in the Drosophila oocyte nucleus. J Cell Biol. Rockefeller Univ Press; 2007;179(5):817–24.

12. Lancaster OM, Breuer M, Cullen CF, Ito T, Ohkura H. The Meiotic Recombination Checkpoint Suppresses NHK-1 Kinase to Prevent Reorganisation of the Oocyte

Nucleus in Drosophila. PLoS Genet. Public Library of Science; 2010 Oct 28;6(10):e1001179.

13. Nikalayevich E, Ohkura H. The NuRD nucleosome remodelling complex and NHK-1 kinase are required for chromosome condensation in oocytes. J Cell Sci. 2015 Feb 1;128(3):566–75.

14. Margalit A, Brachner A, Gotzmann J, Foisner R, Gruenbaum Y. Barrier-to-autointegration factor--a BAFfling little protein. Trends Cell Biol. 2007 Apr;17(4):202–8.

15. Bengtsson L, Wilson KL. Barrier-to-autointegration factor phosphorylation on Ser-4 regulates emerin binding to lamin A in vitro and emerin localization in vivo. Mol Biol Cell. 2006 Mar;17(3):1154–63.

16. Gorjánácz M, Klerkx EPF, Galy V, Santarella R, López-Iglesias C, Askjaer P, et al. Caenorhabditis elegans BAF-1 and its kinase VRK-1 participate directly in post-mitotic nuclear envelope assembly. EMBO J. 2007 Jan 10;26(1):132–43.

17. Nichols RJ, Wiebe MS, Traktman P. The vaccinia-related kinases phosphorylate the N' terminus of BAF, regulating its interaction with DNA and its retention in the nucleus. Mol Biol Cell. 2006 May;17(5):2451–64.

18. Ashton-Beaucage D, Udell CM, Gendron P, Sahmi M, Lefrançois M, Baril C, et al. A Functional Screen Reveals an Extensive Layer of Transcriptional and Splicing Control Underlying RAS/MAPK Signaling in Drosophila. PLoS Biol. Public Library of Science; 2014;12(3):e1001809.

19. Swarup S, Pradhan-Sundd T, Verheyen EM. Genome-wide identification of phospho-regulators of Wnt signaling in Drosophila. Development. 2015 Apr 15;142(8):1502–15.

6. Chapter 6: Conclusions and Future Directions

Introduction

banshee (*bshe*) was initially found in a genetic screen looking for mutants that dominantly enhanced *white* variegation in *Pci*, through *P* element dependent silencing (PDS) (1). Its role as an enhancer of PDS was supported by the identification of a kinase-like domain, leading to the hypothesis that it is a presumed histone kinase. My research into this unstudied protein began with bioinformatics studies to learn more about this gene and its protein. By identifying genes with similar sequences, clues to the function of *bshe* might be identified. Next, I looked at its mutant phenotype and RNAi knockdown effects to determine its developmental stage of lethality, and if that could tell us anything more about its role. Finally, I began optimizing antibody protocols for Western and immunofluorescence analysis. Here I will briefly summarize those findings, state the conclusions, and propose what steps should be taken next.

Summary of Results

Bioinformatics

In my phylogenetic tree, *bshe* is placed in the CK1 kinase family, as previously supported (2). Five other groups also were found that make up the known CK1 kinase family, *ballchen*, *asator*, *casein kinase 1α, gilgamesh,* and *discs overgrown,* with also one unnamed CK1-like *Drosophila* gene. The gene with the most similar kinase domain sequence to *bshe* is *ballchen* (*ball*), a *Drosophila* VRK-1 homolog.

The amino acid sequence of *bshe* has a kinase domain, but with a large interruption in it in the middle of the catalytic domain. My protein structure prediction suggests that this interruption should not affect the kinase domain's structure and thus presumably its function. In BSHE the inserted region loops out from the kinase domain, allowing the catalytic portion of the kinase domain to stay in correct conformation. The exact location of the insert within the kinase domain is the same in all *bshe* orthologs, but the size and sequence of the insert is not conserved. Also, while *Drosophila bshe* has three regions of acidic amino acids, this is also not seen in other *bshe* orthologs

Both *bshe* and *ball* have longer branch lengths than the other members of the CK1 kinase family, showing evidence that they have a later point of divergence either due to

evolutionary time or selective pressure. From the results, *bshe* is only found within insects and is missing from the Arachnid outgroup.

Mutant analysis

The phenotypic ratios of three different mutant larvae (*3a52a*, *3a66a*, and *3a90a*) were observed at different stages of development. These ratios show some difference in when each larvae dies, but all die before pupating. *3a52a* dies before third instar, *3a66a* dies mostly during embryogenesis, but some persist to third instar, and *3a90a* dies before second instar. Residual effects of hypomorphic alleles, or homozygosity of other latent recessive mutant genes may cause different stages of lethality for different mutants.

I next looked more closely at when in development the mutants were lethal by following individual larvae throughout their life. Four trials of this were undertaken: Trial #1 in which mutant stock *3a52a* was crossed to itself, Trial #2 which a female *3a52a* mutant was crossed to a male *bshe* deficiency, and Trial #3 and #4 in which a female *bshe* deficiency was crossed to a male *bshe* mutant, either *3a52a* or *3a66a* for both trials. The experiment was to collect the 25% of the larvae that were hemizygous mutants to observe their lethal period. Trial #1 and #2 had mutants surviving to variable periods of larvalhood, with a delay in molting before dying. Trial #3 and #4 had little to no mutant larvae hatch, and so were lethal during embryogenesis.

As an alternative method for looking at development, RNAi knockdowns of *bshe*, with an *ey-GAL4* driver showed decreased and disorganized eye phenotype, though at a low penetrance (6-52% of non-balancer progeny). Comparisons to a *ball* knockdown with the *ey-GAL4* driver show that *ball* has very little effect in these cells based upon almost no non-balancer progeny having any abnormalities. Knockdown of *bshe* using the *neur-GAL4* driver showed some bristle defects in all *bshe* and in *ball* knockdowns, but again with a low penetrance (5-38% of non-balancer progeny). Knockdown with an *actin* driver for one *bshe* line had a lethal effect in pupae, and in the other *bshe* and *ball* drivers, it did not have a large lethal effect, but did show bristle defects.

Antibody Optimization

Three antibodies against peptides from BSHE were designed, one for the N-terminus and two for the C-terminus. The antibodies were used with Western Blots to see if they were specific to BSHE's 113.8 kDa protein. Through optimization, some bands were present at approximately the expected length. There were many non-specific bands as well. One at approximately 42kDa appeared with all three antibodies, which suggests this common band is due to something within each of the antibody preps. It is otherwise unexpected that a similar protein at that size is found consistently across all of the different antibodies. Negative controls with *bshe* deletion were inconclusive at this time as the loading controls did not appear and wild type control did not recapitulate previous trials. For all trials embryos were inappropriately fixed prior to sample preparation, and so that will negatively affect the outcome of the Western blot.

Immunofluorescence staining of embryos has shown that antibody #2 appears to be specific. In preparations where ¼ of the progeny were predicted to have no BSHE protein, ¼ of the embryos lacked fluorescence (Figure 5.7). In wild type embryos, fluorescence was seen in the cytoplasm within interphase embryos (Figure 5.6). The fluorescence in embryos during mitosis did not have any discernable pattern. Some embryos show foci but I am unsure at this time if this is involved in a specific process or associated with a specific part of the cell.

Conclusions and Future Directions

BSHE is an insect specific protein with a kinase insert region

While inserts within kinase domains are not unheard of, they are relatively rare. Platelet-derived growth factor (PDGF), and other kinases in its family like colony-stimulating factor (CSF-1), are receptor tyrosine kinases that all have inserts within their kinase domains, known as kinase inserts (3). Like the BSHE orthologs, proteins in this family have similar kinase domains, but dissimilar kinase inserts in both sequence and length. The αPDGF receptor has 104 amino acid insert (4). These inserts do show functional significance, as deletion and substitution of the amino acids in the kinase insert differentially impair the kinase activity (5). There are also some examples of kinase inserts in other serine/threonine kinases, like proteins in the eukaryotic initiation factor 2 (eIF2) family including the interferon-induced protein kinase (PKR). PKR has a

32 amino acid kinase insert between the kinase subdomains V and VI, which appears to be just prior of the catalytic loop (6). Modification of this kinase insert region abolishes kinase activity, but pseudosubstrate interaction is not disrupted (7). While neither PDGF nor PKR have kinase inserts in the same region as *bshe*, they do show possibilities for potential function in kinase activity or protein interaction.

The insert does not appear to affect the structure of the kinase domain based on protein structure predictions. The insert is also seen in all other *bshe* orthologs, and the location is the same, but the sequence and size of sequence is different. A hypothesis for the purpose of this insert that it doesn't necessarily have a function specific to its sequence, but rather just having an insert of any size at that specific location is necessary for *bshe*'s function. If *bshe*'s function could be assayed then that could be used to monitor any modified *bshe* transgene, which could be made with a variable sized or completely removed insert to observe whether the insert is necessary for *bshe*'s function. This could further be supported with a transgene rescue if the deletion of the insert does affect the function.

<u>BSHE and BALL are ancient proteins</u>

As discussed in detail in Chapter 3, there are three hypotheses for why *bshe* and *ball* have much longer branch lengths than the other groups in the CK1 kinase family. This is both comparing them to the other groups overall, as well as much longer branch lengths within *ball* and *bshe* between phylogenetic orders.

The first being that the common ancestral protein of *bshe* and *ball* originated prior to the origin of insects, and that *bshe* was lost in other phyla but retained in insects.

The second hypothesis is that the divergence of *bshe* and *ball* occurred near the origin of insects. Prior to that it was just a VRK-like ancestral protein, which split into *bshe* and *ball* after insects were formed.

The third is that *bshe* and *ball* are not any more ancestral than the other CK1 family kinases, but that both have been under more selective pressure, either at a certain point or on an ongoing basis, and so with more changes from the selective pressure has cause the branches to be longer.

All three hypotheses have pros and cons, which are discussed in detail in Chapter 3, and so none at this time stand out as more likely than another. At this time I'm unsure of a way to test any of the hypotheses.

Maternal genotype affects lethality

The different crosses I completed to find when *bshe* is lethal showed two very different results. Either the hemizygous mutants all hatched, and died at a point during the larval stage, or few to no larvae hatched. The difference that causes the earlier embryonic lethality is apparent when the deletion strain is the female parent of the cross. This is described in detail within Chapter 4. It looks as if there is a maternal affect having to do with the deletion strain. This could either be because one of the other genes within the deficiency, coupled with the *bshe* mutation confers an earlier lethality.

Another option is that there is a threshold of maternally deposited protein necessary for surviving further into the larval stage. If the female deletion parent has less BSHE in the ovaries because she is hemizygous, then that coupled with the mutation may not allow enough protein to survive later than the embryo stage. This would occur only if the *bshe* mutant used is not a null but has some residual function, because if it were a true null then the same affect would be seen if the female mutant was used, which is not the case. The mutant *3a52a* is a suspected null, as the truncated protein is missing half of its kinase domain, including all of the catalytic regions. If *bshe* is not a kinase, a truncated protein could still have some residual function.

There are two ways to test for the cause of difference in lethality. Firstly, if the N-terminal antibody is optimized and specific it could be used to test if the mutants are nulls or not, by noting if there is any protein present in suspected null mutant embryos through Western blots. The assumption being if the protein is non-functional that it would be quickly degraded. Additionally, Western blots could also be used to compare the maternally deposited protein levels of early embryos. If the maternal affect threshold hypothesis holds true, then we would suspect hemizygous embryos with the deficiency female parent to have lower protein levels than the hemizygous embryos with the mutant female parent.

In addition to clearly identifying the lethal stage of *bshe* mutants, the larval measurement experiment should be repeated with two different mutant parents (eg. *3a52a* x *3a66a*). Repeating this with reciprocal crosses, and with multiple mutant combinations should show an average of lethal stages and find a more accurate representation of the mutant lethal phenotype. This should prevent homozygosity of any second site EMS mutations, while not having the early lethal problems associated with the hemizygous deficiency parent. A transgene rescue experiment could then be used later to confirm the *bshe* mutants cause the phenotypes.

One way to study maternal affect of *bshe* is through a germ line mosaic. By using the ovo^{D} and FLP/FRT recombinase a germ line mosaic female can be produced (8). These females would either have nonfunctional ovaries because of the ovo^{D}, or be homozygous for the mutant *bshe*. Then we could assay the progeny to determine if there truly is a maternal affect with the *bshe* mutants.

RNAi knockdowns have variable penetrance

The RNAi knockdowns of *bshe* and *ball* strains using various GAL4 drivers had mixed results. On one hand, some showed consistent and useable results. For example, the ubiquitous *act-GAL4* driver with the *bshe* KK strain showed near complete lethality, but with larvae living until pupa stage before dying. Because *bshe* is an essential gene with a lethal mutant phenotype, the knockdown of *bshe* using a ubiquitous driver supports that the particular UAS strain is effective. The fact that they die late in development can also be useful. With the mutants, larvae die either during embryogenesis or early to mid-larval stages making it difficult to dissect and observe the internal structures. With *act-GAL4* driver dying in the pupal stage allows for dissection of living third instar larvae to observe the presence of any possible defective or disorganized internal structures. The other *UAS-bshe* strains and the *UAS-ball* strain with the *act-GAL4* driver do not show as complete a penetrance in either lethality or an adult phenotype, suggesting that the knockdown is not as complete using these strains, making them less ideal candidates for further research. If the Western blot protocol is improved, Western blots and qPCR can confirm the strength of the knockdown for each construct.

The other GAL4 drivers did not show a noticeable or highly penetrant knockdown phenotype. The *elav-GAL4* driver did not show any noticeable adult phenotype with any UAS strain, and so would not be a good driver to use for further research. The *neur-* and *ey-GAL4* drivers did show some phenotypes, but penetrance was variable. With *neur-GAL4* the bristle defects were very subtle and would be difficult to study in future research. The *ey-GAL4* did show a more noticeable phenotype that may be interesting to observe the eye imaginal discs within larvae to observe disrupted or disorganized morphology of the cells. Again, the low penetrance would make this difficult to reliably make conclusion, but it still could be worthwhile to explore. For example, if *bshe* is involved in mitosis, similar to *ball*, then the mitotic wave of the morphogenetic furrow across the eye imaginal disc could be studied with immunofluorescence or other assays. A way to improve penetrance and phenotype that could be explored is conducting the crosses at a higher temperature. An increase in temperature will increase the production of GAL4, which should increase the amount of the dsRNA produced.

RNAi has recently come into question in its viability as a research tool. While it still is used in Drosophila as a way of screening knockdown genes in various studies, it also has been shown to have false positives, false negatives and off-target-effects (9,10). While not completely discounting results found from RNAi experiments, it does suggest that future research with this should proceed with caution and proper controls for accurate knockdown be used.

Western blot BSHE antibodies have non-specific bands

Optimization of the BSHE antibodies is still on going. A few bands were seen in multiple antibodies that have an appropriate size of approximately 113.8 kDa, but as of right now none have been definitively identified as BSHE. There are also many non-specific bands, including a 42 kDa band found across all three antibodies, which suggests a contaminant within all primary antibody solutions. Another possibility is that this band is the BSHE protein, but folded and crosslinked so that it does not run as expected.

With further optimization and proper negative controls a BSHE specific band could be identified. After that, optimization to increase the signal of the BSHE specific band and decrease the background noise and non-specific bands could give antibodies that

would be very useful for further research. Observing relative protein levels of different stages of development and different tissues could identify the spatial and temporal patterns of BSHE expression. These can also be used to compare the differences and viability of the truncated mutant proteins.

BSHE is found in the cytoplasm in early development.

Initial immunofluorescence analysis with one antibody show more definitive results than the Western blots. BSHE fluorescence is seen in the cytoplasm in interphase embryos. The *bshe* deficient strain appears to have embryos with no fluorescence, suggesting that the antibody is specific for *bshe*. This will need to be confirmed though. To do this, fixed embryos would be scored for the presence or absence of antibody staining, and then a PCR can be developed to confirm that the unstained embryos are the deficiency homozygotes. Another way to confirm antibody specificity is to create a transgene that is expressed in stripes within the developing embryo, using expression patterns of *engrailed* for example. A striped embryo of staining and lack of staining should be obvious in this assay, further confirming antibody specificity.

Once this negative control can be confirmed, then the tissue and sub-cellular location of BSHE can be studied in more detail. I would suggest confirming the cytoplasmic specific localization during interphase and attempting to find a pattern of localization during mitosis. This will help understand when and where BSHE is functioning. This can also be repeated in larval tissues to see if this cytoplasmic localization is consistent, or tissue specific.

So far only antibody 2 has been tested for immunofluorescence. The other two antibodies should also be tested to see if one is more consistent and specific than another. Also if multiple are optimized, then it will allow for further confirmation of the results. Since there are antibodies for both the N- and C- terminus it may allow us to see if the truncated mutant embryos are persisting, and possibly having residual activity.

Future experiments with BSHE antibodies

If the antibodies are specific to BSHE, they can be used for many experiments to help understand more of BSHE's function. The antibody can aid in purification of BSHE in order to be used for a variety of assays. Of particular interest is understanding if

BSHE has kinase activity. A kinase assay could be used, initially testing histones or chromatin like *ballchen* to see if it has a similar substrate. Other potential substrates could be the known proteins in the WNT or RAS/MAPK pathway, of which *bshe* has already been identified as having a role (11,12). If BSHE shows a positive result from the kinase assay, that will support the evidence of my protein prediction models that the insert does not have a negative affect on the kinase domain.

Antibodies can also be used in a co-immunoprecipitation to identify partners or substrates for phosphorylation. Candidates for substrate interactions, like histones or members of the WNT or RAS/MAPK pathway can be tested first, mass spectroscopy can also be used to help identify unknown protein interactions (13,14). Finding complexes that BSHE interacts with, regulatory partners or substrates will be an essential step in understanding BSHE's essential role in development.

References

1. McCracken A, Locke J. Mutations in CG8878, a novel putative protein kinase, enhance P element dependent silencing (PDS) and position effect variegation (PEV) in Drosophila melanogaster. PLoS ONE. 2014;9(3):e71695.

2. Manning G, Plowman GD, Hunter T, Sudarsanam S. Evolution of protein kinase signaling from yeast to man. Trends Biochem Sci. 2002 Oct;27(10):514–20.

3. Yarden Y, Escobedo JA, Kuang WJ, Yang-Feng TL, Daniel TO, Tremble PM, et al. Structure of the receptor for platelet-derived growth factor helps define a family of closely related growth factor receptors. Nature. 1986 Sep;323(6085):226–32.

4. Qiu FH, Ray P, Brown K, Barker PE, Jhanwar S, Ruddle FH, et al. Primary structure of c-kit: relationship with the CSF-1/PDGF receptor kinase family--oncogenic activation of v-kit involves deletion of extracellular domain and C terminus. EMBO J. 1988 Apr;7(4):1003–11.

5. Heidaran MA, Pierce JH, Lombardi D, Ruggiero M, Gutkind JS, Matsui T, et al. Deletion or substitution within the alpha platelet-derived growth factor receptor kinase insert domain: effects on functional coupling with intracellular signaling pathways. Mol Cell Biol. 1991 Jan;11(1):134–42.

6. Meurs E, Chong K, Galabru J, Thomas NS, Kerr IM, Williams BR, et al. Molecular cloning and characterization of the human double-stranded RNA-activated protein kinase induced by interferon. Cell. 1990 Jul 27;62(2):379–90.

7. Craig AW, Cosentino GP, Donzé O, Sonenberg N. The kinase insert domain of interferon-induced protein kinase PKR is required for activity but not for interaction with the pseudosubstrate K3L. J Biol Chem. 1996 Oct 4;271(40):24526–33.

8. Perrimon N. Creating mosaics in Drosophila. Int J Dev Biol. 1998;42(3):243–7.

9. Mohr SE, Perrimon N. RNAi screening: new approaches, understandings, and organisms. Wiley Interdiscip Rev RNA. 2012 Mar;3(2):145–58.

10. Booker M, Samsonova AA, Kwon Y, Flockhart I, Mohr SE, Perrimon N. False negative rates in Drosophila cell-based RNAi screens: a case study. BMC Genomics. 2011;12:50.

11. Swarup S, Pradhan-Sundd T, Verheyen EM. Genome-wide identification of phospho-regulators of Wnt signaling in Drosophila. Development. 2015 Apr 15;142(8):1502–15.

12. Ashton-Beaucage D, Udell CM, Gendron P, Sahmi M, Lefrançois M, Baril C, et al. A Functional Screen Reveals an Extensive Layer of Transcriptional and Splicing Control Underlying RAS/MAPK Signaling in Drosophila. PLoS Biol. Public Library of Science; 2014;12(3):e1001809.

13. Free RB, Hazelwood LA, Sibley DR. Identifying novel protein-protein interactions using co-immunoprecipitation and mass spectroscopy. Curr Protoc Neurosci. 2009 Jan;Chapter 5:Unit5.28.

14. Comai L. Coimmunoprecipitation Assay for the Detection of Kinase-Substrate Interactions. Cancer Cell Signaling. New Jersey: Humana Press; 2002. pp. 277–84.

7. Appendix

Introduction

The following appendix consists of experiments that were not appropriate for full analysis, but are still evidence of work completed.

The first section is a summary of mutant length and activity analysis that was done with homozygous mutants as opposed to hemizygous mutants. The second section is of a rough BLAST and sequence alignment to account for Crustacea, which was not included in the initial phylogenetics search for other organisms that have *banshee* (*bshe*). The third section is of the sequencing I completed for the gene *combgap* (*cg)* searching for lesions of two mutants, and is not related to my *banshee* characterization.

Homozygous mutant length analysis

The following are results collected from the initial mutant length analysis using homozygous *3a52a* mutant. Larvae were collected and measured as described in Method 1 in Chapter 2. Length, molting times and activity at the time of measurement were recorded and presented below.

A

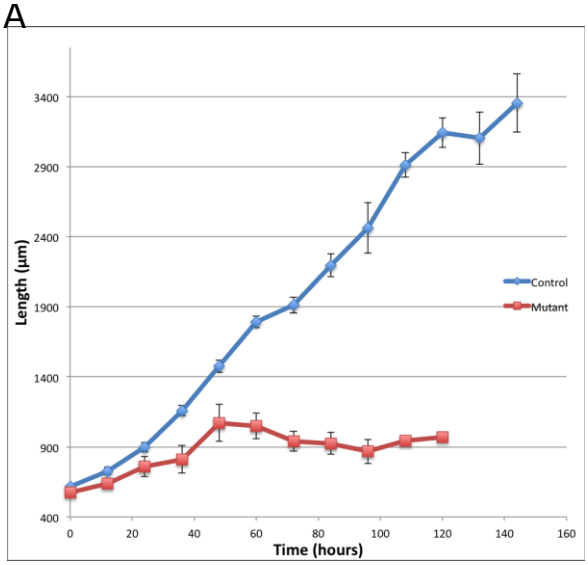

B

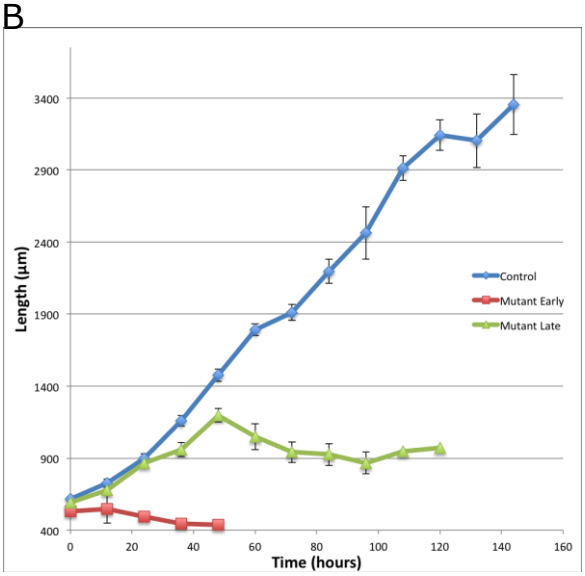

Figure 7.1. Mutant larval growth rates over time. (A) A comparison between control (blue) and mutant (red) larvae. (B) Same data presented here as in (A), but this case the mutants were separated into two cohorts, those that died before the first molt (red), and those that lived longer (green). Mutants that died in the first molt did not grow at all, while those in the second molt grew relatively normally for the first part of their lifespan.

A

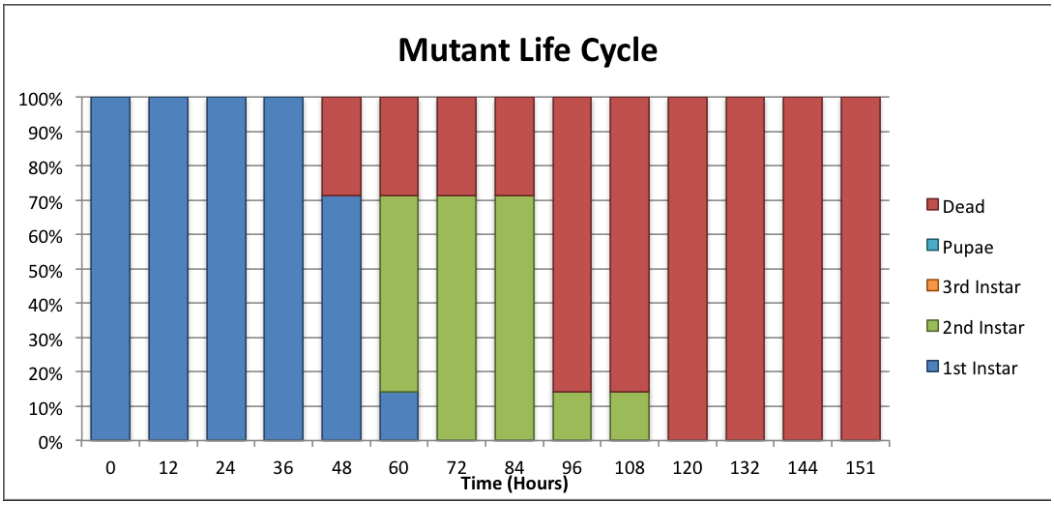

B

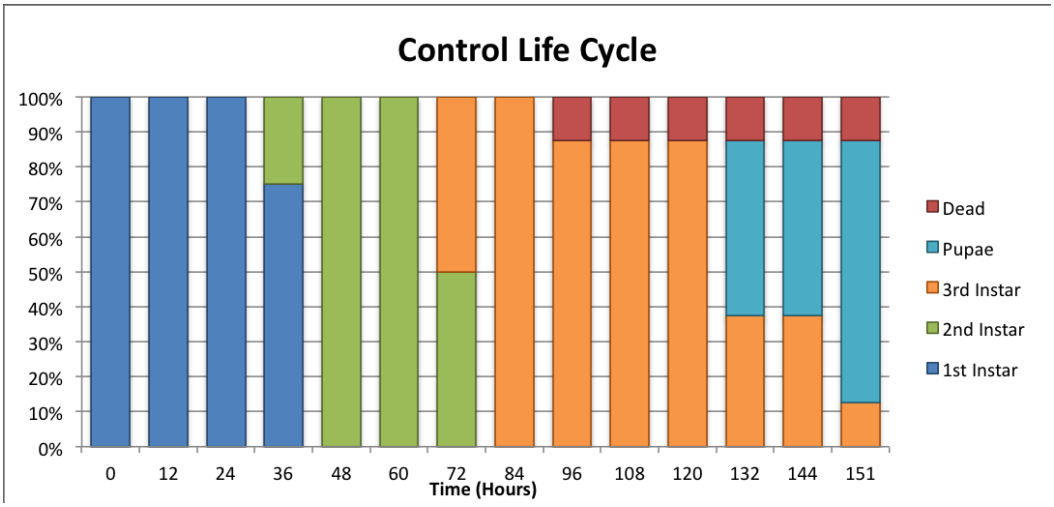

Figure 7.2. Percentage of life cycle stages at each time point of mutant larvae (A) and control larvae (B). Mutant larvae completed their first molt much later than control larvae, and those that did complete their first molt did not survive to their second molt.

A

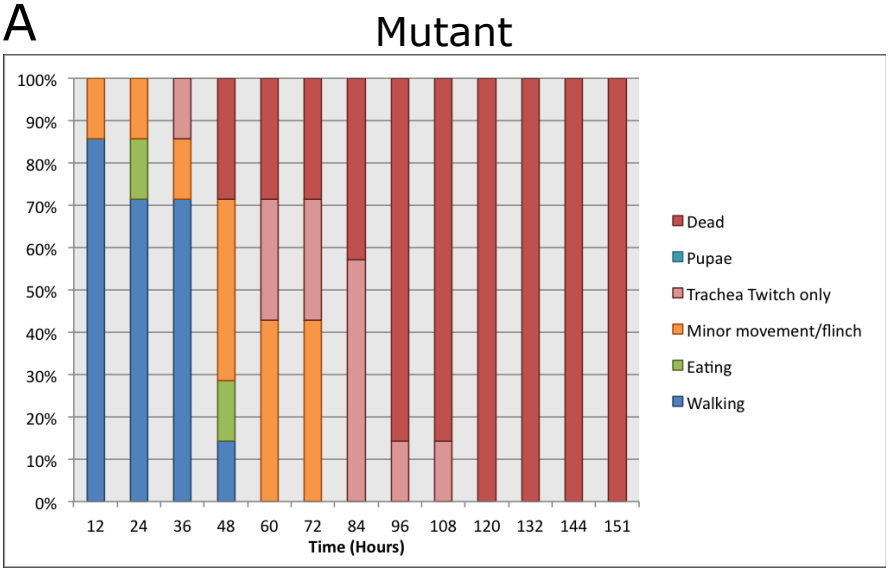

B

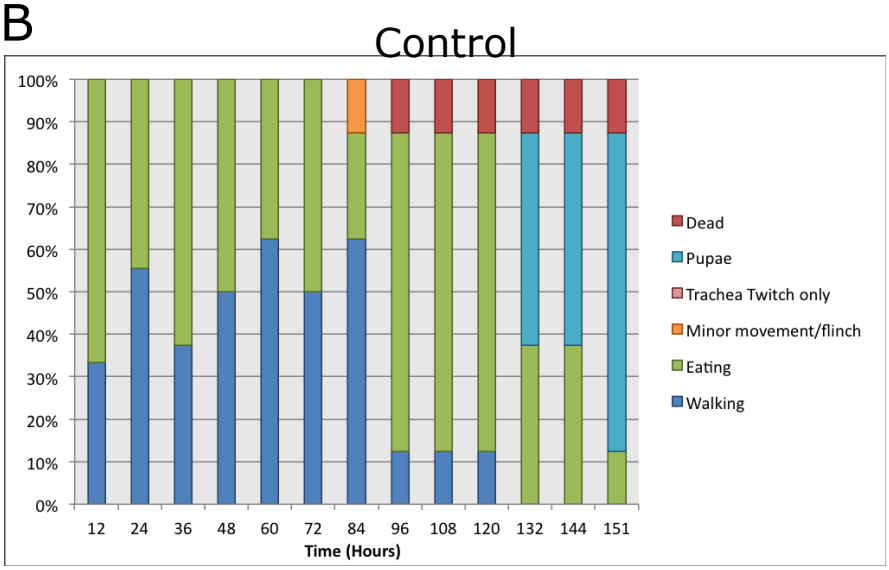

Figure 7.3. Activity of mutant (A) and control (B) larvae as observed at time of measurement. Larvae were scored on their activity immediately prior to measurement. Trachea twitch only means that the larvae no longer move or flinch on light contact, but when observed closely do have minor muscle spasms visible within the trachea. The spasms are constant and not associated with light or physical disturbance. Minor movement/flinch means that the larvae were not moving or not moving efficiently, but will still flinch and move when lightly touched. Eating means that the larvae were within the media. Walking means larvae were crawling along the surface of the media.

Crustacea alignment

The *Drosophila melanogaster banshee (*BSHE*)* kinase domain polypeptide sequence was submitted to BLAST using only the Crustacea database sequences. Currently only *Daphnia pulex* is completely sequenced within Crustacea, so only sequences from *D. pulex* were expected. Sequences from other Crustacea did get returned, but were not included due to that species being incompletely sequenced.

Sequences lower than a $1e^{-08}$ e-value threshold were chosen. This threshold is less stringent than the phylogenetic tree built in Chapter 3, which had a threshold of $9.9e^{-20}$. This was done in order to identify all Casien Kinase 1 family proteins, and because BLAST is less stringent than the profile Hidden Markov Models used with HMMER. Crustacean sequences that were higher than the $1e^{-08}$ threshold did not align well with the sequences already included. The Crustacean sequences along with the *D. melanogaster* Casein Kinase 1 family proteins were aligned using CLUSTALW, and a rooted UPGMA tree with branch length was constructed from that.

Figure 7.4 is the initial alignment using the full protein of all sequences. Note that this is different than the method for tree building used in Chapter 3, where only sequences with less than 10% gaps in the alignment were used. GI321468460 aligns more closely with BALL than with BSHE. GI321458037 aligns with CK1A, GI321478363 aligns with GISH, and GI321468883 aligns with ASATOR. Two proteins did not align closely with any specific *D. melanogaster* protein, but GI321453624 appears GISH-like and GI 321479006 appears CK1A like. No *D. pulex* DISC protein was found.

Alignments using the entire kinase domain were also completed of just GI321468460 and *D. melanogaster* BSHE and BALL, both with Figure 7.5 and without Figure 7.6 the BSHE insert region. In both cases, GI321468460 aligns more closely with BALL, with no noticeable insert within the kinase domain, suggesting that this sequence is a BALL ortholog as opposed to a BSHE ortholog.

This initial evidence suggests that the Crustacean *D. pulex* is like the Arachnida outgroup, where it does not have the BSHE protein, and only has BALL, further supporting the evidence than *bshe* is an insect specific gene.

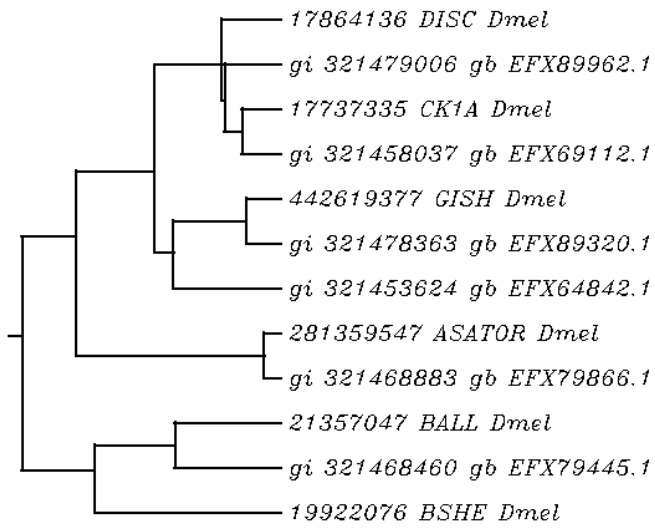

Figure 7.4. CLUSTALW protein alignment of top six *Daphina pulex* proteins from a BLAST of the *Drosphila melanogaster* BSHE kinase domain. These sequences were aligned to the *Drosophila melanogaster* Casein Kinase 1 family proteins to identify if *D. pulex* contains BSHE.

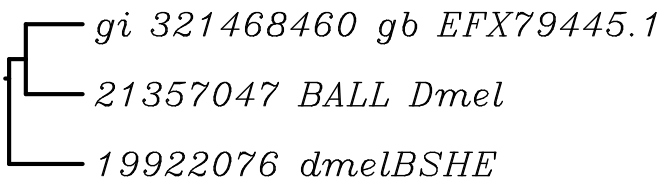

Figure 7.5. CLUSTALW protein alignment of only the kinase domain of the most similar *Daphina pulex* protein to *Drosophila melanogaster* BALL and BSHE with insert sequence included.

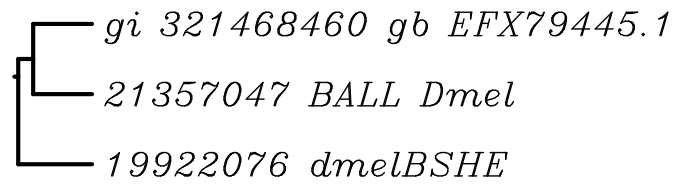

Figure 7.6 CLUSTALW protein alignment of only the kinase domain of the most similar *Daphina pulex* protein to *Drosophila melanogaster* BALL and BSHE without insert sequence.

Sequencing *combgap*

All expected exons of *combgap* were sequenced in the parental genotype, as well as the two mutant 4a29a and 4a30a. These sequences were compared to the given reference sequence (GI: 671162315) to locate polymorphisms as well as mutation points. Mutations were observed as double peaks on the chromatograph. Exons were predicted using isoform F (GI: 665400843) and then translated using the online ExPASy translate tool and compared to the isoform F protein sequence (GI: 161077054). There were many regions of polymorphism when comparing both mutants and parental to the reference sequence. In addition, two point mutations were found in 4a29a and one point mutation was found in 4a30a.

There were large regions of polymorphic differences between the parental and reference sequence. These include single nucleotide changes, and missing or gaining one or more additional nucleotides in regions. These are mostly in the introns (61 intronic polymorphisms, 5 in exons), with the polymorphisms in the exons still coding for the conserved amino acid sequence.

4a29a has a G to A transition, which creates a missense mutation of a C to Y at amino acid 389. This residue is within a zinc finger domain. The second lesion is a C to A transversion, which creates a missense mutation of Q to K at amino acid 485. This amino acid change is between similar amino acids, and it is not within a known domain of combgap.

4a30a has a C to T transition. This creates an R to C missense mutation at amino acid 404. Additionally, this mutation occurs at the -2 position of the 5’ splice site. This might cause a splicing mutation, but splice site consensus puts a T or C at equal likelihood at this location, with A being the preferred nucleotide (Mount 1992). If it does in fact prevent splicing at that location, an intronic stop codon would lead to a truncated protein.

Mount SM, Burks C, Hertz G, Stormo GD, White O, Fields C. Splicing signals in Drosophila: intron size, information content, and consensus sequences. *Nucleic Acids Research*. 1992;20(16):4255-4262.

```
Combgap          TGGTCACGCACAGCAAGTTCCACGCCGGCGAACGACCATATGTATGCGAGGAATGTGGTG
4a29a            TGGTCACGCACAGCAAGTTCCACGCCGGCGAACGACCGTATGTATGCGAGGAATRTGGTG
                 ************************************ *************** *****
```

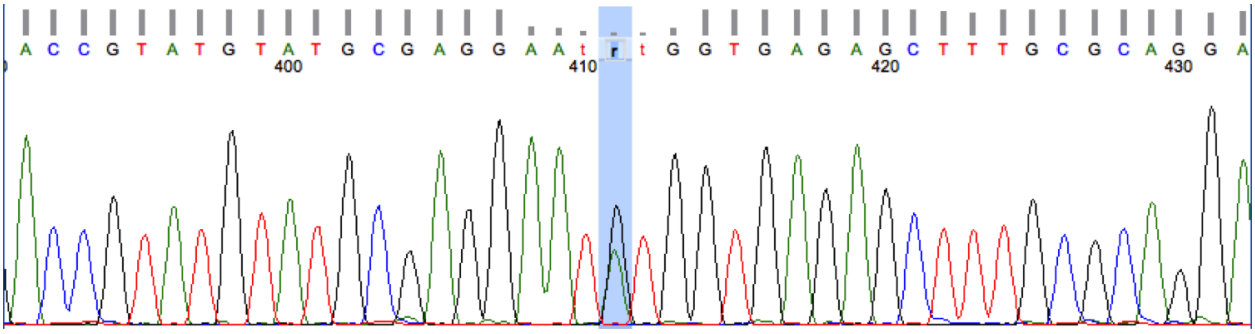


```
Combgap          CGCATCCCTGCGTCAGCTGTGGCGAGGGATTCCTCACCAAGGCCGAACTGCATCAGCATG
4a29a            CGCATCCCTGCGTCAGCTGTGGCGAGGGATTCCTCACCAAGGCCGAACTGCATMAGCATG
                 ************************************************** ******
```

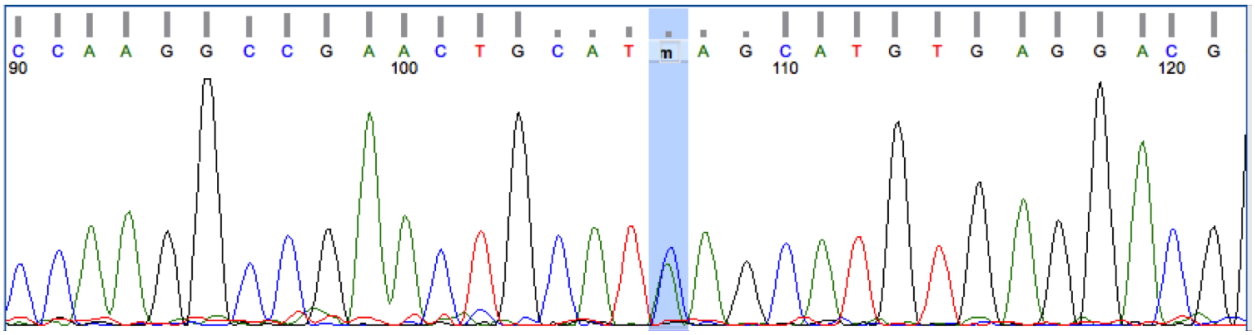

Figure 7.7. Single base pair mutations of *combgap* mutant *4a29a.*

```
Combgap          AGAGCTTTGCGCAGGAAAACCACCTGATTATGCACTCTCGgtaagttggctcttttaata
4a30a            AGAGCTTTGCGCAGGAAAACCACCTGATTATGCACTCTYGgtaagttggctcttttaata
                 **************************************** ********************
```

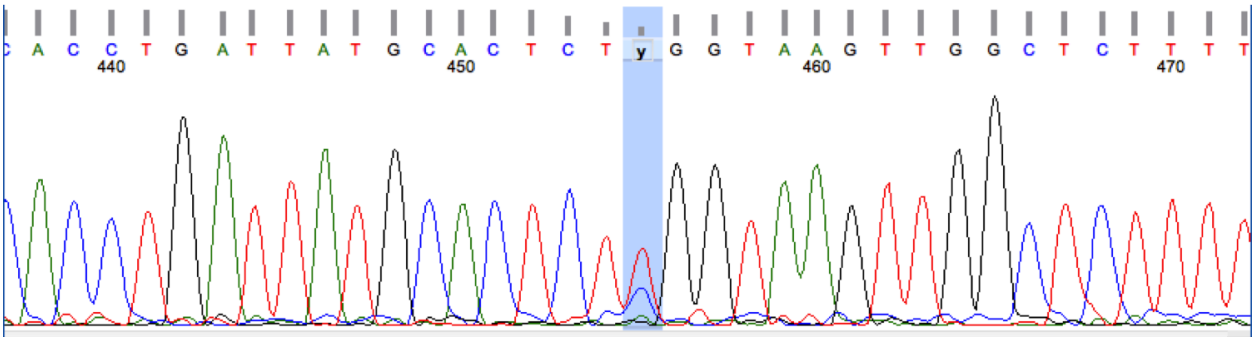

Figure 7.8. Single base pair mutations of *combgap* mutant *4a30a.* In the alignment, uppercase indicates exons while lowercase indicates introns.

Works Cited

Ahmad K, Henikoff S. The histone variant H3.3 marks active chromatin by replication-independent nucleosome assembly. Mol Cell. 2002 Jun;9(6):1191–200.

Aihara H, Nakagawa T, Yasui K, Ohta T, Hirose S, Dhomae N, et al. Nucleosomal histone kinase-1 phosphorylates H2A Thr 119 during mitosis in the early Drosophila embryo. Genes Dev. 2004 Apr 15;18(8):877–88.

Ashburner M. Drosophila: A laboratory manual. Cold Spring Harbor Laboratory Press; 1989. 1 p.

Ashton-Beaucage D, Udell CM, Gendron P, Sahmi M, Lefrançois M, Baril C, et al. A Functional Screen Reveals an Extensive Layer of Transcriptional and Splicing Control Underlying RAS/MAPK Signaling in Drosophila. PLoS Biol. Public Library of Science; 2014;12(3):e1001809.

Bao X, Deng H, Johansen J, Girton J, Johansen KM. Loss-of-function alleles of the JIL-1 histone H3S10 kinase enhance position-effect variegation at pericentric sites in Drosophila heterochromatin. Genetics. 2007 Jun;176(2):1355–8.

Bártová E, Krejcí J, Harnicarová A, Galiová G, Kozubek S. Histone modifications and nuclear architecture: a review. J Histochem Cytochem. 2008 Aug;56(8):711–21.

Behrend L, Stöter M, Kurth M, Rutter G, Heukeshoven J, Deppert W, et al. Interaction of casein kinase 1 delta (CK1delta) with post-Golgi structures, microtubules and the spindle apparatus. Eur J Cell Biol. 2000 Apr;79(4):240–51.

Bengtsson L, Wilson KL. Barrier-to-autointegration factor phosphorylation on Ser-4 regulates emerin binding to lamin A in vitro and emerin localization in vivo. Mol Biol Cell. 2006 Mar;17(3):1154–63.

Black DM, Jackson MS, Kidwell MG, Dover GA. KP elements repress P-induced hybrid dysgenesis in Drosophila melanogaster. EMBO J. 1987 Dec 20;6(13):4125–35.

Bloomfield VA. DNA condensation. Curr Opin Struct Biol. 1996 Jun;6(3):334–41.

Booker M, Samsonova AA, Kwon Y, Flockhart I, Mohr SE, Perrimon N. False negative rates in Drosophila cell-based RNAi screens: a case study. BMC Genomics. 2011;12:50.

Boulianne GL, la Concha de A, Campos-Ortega JA, Jan LY, Jan YN. The Drosophila neurogenic gene neuralized encodes a novel protein and is expressed in precursors of larval and adult neurons. EMBO J. 1991 Oct;10(10):2975–83.

Brand AH, Perrimon N. Targeted gene expression as a means of altering cell fates and generating dominant phenotypes. 1993.

Brittle AL, Nanba Y, Ito T, Ohkura H. Concerted action of Aurora B, Polo and NHK-1

kinases in centromere-specific histone 2A phosphorylation. Exp Cell Res. 2007 Aug;313(13):2780–5.

Brodie R, Roper RL, Upton C. JDotter: a Java interface to multiple dotplots generated by dotter. Bioinformatics. 2004.

Bushey D, Locke J. Mutations in Su (var) 205 and Su (var) 3-7 suppress P-element-dependent silencing in Drosophila melanogaster. Genetics. Genetics Soc America; 2004;168(3):1395–411.

Carmena M, Wheelock M, Funabiki H, Earnshaw WC. The chromosomal passenger complex (CPC): from easy rider to the godfather of mitosis. Nat Rev Mol Cell Biol. 2012 Dec;13(12):789–803.

Comai L. Coimmunoprecipitation Assay for the Detection of Kinase-Substrate Interactions. Cancer Cell Signaling. New Jersey: Humana Press; 2002. pp. 277–84.

Craig AW, Cosentino GP, Donzé O, Sonenberg N. The kinase insert domain of interferon-induced protein kinase PKR is required for activity but not for interaction with the pseudosubstrate K3L. J Biol Chem. 1996 Oct 4;271(40):24526–33.

Csink AK, Bounoutas A, Griffith ML, Sabl JF, Sage BT. Differential gene silencing by trans-heterochromatin in Drosophila melanogaster. Genetics. 2002 Jan;160(1):257–69.

Cullen CF. The conserved kinase NHK-1 is essential for mitotic progression and unifying acentrosomal meiotic spindles in Drosophila melanogaster. J Cell Biol. 2005 Nov 14;171(4):593–602.

Dernburg AF, Broman KW, Fung JC, Marshall WF, Philips J, Agard DA, et al. Perturbation of nuclear architecture by long-distance chromosome interactions. Cell. 1996 May 31;85(5):745–59.

Eaton S, Kornberg TB. Repression of ci-D in posterior compartments of Drosophila by engrailed. Genes Dev. 1990.

Ebert A, Schotta G, Lein S, Kubicek S, Krauss V, Jenuwein T, et al. Su(var) genes regulate the balance between euchromatin and heterochromatin in Drosophila. Genes Dev. 2004 Dec 1;18(23):2973–83.

Eddy SR. Profile hidden Markov models. Bioinformatics. 1998.

Edgar RC. MUSCLE: multiple sequence alignment with high accuracy and high throughput. Nucleic Acids Res. 2004;32(5):1792–7.

Engels WR. The origin of P elements inDrosophila melanogaster. Bioessays. 1992 Oct;14(10):681–6.

Filion GJ, van Bemmel JG, Braunschweig U, Talhout W, Kind J, Ward LD, et al. Systematic protein location mapping reveals five principal chromatin types in Drosophila cells. Cell. 2010 Oct 15;143(2):212–24.

Free RB, Hazelwood LA, Sibley DR. Identifying novel protein-protein interactions using co-immunoprecipitation and mass spectroscopy. Curr Protoc Neurosci. 2009 Jan;Chapter 5:Unit5.28.

Gallego M, Virshup DM. Post-translational modifications regulate the ticking of the circadian clock. Nat Rev Mol Cell Biol. 2007 Feb;8(2):139–48.

Gelbart WM, Emmert DB. FlyBase High Throughput Expression Pattern Data. 2013.

Girton JR, Johansen KM. Chromatin structure and the regulation of gene expression: the lessons of PEV in Drosophila. Adv Genet. 2008;61:1–43.

Gloor GB, Preston CR, Johnson-Schlitz DM, Nassif NA, Phillis RW, Benz WK, et al. Type I repressors of P element mobility. Genetics. 1993 Sep;135(1):81–95.

Goll MG, Bestor TH. Histone modification and replacement in chromatin activation. Genes Dev. 2002 Jul 15;16(14):1739–42.

Gorjánácz M, Klerkx EPF, Galy V, Santarella R, López-Iglesias C, Askjaer P, et al. Caenorhabditis elegans BAF-1 and its kinase VRK-1 participate directly in post-mitotic nuclear envelope assembly. EMBO J. 2007 Jan 10;26(1):132–43.

Grant PA. A tale of histone modifications. Genome Biol. 2001;2(4):REVIEWS0003

Grewal SIS, Elgin SCR. Heterochromatin: new possibilities for the inheritance of structure. Curr Opin Genet Dev. 2002 Apr;12(2):178–87.

Gross SD. A phosphatidylinositol 4,5-bisphosphate-sensitive casein kinase I alpha associates with synaptic vesicles and phosphorylates a subset of vesicle proteins. J Cell Biol. 1995 Aug 1;130(3):711–24.

Guex N, Peitsch MC. SWISS-MODEL and the Swiss-PdbViewer: an environment for comparative protein modeling. Electrophoresis. 1997 Dec;18(15):2714–23.

Halder G, Callaerts P, Gehring WJ. Induction of ectopic eyes by targeted expression of the eyeless gene in Drosophila. Science. 1995 Mar 24;267(5205):1788–92.

Halder G, Callaerts P, Gehring WJ. New perspectives on eye evolution. Curr Opin Genet Dev. 1995 Oct;5(5):602–9.

Heidaran MA, Pierce JH, Lombardi D, Ruggiero M, Gutkind JS, Matsui T, et al. Deletion or substitution within the alpha platelet-derived growth factor receptor kinase insert domain: effects on functional coupling with intracellular signaling pathways. Mol Cell Biol. 1991 Jan;11(1):134–42.

Herzig B, Yakulov TA, Klinge K, Günesdogan U, Jäckle H, Herzig A. Bällchen is required for self-renewal of germline stem cells in Drosophila melanogaster. Biol Open. 2014 May 29.

Horwich MD, Li C, Matranga C, Vagin V, Farley G, Wang P, et al. The Drosophila RNA methyltransferase, DmHen1, modifies germline piRNAs and single-stranded siRNAs in RISC. Curr Biol. 2007 Jul 17;17(14):1265–72.

Houlden H, Johnson J, Gardner-Thorpe C, Lashley T, Hernandez D, Worth P, et al. Mutations in TTBK2, encoding a kinase implicated in tau phosphorylation, segregate with spinocerebellar ataxia type 11. Nat Genet. 2007 Dec;39(12):1434–6.

Ivanovska I. A histone code in meiosis: the histone kinase, NHK-1, is required for proper chromosomal architecture in Drosophila oocytes. Genes Dev. 2005 Nov 1;19(21):2571–82.

Ivanovska I, Orr-Weaver TL. Histone modifications and the chromatin scaffold for meiotic chromosome architecture. Cell Cycle. Landes Bioscience; 2006;5(18):2064–71.

Jenuwein T, Allis CD. Translating the histone code. Science. 2001 Aug 10;293(5532):1074–80.

Kammermeier L, Leemans R, Hirth F, Flister S, Wenger U, Walldorf U, et al. Differential expression and function of the Drosophila Pax6 genes eyeless and twin of eyeless in embryonic central nervous system development. Mech Dev. 2001 May;103(1-2):71–8.

Kang T-H, Kim K-T. Negative regulation of ERK activity by VRK3-mediated activation of VHR phosphatase. Nat Cell Biol. 2006 Jul 16;8(8):863–9.

Kang T-H, Kim K-T. VRK3-mediated inactivation of ERK signaling in adult and embryonic rodent tissues. Biochim Biophys Acta. 2008 Jan;1783(1):49–58.

Kang T-H, Park D-Y, Choi YH, Kim K-J, Yoon HS, Kim K-T. Mitotic Histone H3 Phosphorylation by Vaccinia-Related Kinase 1 in Mammalian Cells. Mol Cell Biol. 2007.

Kidwell MG, Frydryk T, Novy JB. The hybrid dysgenesis potential of Drosophila melanogaster strains of diverse temporal and geographical natural origins. Drosoph. Inf. Serv; 1983. 7 p.

Kidwell MG, Kidwell JF, Sved JA. Hybrid Dysgenesis In Drosophila Melanogaster: A Syndrome Of Aberrant Traits Including Mutation, Sterility And Male Recombination. Genetics. 1977.

Kim K, Kim J-M, Kim J-S, Choi J, Lee YS, Neamati N, et al. VprBP has intrinsic kinase activity targeting histone H2A and represses gene transcription. Mol Cell. 2013 Nov

7;52(3):459–67.

Knippschild U, Gocht A, Wolff S, Huber N, Löhler J, Stöter M. The casein kinase 1 family: participation in multiple cellular processes in eukaryotes. Cell Signal. Elsevier; 2005;17(6):675–89.

Lancaster OM, Breuer M, Cullen CF, Ito T, Ohkura H. The Meiotic Recombination Checkpoint Suppresses NHK-1 Kinase to Prevent Reorganisation of the Oocyte Nucleus in Drosophila. PLoS Genet. Public Library of Science; 2010 Oct 28;6(10):e1001179.

Lancaster OM, Cullen CF, Ohkura H. NHK-1 phosphorylates BAF to allow karyosome formation in the Drosophila oocyte nucleus. J Cell Biol. Rockefeller Univ Press; 2007;179(5):817–24.

Lemaitre B, Ronsseray S, Coen D. Maternal repression of the P element promoter in the germline of Drosophila melanogaster: a model for the P cytotype. Genetics. 1993 Sep;135(1):149–60.

Lerach S, Zhang W, Bao X, Deng H, Girton J, Johansen J, et al. Loss-of-function alleles of the JIL-1 kinase are strong suppressors of position effect variegation of the wm4 allele in Drosophila. Genetics. 2006 Aug;173(4):2403–6.

Locke J, Kotarski MA, Tartof KD. Dosage-dependent modifiers of position effect variegation in Drosophila and a mass action model that explains their effect. Genetics. 1988 Sep;120(1):181–98.

Lopez-Sanchez I, Sanz-Garcia M, Lazo PA. Plk3 Interacts with and Specifically Phosphorylates VRK1 in Ser342, a Downstream Target in a Pathway That Induces Golgi Fragmentation. Mol Cell Biol. 2009 Feb 11;29(5):1189–201.

Lund H, Cowburn RF, Gustafsson E, Strömberg K, Svensson A, Dahllund L, et al. Tau-Tubulin Kinase 1 Expression, Phosphorylation and Co-Localization with Phospho-Ser422 Tau in the Alzheimer's Disease Brain. Brain Pathol. 2012 Nov 20;23(4):378–89.

Maeshima K, Imai R, Tamura S, Nozaki T. Chromatin as dynamic 10-nm fibers. Chromosoma. 2014 Jun;123(3):225–37.

Manning G, Plowman GD, Hunter T, Sudarsanam S. Evolution of protein kinase signaling from yeast to man. Trends Biochem Sci. 2002 Oct;27(10):514–20.

Margalit A, Brachner A, Gotzmann J, Foisner R, Gruenbaum Y. Barrier-to-autointegration factor--a BAFfling little protein. Trends Cell Biol. 2007 Apr;17(4):202–8.

McCracken A. Modifiers of P-element-dependent silencing in Drosophila melanogaster. Locke J, editor. [Edmonton]: University of Alberta; 2012.

McCracken A, Locke J. Mutations in CG8878, a novel putative protein kinase, enhance P element dependent silencing (PDS) and position effect variegation (PEV) in Drosophila melanogaster. PLoS ONE. 2014;9(3):e71695.

Melcher K. The strength of acidic activation domains correlates with their affinity for both transcriptional and non-transcriptional proteins. J Mol Biol. 2000 Sep 1;301(5):1097–112.

Meurs E, Chong K, Galabru J, Thomas NS, Kerr IM, Williams BR, et al. Molecular cloning and characterization of the human double-stranded RNA-activated protein kinase induced by interferon. Cell. 1990 Jul 27;62(2):379–90.

Milne D. Catalytic Activity of Protein Kinase CK1δ (Casein Kinase 1δ) Is Essential for Its Normal Subcellular Localization. Exp Cell Res. 2001 Feb 1;263(1):43–54.

Misra S, Rio DC. Cytotype control of Drosophila P element transposition: The 66 kd protein is a repressor of transposase activity. Cell. 1990.

Mohr SE, Perrimon N. RNAi screening: new approaches, understandings, and organisms. Wiley Interdiscip Rev RNA. 2012 Mar;3(2):145–58.

Monsalve DM, Merced T, Fernández IF, Blanco S, Vázquez-Cedeira M, Lazo PA. Human VRK2 modulates apoptosis by interaction with Bcl-xL and regulation of BAX gene expression. Cell Death Dis. 2013;4:e513.

Motzny CK, Holmgren R. The Drosophila cubitus interruptus protein and its role in the wingless and hedgehog signal transduction pathways. Mech Dev. 1995 Jul;52(1):137–50.

Muller HJ. Types of visible variations induced by X-rays in Drosophila. Journ of Gen. 1930 Jul;22(3):299–334.

Nakayama T, Nishioka K, Dong Y-X, Shimojima T, Hirose S. Drosophila GAGA factor directs histone H3.3 replacement that prevents the heterochromatin spreading. Genes Dev. 2007 Mar 1;21(5):552–61.

Nichols RJ, Traktman P. Characterization of three paralogous members of the Mammalian vaccinia related kinase family. J Biol Chem. 2004 Feb 27;279(9):7934–46.

Nichols RJ, Wiebe MS, Traktman P. The vaccinia-related kinases phosphorylate the N' terminus of BAF, regulating its interaction with DNA and its retention in the nucleus. Mol Biol Cell. 2006 May;17(5):2451–64.

Nikalayevich E, Ohkura H. The NuRD nucleosome remodelling complex and NHK-1 kinase are required for chromosome condensation in oocytes. J Cell Sci. 2015 Feb 1;128(3):566–75.

O'Hare K, Rubin GM. Structures of P transposable elements and their sites of insertion and excision in the Drosophila melanogaster genome. Cell. 1983.

Perrimon N. Creating mosaics in Drosophila. Int J Dev Biol. 1998;42(3):243–7.

Price MA. CKI, there's more than one: casein kinase I family members in Wnt and Hedgehog signaling. Genes Dev. 2006 Feb 15;20(4):399–410.

Qi H, Yao C, Cai W, Girton J, Johansen KM, Johansen JR. Asator, a tau-tubulin kinase homolog in Drosophilalocalizes to the mitotic spindle. Dev Dyn. 2009 Dec;238(12):3248–56.

Qiu FH, Ray P, Brown K, Barker PE, Jhanwar S, Ruddle FH, et al. Primary structure of c-kit: relationship with the CSF-1/PDGF receptor kinase family--oncogenic activation of v-kit involves deletion of extracellular domain and C terminus. EMBO J. 1988 Apr;7(4):1003–11.

Quiring R, Walldorf U, Kloter U, Gehring WJ. Homology of the eyeless gene of drosophila to the small eye gene in mice and aniridia in humans. Science. 1994. 785 p.

Rio DC. Molecular mechanisms regulating Drosophila P element transposition. Annual review of genetics. 1990.

Robinow S, White K. Characterization and spatial distribution of the ELAV protein during Drosophila melanogaster development. J Neurobiol. 1991 Jul;22(5):443–61.

Roche SE, Rio DC. Trans-silencing by P elements inserted in subtelomeric heterochromatin involves the Drosophila Polycomb group gene, Enhancer of zeste. Genetics. 1998 Aug;149(4):1839–55.

Roy A, Kucukural A, Zhang Y. I-TASSER: a unified platform for automated protein structure and function prediction : Abstract : Nature Protocols. Nat Protoc. 2010.

Saito K, Nishida KM, Mori T, Kawamura Y, Miyoshi K, Nagami T, et al. Specific association of Piwi with rasiRNAs derived from retrotransposon and heterochromatic regions in the Drosophila genome. Genes Dev. 2006 Aug 15;20(16):2214–22.

Sameny A, Locke J. The P-element-induced silencing effect of KP transposons is dose dependent in Drosophila melanogaster. Genome. 2011 Sep;54(9):752–62.

Sanz-Garcia M, Lopez-Sanchez I, Lazo PA. Proteomics Identification of Nuclear Ran GTPase as an Inhibitor of Human VRK1 and VRK2 (Vaccinia-related Kinase) Activities. Mol Cell Proteomics. 2008 Nov 6;7(11):2199–214.

Sato S, Cerny RL, Buescher JL, Ikezu T. Tau-tubulin kinase 1 (TTBK1), a neuron-specific tau kinase candidate, is involved in tau phosphorylation and aggregation. J

Neurochem. 2006 Sep;98(5):1573–84.

Scheeff ED, Bourne PE. Structural Evolution of the Protein Kinase–Like Superfamily. PLoS Comput Biol. Public Library of Science; 2005 Oct 21;1(5):e49.

Scheeff ED, Eswaran J, Bunkoczi G, Knapp S, Manning G. Structure of the pseudokinase VRK3 reveals a degraded catalytic site, a highly conserved kinase fold, and a putative regulatory binding site. Structure. 2009 Jan 14;17(1):128–38.

Schotta G. Central role of Drosophila SU(VAR)3-9 in histone H3-K9 methylation and heterochromatic gene silencing. EMBO J. Nature Publishing Group; 2002 Mar 1;21(5):1121–31.

Schotta G, Ebert A, Reuter G. SU(VAR)3-9 is a conserved key function in heterochromatic gene silencing. Genetica. 2003 Mar;117(2-3):149–58.

Schwartz BE, Ahmad K. Transcriptional activation triggers deposition and removal of the histone variant H3.3. Genes Dev. 2005 Apr 1;19(7):804–14.

Siebel CW, Rio DC. Regulated splicing of the Drosophila P transposable element third intron in vitro: somatic repression. Science. 1990 Jun 8;248(4960):1200–8.

Sillibourne JE, Milne DM, Takahashi M, Ono Y, Meek DW. Centrosomal Anchoring of the Protein Kinase CK1δ Mediated by Attachment to the Large, Coiled-coil Scaffolding Protein CG-NAP/AKAP450. J Mol Biol. 2002 Sep;322(4):785–97.

Steinberg S, de Jong S, Andreassen OA, Werge T, Børglum AD, Mors O, et al. Common variants at VRK2 and TCF4 conferring risk of schizophrenia. Hum Mol Gen. 2011.

Swarup S, Pradhan-Sundd T, Verheyen EM. Genome-wide identification of phospho-regulators of Wnt signaling in Drosophila. Development. 2015 Apr 15;142(8):1502–15.

Takahashi M, Tomizawa K, Sato K, Ohtake A, Omori A. A novel tau-tubulin kinase from bovine brain. FEBS Lett. 1995 Sep;372(1):59–64.

Takata H, Hanafusa T, Mori T, Shimura M, Iida Y, Ishikawa K, et al. Chromatin compaction protects genomic DNA from radiation damage. PLoS ONE. 2013;8(10):e75622.

Talbert PB, Henikoff S. Spreading of silent chromatin: inaction at a distance. Nat Rev Genet. 2006 Oct;7(10):793–803.

Taylor SS, Radzio-Andzelm E. Three protein kinase structures define a common motif. Structure. 1994.

Tomizawa K, Omori A, Ohtake A, Sato K, Takahashi M. Tau-tubulin kinase phosphorylates tau at Ser-208 and Ser-210, sites found in paired helical filament-

tau. FEBS Lett. 2001 Mar;492(3):221–7.

Trojer P, Reinberg D. Facultative heterochromatin: is there a distinctive molecular signature? Mol Cell. 2007 Oct 12;28(1):1–13.

Valbuena A, Castro-Obregón S, Lazo PA. Downregulation of VRK1 by p53 in Response to DNA Damage Is Mediated by the Autophagic Pathway. PLoS ONE. Public Library of Science; 2011 Feb 28;6(2):e17320.

Valbuena A, López-Sánchez I, Vega FM, Sevilla A, Sanz-García M, Blanco S, et al. Identification of a dominant epitope in human vaccinia-related kinase 1 (VRK1) and detection of different intracellular subpopulations. Arch Biochem Biophys. 2007 Sep;465(1):219–26.

Valbuena A, Sanz-García M, López-Sánchez I, Vega FM, Lazo PA. Roles of VRK1 as a new player in the control of biological processes required for cell division. Cell Signal. 2011 Aug;23(8):1267–72

Vázquez-Cedeira M, Lazo PA. Human VRK2 (vaccinia-related kinase 2) modulates tumor cell invasion by hyperactivation of NFAT1 and expression of cyclooxygenase-2. Journal of Biological Chemistry. 2012 Dec 14;287(51):42739–50.

Yakulov T, Günesdogan U, Jäckle H, Herzig A. Bällchen participates in proliferation control and prevents the differentiation of Drosophila melanogaster neuronal stem cells. Biol Open. 2014;3(10):881–6.

Yang Z. Maximum likelihood phylogenetic estimation from DNA sequences with variable rates over sites: approximate methods. J Mol Evol. 1994 Mar 9;39(3):306–14.

Yarden Y, Escobedo JA, Kuang WJ, Yang-Feng TL, Daniel TO, Tremble PM, et al. Structure of the receptor for platelet-derived growth factor helps define a family of closely related growth factor receptors. Nature. 1986 Sep;323(6085):226–32.

Zhang W, Deng H, Bao X, Lerach S, Girton J, Johansen J, et al. The JIL-1 histone H3S10 kinase regulates dimethyl H3K9 modifications and heterochromatic spreading in Drosophila. Development. 2006 Jan;133(2):229–35.

Zhang Y. I-TASSER server for protein 3D structure prediction. BMC Bioinformatics. 2008;9:40.

Zuckerkandl E. A possible role of "inert" heterochromatin in cell differentiation. Action of and competition for “locking” molecules. Biochimie. 1974;56(6-7):937–54.